

Reliability Modelling of a Multi-Terminal High Voltage Direct Current (HVDC) System based on Half-Bridge Modular Multilevel Converter (MMC) Technology

Master Thesis
Zahrina Hafizhah

Reliability Modelling of a Multi-Terminal High Voltage Direct Current (HVDC) System based on Half-Bridge Modular Multilevel Converter (MMC) Technology

By

Zahrina Hafizhah

in partial fulfilment of the requirements for the degree of

Master of Science
in Electrical Engineering

at Delft University of Technology,
to be defended publicly on Wednesday July 26, 2017 at 10:00 AM.

Supervisor:	Prof. Ir. Mart. A. M. M. Van der Meijden	TU Delft
Thesis committee:	Dr. Ir. José L. Rueda Torres	TU Delft
	Dr. Ir. M. Ghaffarian Niasar	TU Delft
	Ir. Bart W. Tuinema	TU Delft

An electronic version of this thesis is available at <http://repository.tudelft.nl/>.

Acknowledgement

All praises and thanks to Allah, the Lord of the Creation, the Compassionate, and the Merciful.

I strongly believe that everybody has the same right and opportunity to reach higher dreams and acquire more knowledge as a personal development for his/her life. Yet, I realize that a lot of people out there are not as lucky as I am to be able to achieve life targets, involving the chance of gaining knowledge.

Having more insight and knowledge is a new kind of happiness I found during this master thesis work. I feel alive when I read, think, and find any solution of problems I deal with, included this master thesis. However, this idea was found through the hardest time in my life in the last two years. In the first quarter of my life in Delft, I was aware that studying here was not easy and never sure I can survive with my condition, competence and skill. I realized that only dreams and interest would not be enough to pass through the life of a TU Delft student. At the time I was doing my master thesis, I found that reading a lot of paper, thinking critically, solving technical problems, doing analysis for improvements are exhausting and challenging, yet at the same time, pleasant. I discover that the topic of my master thesis is very important in purpose of fulfilling electricity demand, for the better human life. This thought is the main motor that brings me to the graduation and to live my life as an electrical engineer in the future.

Once again, all praises and thanks to Allah, whose permission and help enables me to accomplish my study in TU Delft. I would also like to thank dr. Ir. José L. Rueda Torres as a supervisor who gave me the opportunity and guidance to finish the thesis project. Besides, I am thankful to prof. ir. Mart. A.M.M. Van der Meijden (Chair, TU Delft), who gives the insightful statement: "You are here to learn, not to teach." which made me realize that it is okay to make mistakes as a student and motivated me to improve myself day to day. It helps me boost my confidence to finish the task. Also, I thank the rest of the thesis committee: dr. ir. M. Ghaffarian Niasar for the comments, which are very helpful in improving the quality of my work.

Next, I am grateful to my daily supervisor, ir. Bart W. Tuinema for his continuous assistance and his patience to give me more technical guidance. He helped me a lot with improving the quality of my document. In addition, I am thankful to ir. Arcadio D. Perilla Guerra for his time to give me insight about multi-terminal HVDC system and remarks regarding the slide of my presentation.

Last but not least, I want to give my best thanks to my parents. They never stop praying for my success and good things in my life, including my study in TU Delft. They give never-ending support to me in every condition. Next, thanks are also given to Arinda and Roro, my best friends in the Netherlands who give my passion back at my hardest time. Also thanks to the Indonesian guys in ESE, Dedi, Zamroni, Bryan and Ryan as partners of studying most of the subjects in TU Delft who care and support each other. Big thanks given to all Indonesian community members, Keluarga Muslim Delft (KMD) and Perhimpunan Pelajar Indonesia (PPI) Delft, which became my second family and made Delft become like home. Finally, I thank to all my family members and friends both in the Netherlands and Indonesia for the support.

*Zahrina Hafizhah
Delft, July 2017*

Table of Contents

Acknowledgement	v
Table of Contents	vii
List of Figures	ix
List of Tables	xi
Glossary	xiii
Abstract	xv
1 Introduction	1
1.1 Motivation	1
1.2 Literature Review	3
1.3 Research Question.....	4
1.4 Methodology.....	4
1.5 Thesis Outline	4
2 Multi-Terminal HVDC Systems and Probabilistic Reliability Analysis	7
2.1 State-of-the-art of HVDC Design.....	7
2.2 Converter Station Components	9
2.2.1. Transformer	9
2.2.2. Converter Reactor	9
2.2.3. Converter unit.....	9
2.2.4. Line Commutated Converter (LCC).....	10
2.2.5. Voltage Source Converter (VSC)	11
2.2.6. DC Lines.....	11
2.2.7. DC Switchyard.....	12
2.2.8. Auxiliary Systems	12
2.3 HVDC Topologies.....	12
2.3.1. Monopole HVDC System	12
2.3.2. Bipole HVDC System	12
2.3.3. Back-to-Back HVDC Links	12
2.3.4. Multi Terminal HVDC System.....	13
2.4 Modular Multilevel Converter (MMC).....	14
2.5 Basic Reliability Models of Components	15
2.5.1. Basic Reliability Functions.....	15
2.5.2. Bathtub Curve	16
2.5.3. Component Life Cycle	17
2.5.4. Two State Markov Model.....	18
2.6 Reliability Models of Systems of Components	19
2.6.1. Series-Parallel Networks (Reliability Networks)	19
2.6.2. Monte Carlo	21
3 Case Study Description	23
3.1 Offshore Grid Topology	23
3.2 Converter Station	24
3.2.1. Transformer	25
3.2.2. Converter Unit	25
3.2.3. Converter Reactor	26
3.2.4. Control System.....	27
3.2.5. DC Switchyards.....	27
3.3 DC Cable.....	28
3.4 Conclusions.....	29
4 Modelling	31
4.1 Reliability Model of a Converter Unit.....	31
4.1.1. IGBT to Power Modules	32
4.1.2. Power Modules to Converter Arm	33
4.1.3. Converter Arms to Converter Unit.....	33
4.2 Reliability Model of the Converter Station	34

4.3	Reliability Model of a Point-to-Point HVDC Connection	36
4.4	Reliability Model of the Three-Terminal Connection with Offshore Node.....	38
4.5	Monte Carlo Simulation	40
4.6	Conclusion.....	45
5	Results.....	47
5.1	Probabilistic Reliability Analysis of a Converter unit.....	47
5.2	Probabilistic Reliability Analysis of a Converter Station	50
5.2.1.	Onshore Converter Stations.....	50
5.2.2.	Offshore Converter Station.....	53
5.3	Probabilistic Reliability Analysis of a Point-to-Point HVDC System	55
5.4	Probabilistic Reliability Analysis of The Three-Terminal HVDC System	57
5.4.1.	Without Switching Possibilities	58
5.4.2.	With Switching Possibilities	61
5.5	Conclusion.....	69
6	Conclusion & Recommendations	71
6.1	Conclusion.....	71
6.2	Recommendation	72
	Bibliography	73
	Appendix A	77
	The Simulation of Reliability Analysis of Converter Unit.....	77
	• Input.....	77
	• Process.....	77
	• Output.....	78
	Appendix B	81
	The Monte Carlo Simulation of The Subsystems and Systems Reliability Analysis	81
	• Input.....	81
	• Generation of Lifetime Series	82
	• Output	88
	Appendix C	97
	The Result Sampling	97
	• Input.....	97
	• Sampling.....	98
	• Process and Output.....	98

List of Figures

Fig. 1-1 Thesis Outline	5
Fig. 2-1 Breakeven distance of HVDC-HVAC system	8
Fig. 2-2 Single Line Diagram of Symmetric Monopole HVDC System	9
Fig. 2-3 Effect of Firing Angle on Converter Operation [44]	10
Fig. 2-4 Effect of Firing Angle as it Approaches 90° [44]	10
Fig. 2-5 Effect of Firing Angle of 90° [44]	10
Fig. 2-6 Asymmetric Monopole HVDC System with Ground Return	13
Fig. 2-7 Asymmetric Monopole HVDC System with Metallic Return	13
Fig. 2-8 Symmetric Monopole HVDC System	13
Fig. 2-9 Bipolar HVDC System	13
Fig. 2-10 Back to Back Asymmetric Monopole HVDC link	13
Fig. 2-11 Multi Terminal HVDC System - Series Arrangement	13
Fig. 2-12 Multi Terminal HVDC System - Parallel Arrangement	13
Fig. 2-13 MMC HVDC Converter Scheme	14
Fig. 2-14 Series Connection	19
Fig. 2-15 Parallel Connection	20
Fig. 3-1 Multi terminal HVDC Layout of the Case Study	23
Fig. 3-2 Simplified Case Study Layout	24
Fig. 4-1 MMC System Topology of the Case Study	32
Fig. 4-2 Reliability Model of The Power Module	32
Fig. 4-3 Reliability Model of The Converter Arm	33
Fig. 4-4 Reliability Model of The Converter Unit	34
Fig. 4-5 Converter Station Scheme	35
Fig. 4-6 Reliability Model of a Converter Station	35
Fig. 4-7 Reliability Model of a Point-to-Point Connection	37
Fig. 4-8 Reliability Model of a Three-Terminal Connection (without Switching Possibility)	38
Fig. 4-9 Lifetime Cycle of the Point-to-Point Connection in a Year	41
Fig. 4-10 Workflow of the Monte Carlo Simulation	42
Fig. 5-1 Hazard Rate of the Converter unit	47
Fig. 5-2 Reliability Curve of The Converter unit with Four Redundant Power Modules	48
Fig. 5-3 Reliability Curve of The Converter unit without Redundancy	48
Fig. 5-4 Fitted Converter unit Reliability using General Negative Exponential Distribution	49
Fig. 5-5 Fitted Converter unit Reliability using Eq. 5.3	50
Fig. 5-6 Pie Chart of The Onshore Converter Station Components Unavailability based on Table 5-3 using the Analytical Approach	52
Fig. 5-7 Pie Chart of The Onshore Converter Station Components Unavailability based on Table 5-3 using Monte Carlo Simulation	52
Fig. 5-8 Pie Chart of the Offshore Converter Station Components Unavailability based on Monte Carlo Simulation	54
Fig. 5-9 The outage Duration of the Onshore and Offshore Converter Stations	55
Fig. 5-10 Graph of The Expected not-Transmitted Energy of a Point-to-Point Connection	57
Fig. 5-11 Multi-terminal HVDC Layout	58
Fig. 5-12 Range of Time Between Failures in the Subsystems and HVDC System in the Multi-terminal HVDC Project	61
Fig. 5-13 The Year Scenario of The NL Preference in The Offshore Node	65
Fig. 5-14 The Year Scenario of The NL Preference in (a) NL Onshore Node and (b) DK Onshore Node	65
Fig. 5-15 The Year Scenario of The DK Preference in (a) NL Onshore Node and (b) DK Onshore Node	66
Fig. 5-16 The Year Scenario of The Equal Preference in (a) NL Onshore Node and (b) DK Onshore Node	66
Fig. 5-17 The Year Scenario of The Equal Preference in (a) NL Onshore Node and (b) DK Onshore Node	67

List of Tables

Table 2-1 Comparison between LCC and VSC [46].....	11
Table 3-1 Reliability Parameters of The Transformers.....	25
Table 3-2 The Reliability Parameter of The Converter Unit [29]	26
Table 3-3 The MTTR of The Converter Unit.....	26
Table 3-4 Reliability Parameters of The Converter Reactor.....	27
Table 3-5 Reliability Parameters of Control System.....	27
Table 3-6 Reliability Parameters of DC Switchyard	28
Table 3-7 Reliability Parameters of The DC Cables.....	28
Table 3-8 Reliability Parameters of The DC Cables used in The Case Study	29
Table 3-9 Reliability Parameters of all Components in the Onshore Subsystem.....	29
Table 3-10 Reliability Parameters of all Components in the Offshore Subsystem.....	29
Table 4-1 Failure State Probability of a Three Terminal Topology with Switching Possibility ..	39
Table 5-1 List of Reliability Indices of Components inside Converter unit	48
Table 5-2 Reliability Parameters of all Subsystems in the Onshore Subsystem.....	51
Table 5-3 Unavailability of Subsystems in the Onshore Converter Station	51
Table 5-4 Outage Duration of the Subsystems in NL and DK Onshore Converter Station	52
Table 5-5 Reliability Parameters of all Subsystems in the Offshore Node	53
Table 5-6 Unavailability of Subsystems in the Offshore Node	53
Table 5-7 Outage Duration of the Components in the Offshore Node	54
Table 5-8 Unavailability of Subsystems in the Point-to-Point Connection.....	56
Table 5-9 Expected amount of Energy not Transmitted in the Point-to-Point Connection	56
Table 5-10 Unavailability of The Subsystems in Offshore Converter Station.....	58
Table 5-11 Probability and Duration of Subsystem Failure by the Analytical Method.....	59
Table 5-12 Other Analysis Results from Monte Carlo Simulation	59
Table 5-13 The Outage Duration of the Case Study Subsystems and System	60
Table 5-14 Probability and Duration of Subsystem Failure States by the Analytical Method..	62
Table 5-15 Probability and Duration of Subsystem Failure States by Monte Carlo Simulation	62
Table 5-16 The Snapshot of Energy not Transmitted per Year in Three Terminal Topology using Analytical Result	63
Table 5-17 Year Scenario of Energy Transmitted in Three Terminal Topology	67
Table 5-18 Year Scenario of Energy not Transmitted per Year in Three Terminal Topology using Analytical Result	68

Glossary

HVDC	High Voltage Direct Current
MMC	Modular Multilevel Converter
VSC	Voltage Source Converter
IGBT	Insulated Gate Bipolar Transistor
RES	Renewable Energy Source
HVAC	High Voltage Alternating Current
LCC	Line Commutated Converter
PWM	Pulse Width Modulation
MTTF	Mean Time to Failure
MTTR	Mean Time to Repair
TTF	Time to Failure
NL	The Netherlands
DK	Denmark

Abstract

The increase of power generation in Europe using renewable energy sources leads to the application of HVDC for high efficiency transmission. The growth of the energy market and the development of the HVDC technology cause the multi-terminal HVDC based on half-bridge MMC technology to be one of the best options for transmission systems, especially for offshore power grids. The aim of designing transmission systems is to obtain a network with high reliability. In this master thesis, the reliability modelling of multi-terminal HVDC systems based on half-bridge MMC technology is analysed as an important step to designing transmission networks. Firstly, the reliability of all subsystems of the HVDC connection is modelled. The Modular Multi-Level Converter - Voltage Source Converter (MMC-VSC) is discussed, starting from the lowest level. After that, the converter unit and other components such as transformer, converter reactor, control system and DC switchyard in the connection are described by their reliability function and are combined into a reliability model of a converter station. Two types of converter stations (i.e. onshore and offshore) and the required cables assemble the HVDC system, based on the case study. Two possible configurations are modelled: the Point-to-point and the three-terminal configuration. In the three-terminal configuration, two situations are studied: with and without switching possibilities. The reliability modelling is performed using two approaches: an analytical approach and Monte Carlo simulation. After creating the model and collecting the reliability parameter, the reliability analysis is performed. The reliability modelling of the subsystems and systems involve the calculation of availability, unavailability, outage duration, energy not transmitted, failure frequency, average duration per interruption, and the range of time between failures. After having the model and the reliability parameter, the reliability analysis is performed.

From the analysis, it is found that the highest unavailability and, thus, the outage duration in the onshore and offshore converter station have the transformer and the converter reactor, respectively. The offshore converter station is found to have the highest unavailability. The failure frequency, the average duration per interruption, and the time between interruptions, which is produced by Monte Carlo simulation, provide useful information for taking further action regarding asset management of the system. The energy not transmitted of the point-to-point and three-terminal system provides useful information to choose which solution is the most profitable

Keywords: *Reliability Modelling, Multi-Terminal HVDC, Half-Bridge MMC, Converter Station, Point-to-Point, Three-Terminal*

1 Introduction

This chapter introduces the master thesis project. It starts by brief a motivation and the purpose of doing the master thesis in section 1.1. From the motivation, the research that has been done regarding important aspects of this master thesis is briefly described in section 1.2. This leads to several research questions, which are listed in section 1.3. The methodology to finish the master thesis is summarised in section 1.4. Finally, section 1.5 explains the content of all chapters in this master thesis report.

1.1 MOTIVATION

Renewable energy sources (RES) are nowadays playing an important role for sustainable and abundant energy supply. It is accounted that 90% of the newly added energy in the European power grid is generated by RES in 2016 [1]. A variety of RES supports the capacity installed in Europe as wind power constitutes the highest capacity installation, which is 12.5 GW (51%) followed by 6.7 GW solar PV (27%) and 3.1 GW natural gas (13%) in 2016 [2]. It is estimated that the offshore wind farm will achieve up to 40 GW installed capacity by 2020 [3]. This leads to preference of High Voltage Direct Current (HVDC) transmission as a more promising technology than conventional High Voltage Alternating Current (HVAC) transmission.

HVDC has proven to be a new technology for transmission systems with a lot of advantages. In economic aspects, based on the break-even distance, the investment costs will be lower than HVAC after 600-800 km for onshore application and about 50 km for offshore application [4]. Therefore, this technology is advantageous for transferring bulk electrical power over very long distances. Also, it produces lower losses than Alternating Current (AC) transmission in practical applications. HVDC offers efficient technology for transmitting power from, for example, remotely located offshore and onshore energy resources to the consumers [5]. In technical aspects, HVDC enables stable and safe asynchronous interconnection of transmission networks with different frequencies and voltages. For example, the Nordel power system in Scandinavia is connected asynchronously to the Western European power system, even though it has the same frequency. The Nordic power system is located geographically isolated, such that connection by DC technology is preferable for better stability. Another strength of HVDC technology is that it allows the connection of new power plants to the grid without any contribution to the short-circuit current [6]. This is profitable since there is no need to increase the rating of the circuit breakers in the connection. HVDC today has become a promising technology for the transmission system of the future.

The growing electricity market prospect and the improvement of HVDC technology leads to the introduction of multi-terminal HVDC grids. It offers more efficient use of the grid and profitable energy trading [3]. For interconnected offshore power grids, multi-terminal HVDC transmission decreases the investment and operational expense and serves as redundancy, thus offers higher flexibility for energy markets. The excellence of multi-terminal HVDC is supported by the features of the Voltage Source Converter (VSC) [7], while LCC technology faces a more complex control of such a parallel multi-terminal configuration. Multi-terminal HVDC requires power direction changes, which is found to be unreliable for LCC systems to fulfil this requirement [8]. Another requirement of wind offshore grids is a compact and reliable converter technology with high power capacity [9]. Modular Multilevel Converter (MMC) provides a flexible and scalable voltage rating since the MMC consists of hundreds of low voltage rating sub-modules that can allow

production of a variety of discrete voltage steps. The application of the sub-modules demonstrates a better harmonic performance thus minimises the need for filters. The need for a DC capacitor can be decreased by the usage of MMC [10]. The MMC enables elimination of several subsystems thus provides a more compact converter technology. Several alternatives of the circuit are available for the converter. Two of them are the two-level half-bridge converter and the two-level full-bridge converter. The half-bridge converter is preferred due to the lower power losses and costs than a full-bridge converter.

The aim of designing transmission systems including multi-terminal HVDC using half-bridge MMC is to obtain a system with high availability and reliability. The transmission network consists of many connections and components which affect the network reliability [11]. Reliability is the ability of a component or a system to operate in the normal condition for a given period. Reliability analysis is, among others, performed to obtain insight into the time and duration of maintenance, consumer interruptions and producer interruptions. The analysis can be done by two kinds of methods: deterministic and probabilistic. Engineers in practice usually use deterministic methods because these are clear and effective, although these can result in over-dimensioned power systems [12]. For large-scale renewable generation, such as solar and wind, the deterministic methods are less applicable because of the variable nature of these sources. Probabilistic approaches can provide insight into the real risk and thereby lead to a more optimal usage of the power system.

System reliability can be predicted by observation and analysis of the reliability behaviour of all components that build the overall system. HVDC connections basically convert power from the generation from AC to DC and vice versa, thus the component with the most significant role in HVDC connection is the power converter [13]. The power electronics contains a number of valves, and a controllable electronic switch that allows for the power conversion. The valves consist of a number of power semiconductor devices. The thyristor is the first power semiconductor device applied in HVDC connections in the Line Commutated Converter (LCC). Today, the Insulated-Gate Bipolar Transistor (IGBT) is also introduced onto the market and used in the Voltage Source Converter (VSC). These two technologies have their own characteristics and are applied in different situations and with different specifications. Other main components in HVDC connections are transformers, DC filters, and the DC smoothing reactor. All the components connect each other and become one subsystem, a converter station. Knowing the configuration and the connection of all components is very useful to determine the reliability of the HVDC connection [14].

The challenge of reliability analysis of a system is how the system can be modelled. This requires sufficient knowledge about how the components interact with each other. Parallel connections in a physical network, for instance, cannot be directly translated into parallel connections in a reliability model. The number of redundant components and the complexity of the system influence the decision of which approaches must be employed. Also, the understanding about the life characteristic of each component, which builds the system, is necessary. This is very useful to decide which type of failure probability distribution should be applied to the components. Another challenge of reliability analysis is the limited component failure data, especially for MMC VSC as a new HVDC technology. This demands further analysis to estimate which data is suitable for the specific power and voltage rating of the analysed HVDC connection. Thus, this thesis will research on how the reliability of multi-terminal HVDC connections based on half bridge MMC can be modelled based on its component characteristics and its network.

1.2 LITERATURE REVIEW

HVDC technology is described in several previous research papers. Paper [11] gives a broad overview of HVDC technology and the motivation of its use, the aim of reliability assessment, and a literature review about reliability assessment of HVDC systems. HVDC plus, a converter technology assumed for the case study in this master thesis, is discussed in a technical article released by SIEMENS [15, 16].

Paper [17] provides a reliability analysis of one of the subsystems inside the HVDC system, which is the converter transformer. The reliability of a variety of the component models and configurations is assessed with a Markov model approach using a statistical survey from CIGRE. The reliability equivalence and sensitivity analysis of the converter transformer, and finally the converter station are proposed in [18]. Paper [19] applies reliability evaluation for the comparison of reliability of different types of converter technologies inside a converter station: LCC, VSC, and integrated power electronics.

Several papers have discussed the reliability evaluation of multi-terminal HVDC. The modelling and evaluation of the reliability of point-to-point LCC HVDC systems using computer simulation are discussed in [20]. The reliability of HVDC transmission connecting a generation bus and a load bus connected to a tapping station is evaluated in [21]. The evaluation of reliability of hybrid multi-terminal HVDC sub-transmission consisting of several VSCs and LCCs, a cable system and a system controller are also determined [22, 23]. The reliability of VSC HVDC is particularly modelled with a comparison of several possible configurations using analytical and computer simulation in [24]. The availability of a point-to-point terminal containing MMC technology is analysed in several papers in [25] and [26]. The reliability investigation of 150 kV point-to-point offshore HVDC system using VSC is described in [27]. The reliability of an offshore HVDC grid using MMC technology is modelled, taking into account several topologies and scenarios (radial, multi-terminal, meshed, bipolar, etc.).

The converter technology reliability is also particularly discussed in several references. The reliability of MMC converter valves released by ABB is represented by the failure rates and analysed for different voltage rating using Markov models in [28]. The reliability of both single IGBT modules and series-connected IGBT modules in MMC technology is also modelled [29]. In [30], the reliability model of MMC is provided considering periodic preventive maintenance. The reliability model of MMC technology including the capacitor inside the power module is discussed in [31].

The reliability modelling of three-terminal HVDC systems using half-bridge MMC in all converter stations has however not been described in earlier research work. This master thesis models the reliability of point-to-point and three-terminal VSC HVDC systems in which the MMC technology of HVDC Plus is utilised in all the converter stations. Due to unavailability of reliability data of the components inside the converter unit, the data of MMC converters manufactured by ABB is applied. The reliability is modelled by two approaches: an analytical and Monte Carlo simulation, as recommended by most of papers in the literature review. Another improvement that has been done in this master thesis for improved reliability assessment of HVDC systems is that this master thesis implements reliability parameters based on the DC voltage level of the case study. The capacitor inside the power module as the lowest level subsystem is included in the model, thus included in the reliability analysis of the system. Therefore, it is expected that it will give more realistic results and representative information about the system.

1.3 RESEARCH QUESTION

Based on the motivation above, the objective of this work is to develop a reliability model of (two- and three terminal) HVDC connections, based on half-bridge MMC technology. The main research question can be defined as follows.

“How can the reliability of multi-terminal HVDC systems based on half-bridge MMC technology be modelled?”

This can be split into the three research questions below:

- How to model the reliability of subsystems in a multi-terminal HVDC system based on half-bridge MMC technology?
- How to model the reliability of multi-terminal HVDC systems based on half-bridge MMC technology?
- What is the reliability of the connection for several different scenarios and which components are the most critical in affecting the connection reliability?

1.4 METHODOLOGY

In this master thesis, the reliability of each component is to be modelled in terms of reliability. Therefore, the first step of the research is to study the components inside the half-bridge modular multilevel converter (MMC) and the connection between all components inside. The subsystems within the converter using MMC-VSC technology are then studied. Next, the reliability parameters of all components and subsystems inside the converter station considering the voltage level of the case study are collected and used for further analysis. After obtaining the reliability parameter as input, the reliability model of all subsystems and the complete systems can be created. Two approaches are utilised to construct the reliability model: an analytical approach and Monte Carlo simulation. First, the model of the converter unit based on half-bridge MMC technology is created. This is then followed by the reliability modelling of other subsystems inside the converter station. From the reliability models of the subsystems, the converter station can be also modelled. The next step is to analyse the reliability of a three-terminal configuration, including an offshore converter station. The point-to-point connection, which only includes the onshore converter station, is first modelled. From the entire model, the reliability analysis is performed considering several factors, calculating reliability indicators like the outage duration and energy not transmitted through the system.

1.5 THESIS OUTLINE

This master thesis is organised as follows. Chapter 2 describes HVDC systems in general, the widely used topologies of HVDC, the converter station and the subsystems within the converter station. This chapter also includes a description of reliability analysis. It consists of reliability analysis of components and small systems, which will be useful for this research.

In Chapter 3, the case study used for the reliability modelling is described. The description is from the highest level, which is the complete HVDC system, to the lowest level, which are the IGBTs. In this chapter, the reliability parameters from all references will be collected, selected and discussed.

In Chapter 4, several models used in the reliability analysis will be discussed based on the specifications of the case study. It begins with the IGBTs inside the converter unit and continues until the complete multi-terminal system.

In Chapter 5, the results of the reliability analysis are described. These include the results of the two approaches as mentioned before which will be compared to determine whether one approach can be used to verify the other.

In Chapter 6, the conclusion of this thesis project and several recommendations for future work will be mentioned.

Fig. 1-1 shows the whole thesis outline.

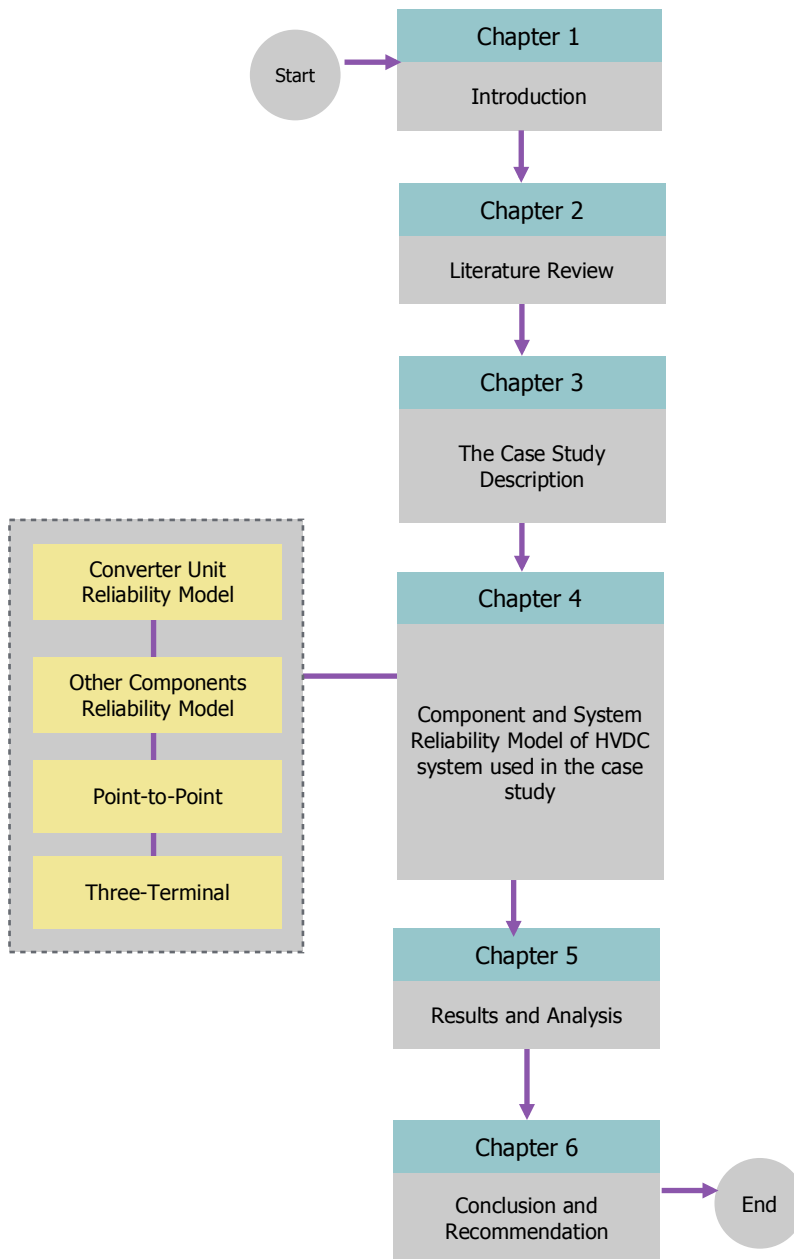


Fig. 1-1 Thesis Outline

2 Multi-Terminal HVDC Systems and Probabilistic Reliability Analysis

2.1 STATE-OF-THE-ART OF HVDC DESIGN

The electricity demand today is increasing with the growth of the world population. To meet this demand, a reliable and efficient electrical power transmission network to transport the energy with high quantity and quality is required. The development of commercial electrical power began after the 1900s; the transformer was invented to enable voltage transformation for the various voltage ratings of the loads using alternating current. This made electrical transmission lines and grids become an important infrastructure for industrialised countries. The human population growth induces the spread of bulk electrical power transmission. High Voltage Alternating Current (HVAC) is the technology which became popular for transferring power from conventional energy sources to the consumers.

Renewable generation is one development of commercial electrical power. The power is gained from natural resources such as solar, wind, hydro, and geothermal. The variable nature of most of these sources requires a transmission grid that can withstand dynamic power flows. In addition, it often needs to bridge longer distances to transmit the energy from the source to the consumer. The introduction of High Voltage Direct Current (HVDC) promises better quality of electrical power transmission for the connection of remote renewable sources. In the early 1900s, the first technology of mercury-vapour rectifiers and then, high-voltage valves was born. The research and development became a real application in 1954 when HVDC transmission was firstly operated by a 96 km sea cable of 20 MW between the mainland of Sweden to the island of Gotland [11]. After that, it was followed by power systems all around the world and the number of applications is still increasing.

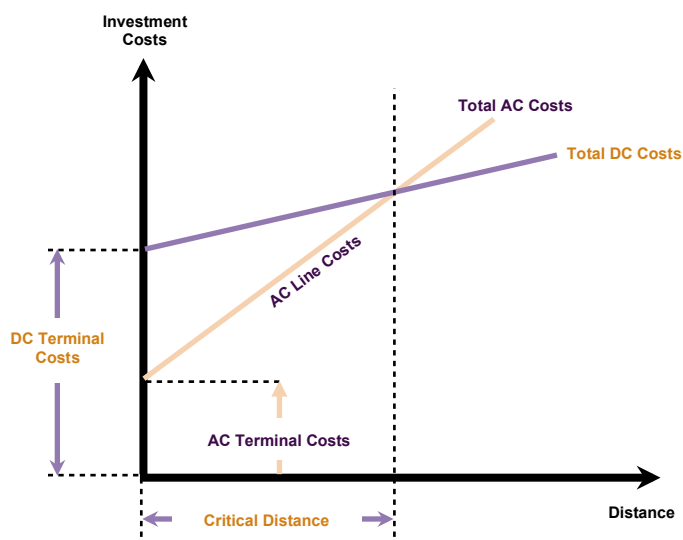


Fig. 2-1 Breakeven distance of HVDC-HVAC system

One of the reasons why HVDC is widely used is illustrated in Fig. 2-1. Fig. 2-1 shows the investment costs of DC and AC connections. The investment costs consist of the terminal costs and the line costs. The line costs are proportional to the length of the connection, while the terminal costs are constant. In Fig. 2-1, DC terminal costs are higher than AC terminal costs due to additional components in the DC terminal, e.g. the converter unit which converts the power from AC to DC and vice versa. However, for increasing distance, there is a break-even distance at approximately 600-800 km, where the total DC costs equal the total AC costs. A longer distance results in more line costs for each technology but the total DC costs are lower. This is caused by the smaller electrical losses of long DC connections compared to AC and the fact that for a DC connection only two lines are needed instead of three for an AC connection. Thus, HVDC gives the lowest expense for very long distances in transmission systems. For subsea application, the breakeven distance is typically much shorter, approximately 50 km [32].

A preference for HVDC systems can also be driven by several lacks of existing HVAC systems [33]:

- Limitation of transmission capacity due to capacitive and inductive elements in AC cables and overhead lines.
- Limitation of transmission distance due to the reason mentioned above. AC cables can only effectively transmit electrical power in the range of 40 to 100 km.
- Incapability to connect two AC systems with different frequencies.
- Incapability to connect two AC systems with the same frequency due to instability, undesirable power flow and short circuit levels.

HVDC transmission denotes the application of Power Electronics (PE) [34] and a main focus on HVDC technology development. The Current Source Converter (CSC) was the first thyristor valve-based technology applied and is now majorly used in HVDC technology all around the world. Another new technology of power electronics, the IGBT (Insulated-Gate Bipolar Transistor) made the application of Voltage Source Converters (VSC) possible. The latest development of HVDC systems is the multi-terminal HVDC system, introduced to optimise the use of DC transmission lines/cables and flexibility in the operation [35]. All those HVDC technologies will be explained further in the next section after describing the components in the converter station.

2.2 CONVERTER STATION COMPONENTS

One of the most important components of an HVDC connection is the converter station. The HVDC converter station is a particular substation, which contains several components as terminal equipment of an HVDC system [36]. Fig. 2-2 illustrates a monopole HVDC converter station, which consists of a transformer, a control system as a subsystem inside an auxiliary system, a converter reactor, an HVDC converter unit, and two DC switchyards.

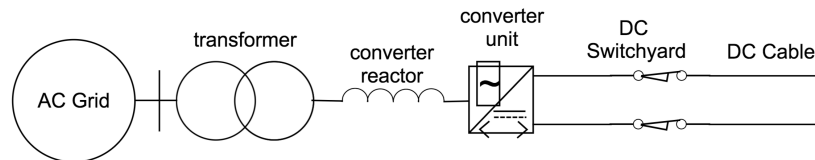


Fig. 2-2 Single Line Diagram of Symmetric Monopole HVDC System

2.2.1. Transformer

The AC network is interfaced by a transformer to interconnect with the converter unit. The main function of the transformer is to transform the voltage level of the AC network to a level suitable for the converter unit [37-39]. Its design depends on the nominal power transmitted and possible transport requirements [40]. LCC HVDC utilises a special transformer called converter transformer which can withstand DC stresses [41] and has several additional features such as on-load tap changers [41, 42]. In VSC HVDC systems, conventional AC transformers can be used.

2.2.2. Converter Reactor

The current produced by the three phases of a voltage source converter possibly result in a slight differences. A converter reactor is installed in each converter arm to reduce the balancing current among the phases to a very low level with the help of proper control. Besides, it also lowers the effect of faults from inside or outside the converter. The increased current of only a few tens of amperes per microsecond due to critical faults can be resolved. The idea of the converter reactor is a technology proposed by SIEMENSTM in their product, HVDC Plus. In their technical paper [43], reliable protection of the system is achieved by this method because such a critical fault can be quickly detected and it can produce a relatively low rise of current rates, thus the IGBT can be switched off at an uncritical current level.

2.2.3. Converter unit

An HVDC converter unit consists of several converter valves (thyristors for CSC, IGBTs for VSC) connected in series. It is an essential component as it is responsible for converting AC to DC or DC to AC [33]. In practice, it is connected as twelve-pulse bridges. In the whole system, the HVDC converter unit has redundancy in order to achieve a high reliability [11]. In the back-to-back HVDC link, the sending and receiving end are associated with the same kind of valve hall [33, 44].

There are two basic HVDC converters that are commonly used: Line Commutated Converter (LCC) and Voltage-Sourced Converter (VSC). The growth of HVDC application is made possible by the development of power electronics, especially in converter technology. The methods have different characteristics to be implemented under different conditions and requirements.

2.2.4. Line Commutated Converter (LCC)

LCC, also known as Current Source Converter (CSC), was first introduced in the 1960s following the development of thyristor-based valve technology. This technology is used in most of HVDC applications in the world [11]. The term is used because it uses line voltage AC connected to the converter to trigger the gate of the thyristor and turn it on. The gate will be turned off when reaching the zero current crossing. Due to the need for a voltage source to commute, LCC lacks the possibility of black start operation. In this converter, the DC current does not change direction and flows through the large inductance grid so it is considered to be a constant DC current. On the AC side, the converter acts as a current source that injects current with a specific frequency and harmonic current. The power can be obtained by reversing the DC voltage polarity on both sides. This technology has the highest voltage and power rating of all HVDC technologies, up to 6250A current and 10 kV blocking voltage [42].

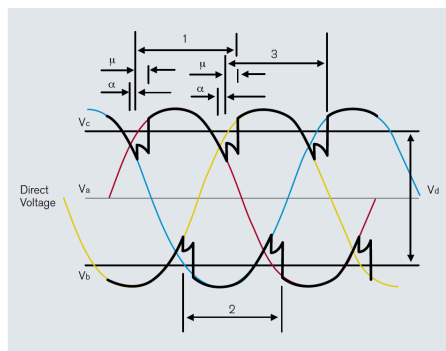


Fig. 2-3 Effect of Firing Angle on Converter Operation [44]

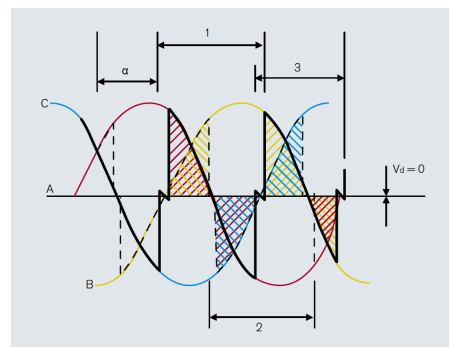


Fig. 2-4 Effect of Firing Angle as it Approaches 90° [44]

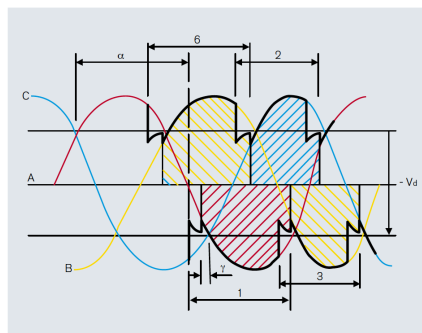


Fig. 2-5 Effect of Firing Angle of 90° [44]

Controlling the firing angle α is the fastest way to control the converter. The firing angle is a representation of the time delay when the thyristor is turned on and the voltage across the valve is positive. It will also control the amplitude of the DC output voltage generated by the rectifier. Raising the angle decreases the magnitude of the DC output voltage. In the rectifier, the control of the firing angle goes up to 90°, as illustrated in Fig. 2-3-Fig. 2-5. If the firing angle is increased above 90°, the DC output will become dominantly negative, leading to an inversion process in which the DC terminal voltage will be negative. The angle is more commonly known as extinction angle γ , which is a representation of the time between the end of the overlap period and the time when the phase voltage of the outgoing valve become more positive/negative than that of the next valve [44]. It is also a measure of the turn off time for the valve from when the valve is fired.

The largest voltage and power and the longest transmission line in the world using LCC technology is Zuandhong-Sichuan HVDC system which has a voltage of 1100 kV and a power of 10000 MW [42].

2.2.5. Voltage Source Converter (VSC)

VSC uses IGBTs to convert power from AC to DC and vice versa. The IGBT, unlike the thyristor, is a controllable converter that can self-commutate without an AC source. In this kind of converter, Pulse Width Modulation (PWM) is used to control the frequency of the gate switching. By using PWM, a VSC can also independently and instantaneously control the active and reactive power flow, acting like a synchronous machine in the power system. This leads to self-controlled short circuit contribution, which is promising when it comes to solve future network constraints frequently met in the power system when using renewable energy generation. However, this technology is more costly compared to LCC [40]. In multi terminal applications, VSC is well applicable as it is easy to control and build parallel connections for which using LCC causes several technical problems, such as the power direction in a single converter, and tends to be unreliable [8]. Table 2-1 below gives a comparison of LCC and VSC [45, 46].

Table 2-1 Comparison between LCC and VSC [46]

LCC	VSC
The type of semiconductor is thyristor	The type of semiconductor is IGBT
Control only for turning on	Control both for turning on and off
Minimum short circuit ratio: >2	Minimum short circuit: 0
Black start capability provided by additional component	Black start capability
Controls active power only	Control both for active and reactive power
AC filters needed	No AC filters needed
Larger site area due to AC filter	Compact site area
Lower cost	Higher costs
Lower station losses	Higher station losses
Higher reliability	Lower reliability
Converter transformer is needed	Conventional transformer is used
More mature technology	Less mature technology
Power reversed by changing the polarity of the converters	Power reversed by changing the current flow direction

2.2.6. DC Lines

There are two types of DC lines: overhead lines and cables. A connection over land usually uses overhead lines and DC cables are preferred for submarine transmission [37]. However, reliability of the HVDC system and the effect on the environment also affect the selection between them [40]. Neither DC cables nor overhead lines are required for a back-to-back HVDC system.

2.2.7. DC Switchyard

The DC switchyard is basically utilised for switching operation [20]. The components in a DC switchyard differ based on the converter unit. In HVDC systems using VSC, the DC switchyard consists of switchgear, measurement transducers, line reactors and an HV capacitor bank, while in LCC systems, it contains DC harmonic filters, smoothing reactors, measurement transducers and switchgear [25].

2.2.8. Auxiliary Systems

Auxiliary systems contain control systems, converter valve cooling, transformer cooling and battery backup. Auxiliary systems are very useful when an outage which can endanger the valves occurs [11].

2.3 HVDC TOPOLOGIES

There are a number of possible configurations based on the converter bridge arrangement. It can be arranged as a monopole or bipole depending on the requirements and location of the converter stations. Typical arrangements are illustrated in Fig. 2-6 to Fig. 2-11 [45].

2.3.1. Monopole HVDC System

There are two types of monopole HVDC systems: asymmetric and symmetric. In an asymmetric monopole system, the system uses a single high voltage cable to connect one or more converters at each end and returns through either a ground return current path to earth or sea or a metallic return current path, as shown in Fig. 2-6 and Fig. 2-7 [44, 47]. In symmetric monopole systems, as shown in Fig. 2-8, there are double conductors, for positive and negative voltage polarities [45]. Two DC circuit breakers are required in this system, which is double that in asymmetric monopole HVDC systems [48, 49]. One of the projects using an HVDC monopole system is the NorNed Project with a power rating of 700 MW and a voltage rating of ± 450 kV [50].

2.3.2. Bipole HVDC System

This configuration, as shown in Fig. 2-9, is frequently used in HVDC systems worldwide due to its high reliability. It uses two converters per converter station and two pole conductors. If one converter station fails and does not operate, the other can still work and the HVDC system can still work at half capacity [51]. The two converters are independent of each other and each might even use a different technology. Under normal conditions, no ground current exists in the system since the current in each pole is equal [40, 52]. The HVDC links between Norway and Denmark known as Skagerrak 3 and Skagerrak 4 are examples of bipole HVDC systems [53].

2.3.3. Back-to-Back HVDC Links

Back-to-back HVDC links can be used with either monopole or bipolar HVDC converters. In this configuration, two converter stations are installed at the same site so that no transmission line is required between them. Generally, it is implemented to transmit power between two power systems with different frequencies. Compared to HVDC systems with links to overhead lines, it has a low

DC rating voltage and a high thyristor valve current rating [44, 54]. An example of this configuration is the HVDC system on the Brazil-Argentina border, 1100 MW Garabi Converter Station [54]. Fig. 2-10 shows the scheme of a back-to-back HVDC link [44].

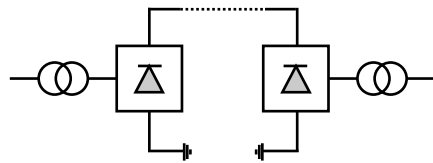


Fig. 2-6 Asymmetric Monopole HVDC System with Ground Return

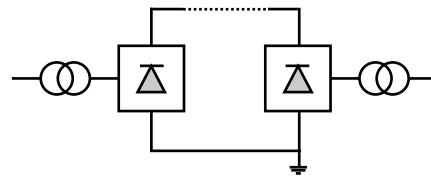


Fig. 2-7 Asymmetric Monopole HVDC System with Metallic Return

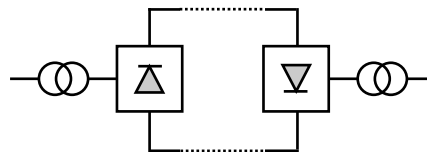


Fig. 2-8 Symmetric Monopole HVDC System

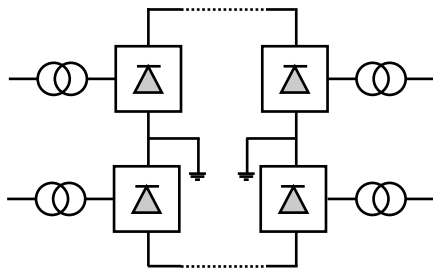


Fig. 2-9 Bipolar HVDC System

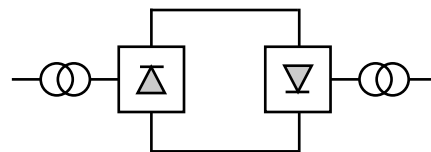


Fig. 2-10 Back to Back Asymmetric Monopole HVDC link

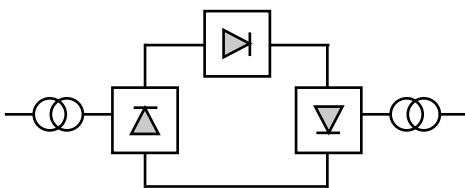


Fig. 2-11 Multi Terminal HVDC System - Series Arrangement

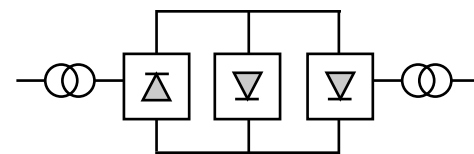


Fig. 2-12 Multi Terminal HVDC System - Parallel Arrangement

2.3.4. Multi Terminal HVDC System

The Multi Terminal HVDC Scheme comprises several converters connected to a DC network. There are two types of arrangement of the multi-terminal HVDC system: series multi-terminal HVDC system and parallel multi-terminal HVDC system. Those arrangements are shown in Fig. 2-11 and Fig. 2-12 respectively. One of the improvements made to this system involves the hybrid multi-terminal HVDC system, a combination of

series-parallel connection [40]. The large-scale multi terminal HVDC system was firstly commissioned is Hydro-Quebec New England Transmission [35].

2.4 MODULAR MULTILEVEL CONVERTER (MMC)

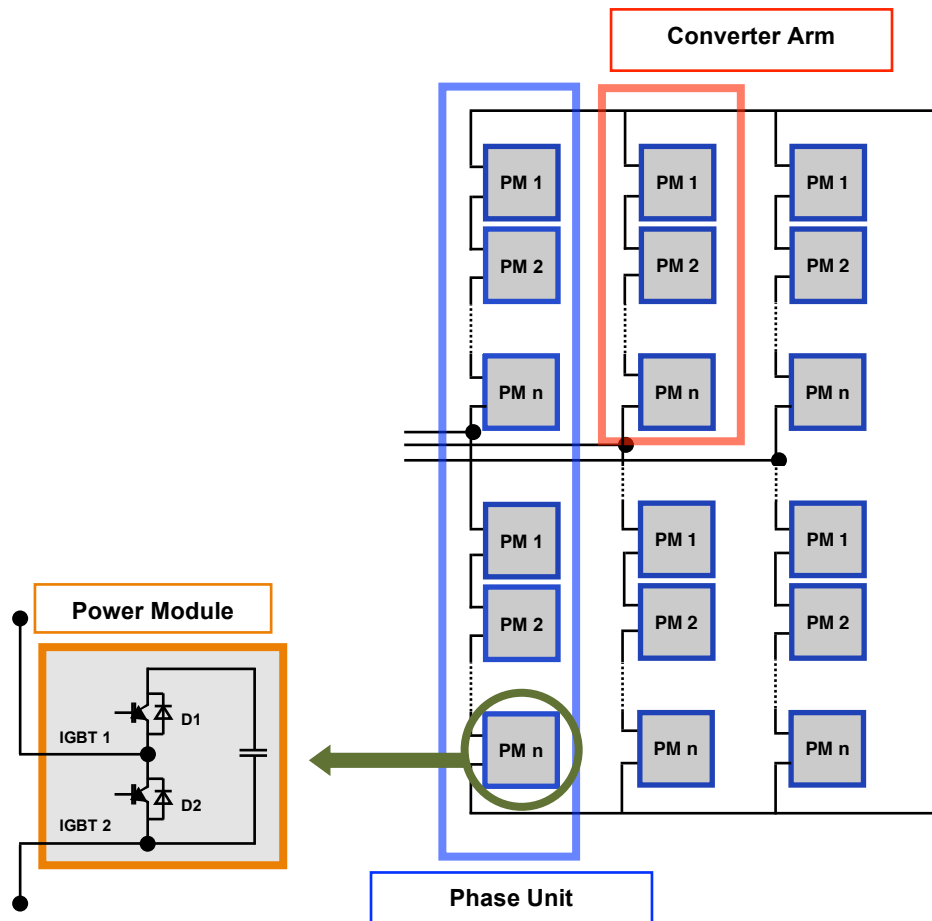


Fig. 2-13 MMC HVDC Converter Scheme

The Modular Multilevel Converter is one of the possible topologies of multilevel Voltage Source Converters. Other topologies are Neutral Point-Clamped (NPC) VSC, Cascaded H-Bridge Converter (CHB) and Flying Capacitor Converter (FCC) [29]. MMC consists of **converter arms**, which produce a wide range of discrete voltages, enabling to form an approximate sine wave with specific voltage magnitude for the AC terminal. Each converter arm is built by a number of converter modules and one converter reactor. A **converter module** is a number of series-connected power modules. The number depends on the magnitude of the DC voltage desired in the system. To withstand the overstress due to overcurrent and overvoltage, power modules are assembled in a converter tower. **Power modules** are an assembly of a sub-module (two series connected IGBT half-bridges), diodes, a DC storage power capacitor, a gate interface board, a bypass switch and a protection thyristor. All the sub-modules in each converter arm are controlled to obtain a DC terminal voltage and a sinusoidal AC terminal voltage after ratio adjustment [16]. All the components mentioned above are shown in Fig. 2-13.

Redundant power modules are installed without any mechanical switches to allow for and increase the safety and availability of the converter station. It is also designed to prevent high voltages in the remaining power modules when a fault

occurs. The power module is shorted by a bypass switch to allow the current to flow without any interruption and improve converter functionality [16].

2.5 BASIC RELIABILITY MODELS OF COMPONENTS

The increasing dependency on electricity requires a reliable power system. More advanced challenges are also faced by the power system:

- Increasing number of consumers
- Changes in the network structure
- Changes in operation policies
- Ageing of the components in the power system

With these challenges, the power system, including HVDC, is required to provide maximum capabilities. To answer the challenge, new techniques and technologies are applied without evoking blackouts in the system. Generally, there are two kinds of methods: deterministic and probabilistic methods. The N-1 redundancy criterion is one example of a deterministic criterion. It requires the condition that the loss of any component in the power system will not affect the electricity supply. Although it is relatively clear and effective, the power system resulting from it might be over-dimensioned. Probabilistic methods, meanwhile, are able to produce more optimal and real reliability results using realistic risks. However, the challenge of probabilistic methods is that the results must be translated into acceptable and desirable reliability indicators.

Firstly, reliability should be clearly defined. Taking one definition of system reliability: System reliability is the ability of a system to fulfil its function [12]. A system, generally, is a group of components working together to fulfil the system function, which considers a system boundary. A component is the smaller part of the system, which has its own characteristics and functions when working in the system. From the definition mentioned above, the system reliability is strongly influenced by component reliability.

2.5.1. Basic Reliability Functions

There are several ways to describe the **reliability of components**: basic reliability functions, the component life cycle, the bathtub curve, and the two-state Markov model [12].

For unrepairable components, some basic reliability functions are described below.

- Unreliability Function or Failure Distribution $F(t)$

The unreliability function or failure distribution is the probability that a healthy component is found in a failed state after time t . Assuming that t_f is the time when the failure occurred, the unreliability function can be defined as:

$$F(t) = P[t_f \leq t] \quad (2.1)$$

Equation 2.1 shows that the unreliability is the probability that the component fails before (or at) time t . Generally, the component is working at $t = 0$ such that $F(0) = 0$ and the probability of the component has failed at $t = \infty$ is $F(\infty) = 1$. The unreliability function is a continuously increasing function, and it is in fact a cumulative distribution function of the component failure density distribution.

- Reliability Function $R(t)$

In contrast to the unreliability function, the reliability function is the probability that a healthy component is found in a healthy state after time t . The reliability function can be directly calculated from the unreliability function.

$$R(t) = P[t_f > t] = 1 - P[t_f \leq t] = 1 - F(t) \quad (2.2)$$

- Failure Density Distribution $f(t)$

The failure density distribution is the rate at which the component fails at time t . It can be defined by the derivative of the unreliability function $F(t)$ to time t .

$$f(t) = \frac{dF(t)}{dt} \quad (2.3)$$

- Hazard Rate $z(t)$

The hazard rate is the rate at which the component fails at time t given that at that time the component is still healthy. It can also be defined as the ratio of the failure density distribution $f(t)$ and the reliability function $R(t)$.

$$z(t) = \frac{f(t)}{R(t)} \quad (2.4)$$

All these basic reliability functions can be approximated using failure statistics. The failure statistics can be obtained from historical failure data of the components of the same type and with similar operation conditions. These data can be approximated by a specific probability distribution that fits the data.

2.5.2. Bathtub Curve

The bathtub curve is a model for component failure behaviour, particularly the hazard rate that follows a curve like a bathtub. In the beginning of the curve, it represents an infant stage in which the hazard rate is relatively high due to production failures but then decreases after some time. A normal operating stage follows in which the hazard rate stays the same. After a specific time, the component enters the wear-out stage, in which the hazard rate increases due to aging of the component. The high hazard rate can be avoided, such that the component has a low hazard rate when it is installed, by performing accelerated testing. The time that the component is in the normal stage can also be lengthened by performing maintenance on the component. There are mainly two types of maintenance: time-based maintenance, when maintenance is undergone based on time intervals, and condition-based maintenance, when maintenance is performed according to the condition of the component.

As explained above, the basic reliability function can be described by specific probability distributions. Based on the bathtub curve, the constant hazard rate (which is called the failure rate λ) can be described by the **negative exponential distribution**. The unreliability function is then defined as follows:

$$F(t) = 1 - e^{-\lambda t} \quad (2.5)$$

The other reliability functions are as shown below:

$$h(t) = \lambda \quad (2.6)$$

$$F(t) = 1 - e^{-\lambda t} \quad (2.7)$$

$$R(t) = 1 - F(t) = e^{-\lambda t} \quad (2.8)$$

$$f(t) = \frac{dF(t)}{dt} = \lambda e^{-\lambda t} \quad (2.9)$$

From the equations above, the expected component lifetime can be calculated by the equation below:

$$\theta = \frac{1}{\lambda} \quad (2.10)$$

The increasing and decreasing hazard rate during the infant stage and wear-out stage in the bathtub curve can also be described by the **Weibull distribution**. With this distribution, the reliability functions are defined as follow.

$$R(t) = e^{-\left(\frac{t}{\alpha}\right)^c} \quad (2.11)$$

$$(2.12)$$

$$F(t) = 1 - e^{-\left(\frac{t}{\alpha}\right)^c}$$

$$(2.13)$$

$$f(t) = \frac{c}{\alpha} \left(\frac{t}{\alpha}\right)^{c-1} e^{-\left(\frac{t}{\alpha}\right)^c}$$

$$(2.14)$$

$$h(t) = \frac{c}{\alpha} \left(\frac{t}{\alpha}\right)^{c-1}$$

With c is shape parameter ($c \geq 0$) and α is scale parameter ($\alpha \geq 0$).

2.5.3. Component Life Cycle

Most components in power systems are repairable components. Thus, they follow a component life cycle that shows the time when the component normally operates and the time when the component is out of service. This can be described by three main parameters.

The Mean Time to Failure (MTTF or d) is the average time it takes until the component fails. The Mean Time to Repair (MTTR or r) is the average time or duration it takes to repair the component. The Mean Time Between Failures (MTBF or T) is the average time between two failures occurring in the component. From these three parameters, some other parameters can be derived.

Failure rate is the rate at which the healthy component fails.

$$\lambda = 1/MTTF \quad (2.15)$$

Repair rate is the rate at which the failed component is repaired.

$$\mu = 1/MTTR \quad (2.16)$$

Failure frequency is the average frequency at which the component fails.

$$f = 1/MTBF \quad (2.17)$$

Availability (A) is the probability that at an arbitrary time the component is in a normal and healthy condition.

$$A = \frac{MTTF}{MTBF} = \frac{MTTF}{MTTF + MTTR} = \frac{f}{\lambda} = \frac{\mu}{\lambda + \mu} \quad (2.18)$$

Unavailability (U) is the probability that at an arbitrary time the component is out of service and under repair.

$$U = \frac{MTTR}{MTBF} = \frac{MTTR}{MTTF + MTTR} = f \cdot MTTR$$

$$U = \frac{\lambda}{\lambda + \mu} = 1 - A \quad (2.19)$$

2.5.4. Two State Markov Model

The Markov model is also one method frequently used in reliability analysis for power system components. This model gives an overview of the possible states (or condition) of the component and the possible transitions between these states. In Markov models, two important stochastic parameters are used: the state (S) and time (t). These two parameters can be discrete or continuous. This results in four kinds of Markov models. A Markov model which has discrete states with continuous time is called a Markov process. The Markov models for repairable and unrepairable components are discussed below.

- **Unrepairable Component**

For a single unrepairable component, there are two states: the UP-state (or S_0) and the DOWN-state (or S_1). Each state has its probability, represented by P_{S_0} and P_{S_1} . The Markov model shows the transition from state S_0 to S_1 , which means the process of a component failure. The probability of this transition can be related to the reliability function as the following equation shows,

$$P_{ij}(t, \Delta t) = h_{ij}(t)\Delta t \quad (2.20)$$

In which h_{ij} is the transition rate between states S_i and S_j . The probability that the component is in a specific state is influenced by the probability the system was in the other state, the transition rate from state S_i to S_j and time. For Markov models:

$$p(t + \Delta t) = p(t)T(\Delta t) \quad (2.21)$$

Where p is the state probability vector and T is the transition matrix. If the transition rate is independent of time, the transition rate

becomes the failure rate and the Markov model is called homogeneous. The transition matrix can be described as follows

$$T = \begin{bmatrix} 1 - \lambda & \lambda \\ 0 & 1 \end{bmatrix} \quad (2.22)$$

- **Repairable Component**

As discussed in the previous paragraph, the state transition shows the transition from S_0 to S_1 . For a repairable component, the analysis uses the failure rate λ and repair rate μ . The transition matrix is described as follows.

$$T = \begin{bmatrix} 1 - \lambda & \lambda \\ \mu & 1 - \mu \end{bmatrix} \quad (2.23)$$

Markov models are frequently assumed to be in equilibrium, such that the state probabilities will not change with time or, as can be said, are time-independent.

This means,

$$pT = p \quad (2.24)$$

$$p(T - 1) = 0 \quad (2.25)$$

in which p is the state probability vector.

2.6 RELIABILITY MODELS OF SYSTEMS OF COMPONENTS

After determining the reliability models of each component, the system reliability can be analysed by combining all reliability models of the components. There are several methods for modelling the system reliability:

2.6.1. Series-Parallel Networks (Reliability Networks)

A system consists of components connected to each other, either in series, parallel, or mixed series-parallel. It is also possible that one individual component failure affects another component's performance.

- **Series Connections**

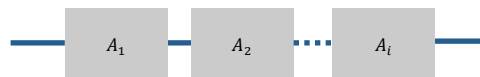


Fig. 2-14 Series Connection

Fig. 2-14 shows the series network, when several components are connected in series. For repairable components, the availability of the connection is

$$A_C = \prod_{i=1}^N A_i \quad (2.26)$$

A_C = Availability of the connection
 N = Number of components in the connection
 A_i = Availability of component i

For unreparable components, the reliability of the connection is

$$R_C(t) = \prod_{i=1}^N R_i(t) \quad (2.27)$$

Where,

R_C = Reliability of the connection
 R_i = Reliability of component i

The failure rate can also be calculated as the sum of all components failure rate.

$$\lambda_C = \sum_{i=1}^N \lambda_i \quad (2.28)$$

Where,

λ_C = Failure rate of the connection
 λ_i = Failure rate of component i

- Parallel Connections

Fig. 2-15 shows the parallel connection, when components are connected in parallel. The availability and the reliability of the connection depend on the number of components required for an available (normal operation) connection.

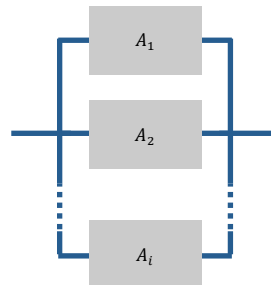


Fig. 2-15 Parallel Connection

- 1-out-of-N

1-out-of-N means that the connection requires at least one available component so that the connection will operate normally. For repairable components, the reliability can be described by the unavailability of the connection, which is:

$$U_C = \prod_{i=1}^N U_i \quad (2.29)$$

U_C = Unavailability of the connection
 N = Number of components in the connection

U_i = Unavailability of component i

- N-out-of-N
N-out-of-N means that all components should be available so the connection can work normally. The series connection can precisely represent this network
- k -out-of-N
 k -out-of-N means that the parallel connection of N components needs at least k components to work normally. For repairable components that have the same availability, the availability of the connection can be calculated as follows.

$$A_C = \sum_{i=k}^N \binom{N}{i} (A_0)^i (1 - A_0)^{N-i} \quad (2.30)$$

For unrepairable components, which have the same reliability, the reliability of the connection can be calculated as follows.

$$R_C(t) = \sum_{i=k}^N \binom{N}{i} R_0^i(t) (1 - R_0(t))^{N-i} \quad (2.31)$$

2.6.2. Monte Carlo

Monte Carlo simulation performs a wide range of applications by generating random values from a certain probability distribution [55]. Two approaches are available: non-sequential and sequential Monte Carlo simulation [56]. Non-sequential Monte Carlo simulation does not consider the time progress and determines a component state based on random samples and the component unavailability. If x is a random sample and the unavailability of n -th component is U_n , then the n -th component is considered to be failed when x is smaller than U_n [12].

In a sequential Monte Carlo simulation, the time progress is considered, enabling analysis by collecting a set of times to failure and times to repair from a specific probability distribution with parameters such as the mean time to failure (MTTF) and mean time to repair (MTTR). The random sampling process produces a time series, which demonstrates the life cycle of components consisting of 'up' states and 'down' states. This is applicable to involve time-behaviour of the system, such as load flow analysis. In addition, it is very practical to analyse a component with many possible failure states and other conditions that are highly complex to deal with in an analytical approach. The weakness of this method is the requirement of a large simulation time to achieve accurate results, which is highly affected by the memory size of the computer.

3 Case Study Description

This chapter describes the case study used in this master thesis. The case study will consider a three-terminal offshore HVDC connection. As the planned HVDC connection between the Netherlands and Denmark is a three-terminal configuration, it is a suitable offshore configuration for this case study. The commercial operation of this offshore HVDC grid will start at the beginning of 2019. Two HVDC converters will be installed at both ends of an HVDC cable, which is a 325 kilometre-long subsea cable below the North Sea. The converter stations, which have a power rating of 700 MW and DC voltage of + 320 kV, are placed at Eemshaven in the Netherlands and Endrup in Denmark. Both converter stations are HVDC Plus VSC in Modular Multilevel Converter (MMC) arrangement [57].

Section 3.1 describes the highest topology, which is the offshore network topology. The subsystems are the onshore converter station in Denmark (DK), the onshore converter station in the Netherlands (NL), the onshore cable part in DK, the onshore cable part in NL, the offshore cable, and the offshore converter station for the offshore wind farm. The converter stations, as subsystems of the network are discussed separately in section 3.2. These are composed of several subsystems such as transformers, converter reactors, converter units, control systems, and DC switchyards, as described before in section 2.2. The DC cable, which connects all three converter-stations involved in the case study, is discussed in 3.3. The data selected for reliability analysis are based on other comparable HVDC systems.

3.1 OFFSHORE GRID TOPOLOGY



Fig. 3-1 Multi terminal HVDC Layout of the Case Study

The topology of the offshore grid is shown in Fig. 3-1. In this case study, there are two onshore converter-stations: the Netherlands and Denmark. The converter station in the Netherlands is connected to the 380 kV transmission network of the Netherlands, while the Denmark converter station is linked to the 400 kV network of Denmark. These two converter-stations are connected to each other by two 325 km DC cables (100 km towards the Netherlands and 225 km towards Denmark). The distance between the offshore converter station and the main cable is 70 km [58]. In the standard offshore topology, there are no switching possibilities at the T-connection. However, for reliability analysis it is interesting to study the effects when there are switching possibilities. Therefore, later in the reliability analysis, it will be assumed that there are DC switches installed at the T-connection in the network.

The simplified layout of Fig. 3-1 is shown in Fig. 3-2.

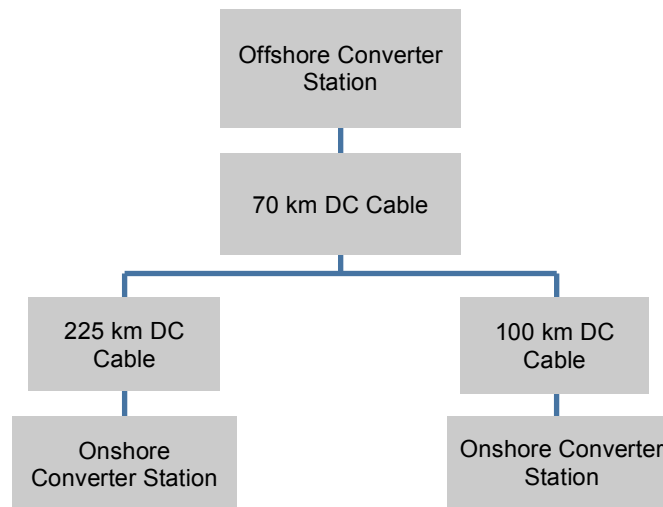


Fig. 3-2 Simplified Case Study Layout

3.2 CONVERTER STATION

One objective of designing an HVDC system, in particular VSC-HVDC transmission systems, is to lower the down-time, especially caused by forced outages [28]. One of the measures to achieve high reliability and availability of an HVDC system is the use of subsystems with a proven high reliability, including the converter station. Thus, selecting the correct requirements for each subsystem in the system is important and can be done when the engineers have determined the desired reliability [29].

The converter stations installed in the network are composed of several subsystems as mentioned in section 2.2: the transformer, converter reactor, converter unit, control system and DC switchyard. For all components, except the converter unit, the failure behaviour can be modelled by negative exponential distributions. Particularly, the failure rate and Mean Time to Repair (MTTR) are the most important reliability parameters, and will be described in section 3.2.1, 3.2.3, 3.2.4, and 3.2.5, respectively. For the converter unit, the Mean Time to Failure (MTTF) will be used instead of the failure rate. The reason is discussed in section 3.2.2.

Choosing the correct input data, based on the DC voltage of the converter station used in the case study, is important to achieve an accurate analysis. The following sections display several reliability parameters from different sources. The sources are listed below:

1. MMC VSC-HVDC from [25]. The reliability parameters listed in this research are based on an industrial report written in [59], several

- academic papers of LCC-HVDC and VSC-HVDC, CIGRE data of VSC-HVDC, older CIGRE data, and an analysis made by the author [25].
2. VSC-HVDC from an industrial report of Stattnet and DNV [59]. The failure statistics from this source will be used specifically for modelling the converter reactor, for which data is only available in this source.
 3. MMC VSC-HVDC from a thesis [48]. The thesis uses CIGRE 2015, SKM 2012, Hodges 2012, ISLES 2012, and Linden 2010 data for analysis of the best, centre, and worst case of reliability scenario.
 4. Offshore VSC-HVDC system from an academic paper [27].
 5. MMC system from an academic paper [29].

In the next sections, all data of each component will be shown and compared based on failure statistics from the sources above. Finally, parameter values will be selected for the further reliability analysis. In the end of this chapter, reliability parameters of all components are listed.

3.2.1. Transformer

The reliability parameters of transformers from several sources are shown in Table 3-1. Because the AC voltage level of the NL and DK nodes is 380 kV and 400 kV respectively, data 1 is chosen as the voltage levels are in the range of the voltage level in source 1. The selection of MTTF from this data is based on the 300-700kV transformer CIGRE data in 1983 and the assumption that the MTTF is higher in more advanced technology nowadays. The MTTR is also picked from the 1983 CIGRE data. The offshore transformer MTTR is a total of normal MTTR (onshore transformer), the time to transport by large vessel, and the time to source spare parts while performing non-invasive tests on offshore platform. The transformer used for analysis in source 3 is new and thus the failure statistic are still unavailable.

Table 3-1 Reliability Parameters of The Transformers

Source	Component	MTTF (Years)	MTTR (Hours)
1	HVDC 41 Onshore Transformer (300-700 kV)	80	1008
	HVDC 41 Offshore Transformer (300-700 kV)	80	1512
2	HVDC 59 Offshore Transformer (132 kV)	225	672
4	Failure Statistic 5 Offshore control system (150 kV)	27	1580

3.2.2. Converter Unit

As mentioned in the beginning of this chapter, the case study utilises MMC-VSC for the converter unit. It consists of six arms, which comprise of a converter reactor and hundreds of power modules in each arm. The six converter reactors are then modelled separately as one component and will be discussed in the next section. The power module contains two half-bridge IGBT cells and a DC capacitor. Thus, the reliability model of a converter unit is based on IGBT cells and a capacitor. Due to the limited information about the converter unit parameters of the case study, data from [29] are used and assumed to be similar to the characteristics of the case study’s converter unit. The converter unit parameters in [29] are selected because the rated DC voltage of the converter unit is identical to that in the case study. All of them are required to perform several calculations in section 4.1, which thereafter are used for the reliability analysis in chapter 5.

Based on [51], the reliability of both onshore and offshore converters are assumed to be similar, thus the IGBT cell reliability parameters are similar for both onshore and offshore converter unit. The number of power modules in each arm depends on the DC and AC voltage across the converter unit and voltage across a sub-module. The calculation is also executed in chapter 4. Redundancy is implemented to improve the availability of the converter unit. The number of redundant power modules is presumed similar to the data of the 320 kV converter unit station in [29].

Table 3-2 lists all parameters of the converter unit that are useful to design the reliability model of the converter unit.

Table 3-2 The Reliability Parameter of The Converter Unit [29]

Symbol	Quantity	Value
S	System Capacity	1000MVA
V_{dc}	Rated DC Voltage	± 320 kV
\hat{V}_o	Peak AC Phase Voltage	320 kV
V_D	Withstanding Voltage of IGBT Module	4.5 kV
η	De-rating Factor of IGBT Module's Voltage	56%
E_{MMC}	Energy Stored in the MMC	30 kJ/MVA
λ_{IGBT}	Failure Rate of the IGBT Module	0.004 failure/year
λ_{CAP}	Failure Rate of the Capacitor	0.000438 failure/year

The MTTRs of a converter unit from all sources are shown in Table 3-3.

Table 3-3 The MTTR of The Converter Unit

Source	Component	MTTR (Hours)
1	Onshore MMC System (300 kV)	12
	Offshore MMC System (300 kV)	60
2	Onshore Converter Unit (300 kV)	24
	Offshore Converter Unit (300 kV)	24
3	Onshore MMC System (320 kV)	3
	Offshore MMC System (320 kV)	3
4	Offshore Converter Unit (150 kV)	4

Because the MMC system has a voltage level of 320 kV and data for exact voltage level is available in source 3, this source is used for reliability parameters in the case study.

3.2.3. Converter Reactor

Due to the limited amount of available data, the reliability parameters of the converter reactor, the MTTF and MTTR, are assumed to be similar to those from source 2, as shown in Table 3-4. The offshore converter reactor MTTF is assumed to be similar to the onshore MTTF and the MTTR is the total of the

normal converter reactor MTTR and the transporting time using a medium vessel, which is analysed in source 1.

Table 3-4 Reliability Parameters of The Converter Reactor

Source	Component	MTTF (Years)	MTTR (Hours)
1	Onshore Converter Reactor	7	24
	Offshore Converter Reactor	7	192

3.2.4. Control System

The MTTF and MTTR of the control system from all sources are shown in Table 3-5. Source 1 is selected because it represents a complete control and protection (C&P) and the voltage level is near to the voltage level used in the case study of this master thesis. According to source 1, the MTTF and the MTTR of the onshore control system are taken from VSC CIGRE in 1983. The offshore control system MTTF is assumed to have the same MTTF. It is also assumed that only 30% of the faults can be solved on-site. Thus, while also assuming that the time required to transport small components is 48 hours, the MTTR can be calculated as the total time to repair a normal control system (onshore control system) and 30% of 48 hours. The voltage level of the control system in source 1 is near to that used in the case study. Moreover, source 3 does not include control systems in the reliability analysis.

The auxiliary system is one of the components, which affect the reliability of the system. Nevertheless this component is not specially modelled in previous studies, thus the reliability parameters are not accessible. The smaller components inside the auxiliary system such as the cooling system of the converter unit and the transformer, when failed, will lead to outages of the main components (converter unit, transformer, etc.). Thus the failure characteristics of the auxiliary system will be included in the main components [48].

Table 3-5 Reliability Parameters of Control System

Source	Component	MTTF (Years)	MTTR (Hours)
1	Onshore Control System (300 kV)	1.6	3
	Offshore Control System (300 kV)	1.6	17
2	Onshore Control System (300 kV)	1	9
3	Offshore Control System (300 kV)	1	9
4	Offshore control system (150 kV)	11	6.05

3.2.5. DC Switchyards

The reliability parameters of DC switchyards are shown in Table 3-6. Data from source 1 is selected instead of source 3 because source 3 only involves the DC circuit breaker, while the DC circuit breaker is only one of the components inside a DC switchyard, of which the data is available in source 1. Besides, source 1 uses data of a 2007-2008 World HVDC survey containing LCC-HVDC back-to-back scheme. This data is used because the DC switchyard in LCC and in VSC HVDC is significantly similar. A back-to-back scheme is selected because it does not need additional components such as a DC filter. This component is still used in

several HVDC systems such as that in source 2. However, in this case study, with the most updated MMC technology, the HVDC system does not require a DC filter anymore. Thus it is sufficient to use this data. The differences between MTTR of onshore DC switchyards and offshore DC switchyards are due to additional time of transport for 80% part using helicopter and for 20% part using small vessels. This analysis is stated in [25].

Table 3-6 Reliability Parameters of DC Switchyard

Source	Source	MTTF (Years)	MTTR (Hours)
1	Onshore DC Switchyard (300 kV)	4.02	26.06
	Offshore DC Switchyards (300 kV)	4.02	98.06
2	DC Circuit Breaker (300 kV)	1.6	17
3	DC Circuit Breaker (320 kV)	12.5	3
4	DC Equipment (150 kV)	11	6.05

3.3 DC CABLE

The DC cable is one of the components of the offshore network. It is included in the reliability analysis of the connection, thus its failure rate and the MTTR data are required. The failure rate is the data available for this component, instead of the MTTF. The chosen reliability parameter is from source 3, as the voltage level used is similar with that in this case study. As shown in Table 3-7, all sources use the same MTTR, which is 1440 hours except the data from source 2. In source 2, the MTTR is the total time of fixed delay, which is 1440 hours and the repair time, which is 120 hours. These data is the best case of reliability parameter as a result of industrial expert analysis from trustworthy reliability data of HVDC.

Table 3-7 Reliability Parameters of The DC Cables

Source	Source	Failure Rate (Years/100km)	MTTR (Hours)
1	DC Cables (300 kV)	0.07	1440
2	DC Cables (300 kV)	0.05	1440
3	DC Cables (320 kV)	0.02	1560
4	DC Cables (150 kV)	0.0706	1440

As stated in section 3.1, there are three DC cables needed for this case study: the NL DC cable (100 km), the DK DC cable (225 km), and the offshore DC cable (70 km). Table 3-8 shows the reliability parameter of all DC cables utilised in the case study.

Table 3-8 Reliability Parameters of The DC Cables used in The Case Study

Components	MTTF (Years)	MTTR (Hours)
DC Cables - NL	50.1717033	1560
DC Cables - DK	22.2985348	1560
DC Cables - offshore	71.67386185	1560

3.4 CONCLUSIONS

After selecting the best data for further reliability analysis, it is helpful to summarise the reliability parameters of all components for the onshore and offshore subsystems (i.e. the converter stations + DC cables), which are shown in Table 3-9 and Table 3-10 respectively. The reliability parameters of components both in the NL onshore node and the DK onshore node are assumed to be similar. It should be clear that the converter unit reliability parameters will be discussed in chapter 4.

Table 3-9 Reliability Parameters of all Components in the Onshore Subsystem

Components	MTTF (Years)	MTTR (Hours)
Control System	1.6	3
Transformer	95	1008
Converter Reactor	7	24
DC Switchyard	4.02	26.06
DC Cables - NL	50.1717033	1560
DC Cables - DK	22.2985348	1560

Table 3-10 Reliability Parameters of all Components in the Offshore Subsystem

Components	MTTF (Years)	MTTR (Hours)
Control System	1.6	17
Transformer	95	1512
Converter Reactor	7	192
DC Switchyard	4.02	98.06
DC Cables - offshore	71.67386185	1560

4 Modelling

From the case study described in chapter 3, the focus of this thesis now shifts to the reliability modelling of each component. It involves all subsystems, from the converter unit to the cables that connect the offshore and onshore nodes in the grid. After modelling the reliability of the subsystems, the reliability model of the complete offshore grid can be developed. The physical connection of all components might be different from that in the reliability model. For instance, it is possible that two components connected in parallel are modelled in reliability analysis as a series connection if those two components are not redundant to each other (i.e. both are needed for successful operation). Therefore, understanding the interaction among the components is very important for modelling the system reliability.

In this chapter, the reliability model of the complete HVDC system is developed in three steps. Section 4.1 discusses the reliability of the converter unit as a subsystem. It describes both the topology and reliability indices from low to high level. The reliability model of the converter station is discussed in section 4.2. Section 4.3 describes the reliability model of a point-to-point configuration. It includes the onshore nodes in Denmark and in the Netherlands with DC cables connecting the onshore nodes as a point-to-point HVDC system. Section 4.4 shows the model of the three-terminal offshore grid. The reliability of the complete three-terminal grid with the offshore node is modelled in this section, comprising several possible failure scenarios.

The reliability modelling is performed using two approaches: an analytical and Monte Carlo simulation. The analytical approach will be used for several kinds of analysis in this chapter. Monte Carlo simulation will be used to model the reliability of all subsystems inside the converter station and the higher level (i.e. the converter station, point-to-point topology and three-terminal topology), which will be described more detail in section 4.5.

The general conclusions will be drawn in section 4.6

4.1 RELIABILITY MODEL OF A CONVERTER UNIT

In this section, the reliability model of the MMC is created. The modelling is started with a single IGBT cell as the lowest-level analysis and continued to a converter unit as the highest-level analysis. All levels will be modelled using an analytical approach in section 4.1.1 until 4.1.3. The output of the model will be the reliability parameter of the converter unit, which will be useful for the next analysis together with the other subsystems inside the converter station.

For convenience, the topology of a MMC system is re-shown in Fig. 4-1.

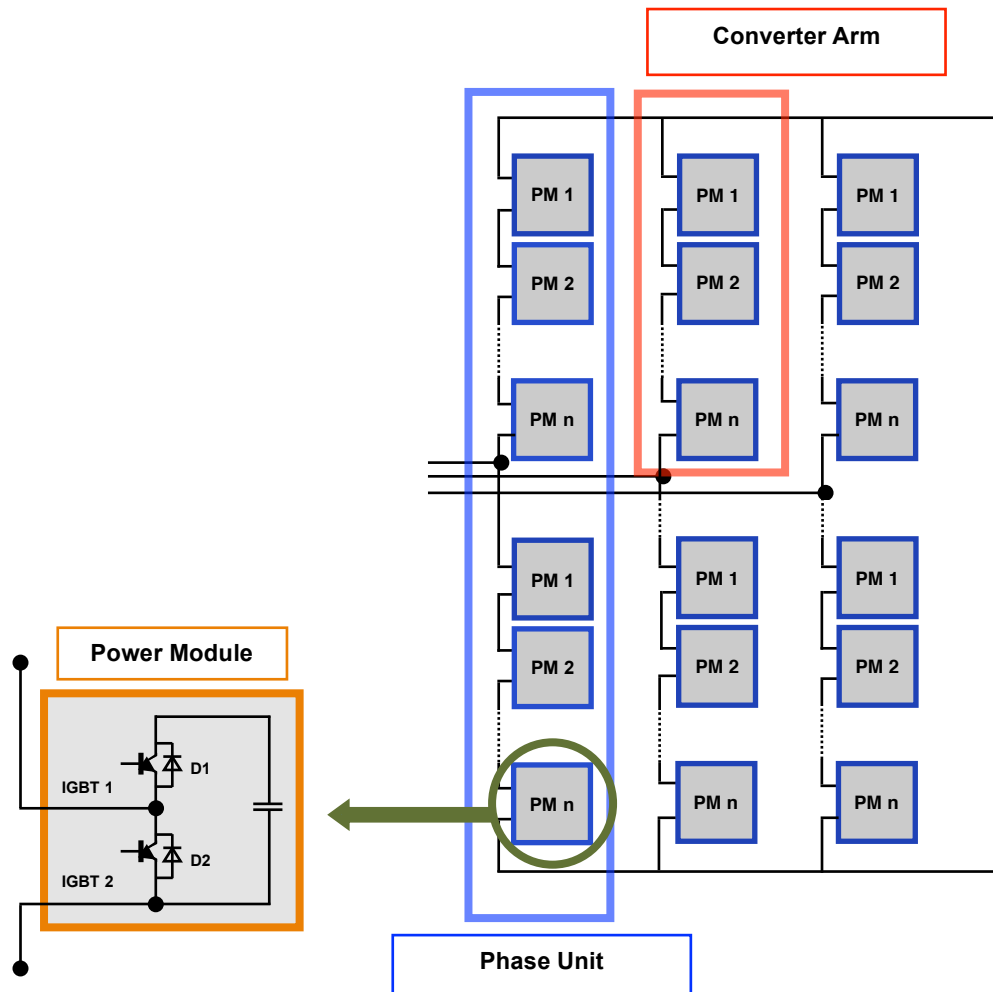


Fig. 4-1 MMC System Topology of the Case Study

4.1.1. IGBT to Power Modules

A power module consists of an IGBT half-bridge and a capacitor [15]. It requires two IGBTs to work perfectly, thus the reliability model is a series block diagram of two IGBTs and a capacitor, as shown in Fig. 4-2. The failure rate of the power module can be considered as a combination of the failure rates of IGBTs and the capacitor [28].



Fig. 4-2 Reliability Model of The Power Module

Thus, according to Eq. 2.27 and Eq. 2.28, the failure rate of the power module is the sum of the failure rates of the IGBTs and a capacitor, while the reliability function is the product of the reliability of the IGBTs and the capacitor. By assuming that all IGBTs have the same reliability, the reliability of the sub-modules can be calculated by Eq. 4.1 and Eq. 4.2.

$$\lambda_{PM} = \lambda_{IGBT1} + \lambda_{IGBT2} + \lambda_{CAP} \quad (4.1)$$

$$R_{PM}(t) = R_{IGBT1}(t) \times R_{IGBT2}(t) \times R_{CAP}(t) \quad (4.2)$$

Also, the reliability of a power module can be defined by equation 4.3.

$$R_{PM}(t) = e^{-\lambda_{PM}t} \quad (4.3)$$

Where,

λ_{PM}	= Failure rate of the power module
λ_{IGBT1}	= Failure rate of the 1 st IGBT
λ_{IGBT2}	= Failure rate of the 2 nd IGBT
λ_{CAP}	= Failure rate of the capacitor
R_{PM}	= Reliability of the power module
R_{CAP}	= Reliability of the capacitor

The next level, which will be discussed in the next section, is a number of power modules assembled to build a converter arm.

4.1.2. Power Modules to Converter Arm

The converter arm normally operates when k (254) out of n (258) power modules work. The reliability model is shown in Fig. 4-3.

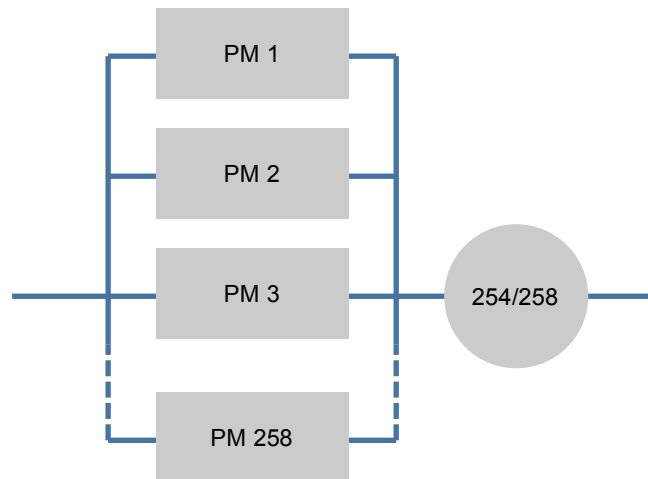


Fig. 4-3 Reliability Model of The Converter Arm

The reliability of a converter arm can be calculated by equation 4.4.

$$R_A(t) = \sum_{i=k}^n \binom{n}{i} R_{PM}(t)^i (1 - R_{PM}(t))^{n-i} \quad (4.4)$$

Where R_A is the reliability of a converter arm.

After that, several converter arms assembling the converter unit will be modelled in the next section.

4.1.3. Converter Arms to Converter Unit

One phase unit consists of two converter arms: a positive arm and a negative arm, which must both be available. The reliability model of the phase unit can be defined as follows:

$$R_{1C}(t) = R_{A+}(t) \times R_{A-}(t) \quad (4.5)$$

Where R_{1C} is the reliability of a phase unit, R_{A+} is the reliability of the positive-polarity-converter arm, and R_{A-} is the reliability of the negative-polarity-converter arm.

The three-phase converter unit reliability R_{3C} can be defined as the product of reliability of three phase units, as mentioned by Eq. 4.6.

$$R_{3C}(t) = R_C^3(t) \quad (4.6)$$

The reliability model of the whole converter is a series connection of the six converter arms. It is shown in Fig. 4-4. It is assumed that each converter arm has similar characteristics.

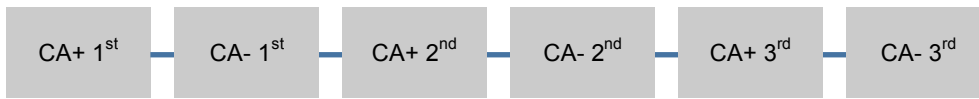


Fig. 4-4 Reliability Model of The Converter Unit

Where,
 CA+ 1st = Positive-polarity 1st phase Converter Arm
 CA - 1st = Negative-polarity 1st phase Converter Arm
 CA+ 2nd = Positive-polarity 2nd phase Converter Arm
 CA - 2nd = Negative-polarity 2nd phase Converter Arm
 CA+ 3rd = Positive-polarity 3rd phase Converter Arm
 CA- 3rd = Negative-polarity 3rd phase Converter Arm

Because redundancy is included in the reliability analysis of the converter unit, the converter unit cannot be modelled by a negative exponential distribution, which has a constant hazard rate (i.e. the failure rate). The best-fit distribution will be discussed based on the results in the next chapter.

However, the expected time to failure of the converter unit can be calculated, as shown in equation 4.7.

$$TTF_{3C} = \int_0^{+\infty} R_{3C}(t) dt \quad (4.7)$$

Next, section 4.2 describes the reliability model of the other subsystems of the converter station and the whole converter station as a subsystem.

4.2 RELIABILITY MODEL OF THE CONVERTER STATION

This section firstly describes the reliability model of the subsystems inside the converter station. One of the subsystems, which is the converter unit, has been discussed in the previous section. After that, the reliability model of the whole converter station will be created. The reliability model of the subsystems inside the converter station and the converter station itself are performed using both the analytical approach and Monte Carlo Simulation. However, this section will only show the model of the analytical approach, while the model of Monte Carlo simulation will be separately shown in chapter 4.5.

A converter station consists of several components, as it was mentioned in section 2.2. For convenience, the configuration of a converter station is re-shown in Fig. 4-5.

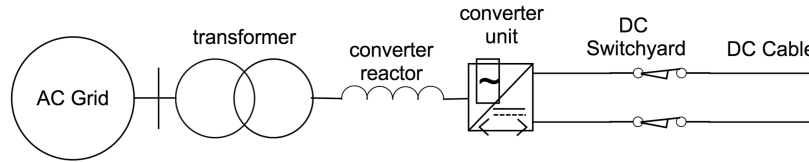


Fig. 4-5 Converter Station Scheme

For this case study, the subsystems considered for the reliability model of the converter station are the AC filter, AC circuit breaker, transformer, converter unit, control system and DC filter. It is assumed that both offshore and onshore converter stations have the same components, yet different reliability parameter, as mentioned before in section 3.2.

All subsystems are first modelled by their availability and unavailability in an analytical approach. Based on 2.18 and 2.19, the availability and the unavailability of each subsystem within the converter station can be found using the equations below.

$$A_{SS} = \frac{MTTF_{SS}}{MTTF_{SS} + MTTR_{SS}} \quad (4.8)$$

$$U_{SS} = 1 - A_{SS} \quad (4.9)$$

Where

- A_{SS} = Availability of the subsystem
- U_{SS} = Unavailability of the subsystem
- $MTTF_{SS}$ = Mean Time to Failure of the subsystem
- $MTTR_{SS}$ = Mean Time to Repair of the subsystem

The data of MTTF and MTTR of each subsystem can be found in section 3.2.

After obtaining all availability and unavailability of the subsystems, the reliability model of the converter station as a subsystem can be performed.

Fig. 4-6 illustrates the reliability model of a converter station.

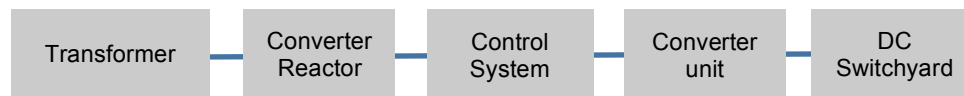


Fig. 4-6 Reliability Model of a Converter Station

All components are in series because all subsystems are needed for successful operation. The availability and unavailability of all types of converter stations in this case study can be calculated as follows.

$$A_{CS} = A_T \times A_{CR} \times A_C \times A_{CS} \times A_{DCS} \quad (4.10)$$

$$U_{CS} = 1 - A_{CS} \quad (4.11)$$

where

- A_T = Availability of the Transformer
- A_{CR} = Availability of the Converter Reactor
- A_C = Availability of the Converter unit

A_{CS} = Availability of the Control System

A_{DCS} = Availability of the DC Switchyard

From the unavailability calculation using Eq. 4.10 and Eq. 4.11, several analyses can be performed. One of them is the calculation of the outage duration. The outage duration during one-year operation is the product of the unavailability and the amount of hours per year. It is explicitly expressed in Eq. 4.12. This expression can be used to get the outage duration of each subsystem inside the converter station and the converter station itself.

$$\text{Outage_Duration_ss} = (1 - A_{SS}) \cdot 8760 \text{ hours/year} \quad (4.12)$$

Where,

Outage_Duration_ss = The total duration when a subsystems of the HVDC system is in the down state

The time between failures of each subsystem can be achieved by executing Monte Carlo simulation. Basically, the Mean Time Between Failures (MTBF) is the sum of the average duration a subsystem is in the 'up' state and in 'down state', as stated in Eq. 4.13. With Monte Carlo simulation, each range of time between failures and the number of its occurrence will be generated to give more insight about the characteristic of the subsystems within the HVDC system.

$$\text{MTBF} = \text{MTTF} + \text{MTTR} \quad (4.13)$$

Where,

MTBF = Mean Time Between Failures

MTTF = Mean Time to Failures

MTTR = Mean Time to Repair

The inverse of MTBF is the failure frequency f , which is the frequency of the subsystems having a cycle of 'up' and 'down' state per year. This will also be obtained from Monte Carlo simulation.

$$f = \frac{1}{\text{MTBF}} = \frac{1}{\text{MTTF} + \text{MTTR}} \quad (4.14)$$

Where,

f = Failure frequency

After possessing the data of all subsystems reliability models, the next level reliability model can be created, which is the reliability model of the complete HVDC system. The next section will demonstrate the reliability model of a point-to-point HVDC system.

4.3 RELIABILITY MODEL OF A POINT-TO-POINT HVDC CONNECTION

This section describes the reliability model of a two-terminal HVDC connection. As explained in the beginning of this chapter, it consists of the NL converter station, the DK converter station and the DC subsea cables connecting the onshore converter stations. All subsystems must be available for successful operation of the system, thus it is modelled as a series connection of three subsystems, which is shown in Fig. 4-7.



Fig. 4-7 Reliability Model of a Point-to-Point Connection

The reliability parameters of the cables were defined in section 3.3 and shown in Table 3-9 and Table 3-10. Since the reliability parameters of the DC cable are failure rates, a conversion should be done first by Eq. 4.15. After that, the availability and the unavailability of the DC cables can be calculated using 4.8 and 4.9.

$$MTTF = 1/\lambda \quad (4.15)$$

The availability and unavailability of the point-to-point HVDC system can be calculated by Eq. 4.16 and Eq. 4.17, respectively. It is a multiplication of three subsystems based on Fig. 4-7.

$$A_{PTP} = A_{CS_NL} \times A_C \times A_{CS_DK} \quad (4.16)$$

$$U_{PTP} = 1 - A_{PTP} \quad (4.17)$$

A_{PTP}	= Availability of a two-terminal connection
U_{PTP}	= Unavailability of a two-terminal connection
A_{CS_NL}	= Availability of the NL onshore node
A_C	= Availability of the cables connecting the DK onshore node and the NL onshore node
A_{CS_DK}	= Availability of the DK onshore node

Another reliability indicator of the point-to-point connection is the amount of energy not transmitted. The calculation of the amount of energy not transmitted utilises a load flow scenario, which contains the hourly load flows for the year 2020. This load flow scenario also contains load flow data for a possible interconnection between the Netherlands and Denmark. Using the total transmitted energy in a year ($E_{total-PTP}$), the expected amount of not transmitted energy can be calculated using Eq. 4.18 below.

$$E_{nottransmitted-PTP} = U_{PTP} \cdot E_{total-PTP} \quad (4.18)$$

Where,

$E_{nottransmitted-PTP}$	= The total energy not transmitted per year in point-to-point topology
$E_{total-PTP}$	= The total energy transmitted per year in a 100% reliable point-to-point topology

The next reliability indicator is the outage duration, which is derived from the unavailability of the point-to-point HVDC system. It can be calculated by multiplying the unavailability by the number of hours in a year, which is 8760, as shown in Eq. 4.19.

$$\text{Outage_Duration_PTP} = U_{\text{PTP}} \cdot 8760 \text{ hours/year} \quad (4.19)$$

Where,

Outage_Duration_PTP = The total duration when the point-to-point HVDC system is in the down state

The range of time between failures and the failure frequency of the point-to-point connection will be determined by Monte Carlo simulation using the theory stated in Eq. 4.13 and Eq. 4.14.

4.4 RELIABILITY MODEL OF THE THREE-TERMINAL CONNECTION WITH OFFSHORE NODE

In this section, the reliability analysis of the three-terminal connection, including an offshore node, is performed. In this analysis, three subsystems are considered to simplify the model and the calculation:

1. The NL Onshore Node, consisting of the NL converter station and 100 km DC Cables
2. The DK Onshore Node, consisting of the DK converter station and 225 km DC Cables
3. The Offshore Node, consisting of the offshore converter station and 70 km DC Cables

The reliability analysis includes the study of the subsystem availability and the study of several failures scenarios, which can occur in this configuration. It should be noted that the offshore wind park connected to the offshore node is assumed to work perfectly.

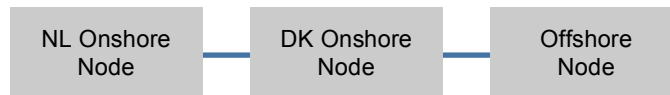


Fig. 4-8 Reliability Model of a Three-Terminal Connection (without Switching Possibility)

First, it is assumed that no circuit breakers are installed at the T-connection in the offshore grid, i.e. there are no switching possibilities in the system. Then the offshore grid is either available or unavailable. The reliability model is built with consideration that all subsystems must be available in the system and modelled as a series connection, as shown in Fig. 4-8. Thus, the availability of the offshore grid can be calculated by multiplying the availability of all subsystems, as can be seen in Eq. 4.20. The unavailability can be obtained using Eq. 4.21.

$$A_{\text{TT}} = A_{\text{CS-off}} \times A_{\text{C-OFF}} \times A_{\text{C-NL}} \times A_{\text{CS-ON}} \times A_{\text{C-DK}} \times A_{\text{CS-ON}} \quad (4.20)$$

$$U_{\text{TT}} = 1 - A_{\text{TT}} \quad (4.21)$$

Where,

A_{TT} = Availability of the three-terminal grid

U_{TT} = Unavailability of the three-terminal grid

$A_{\text{CS-off}}$ = Availability of the offshore converter station

$A_{\text{C-OFF}}$ = Availability of the offshore cable

$A_{\text{C-NL}}$ = Availability of the cable connected to the Netherlands onshore node

A_{CS-ON} = Availability of the onshore node

A_{C-DK} = Availability of the cable connected to Denmark onshore node

The outage duration due to failures in the three-terminal HVDC system will be also analysed using Eq. 4.22.

$$\text{Outage_Duration_TT} = U_{TT} \cdot 8760 \text{ hours/year} \quad (4.22)$$

Where,

Outage_Duration_TT = The total duration when the point-to-point HVDC system is in the down state

Similar with the previous analysis, the range of time between failures, the number of the occurrence of each time between failures, and the failure frequency will be determined in a Monte Carlo simulation.

Second, switching possibilities are applied in the three-terminal HVDC system. Since there are three subsystems within the three-terminal configuration, there will be $2^3 = 8$ possible system states, as shown in Table 4-1. In the table, the working subsystems are denoted as '1' and the failed subsystems are marked by '0'. Failure state 1 occurs when all subsystems are available. Failure states 2, 3, 4 are the states in which one of the subsystems suffers from failure, thus is unavailable. These states still enable the system to transmit the energy, yet can still cause either energy loss or energy excess in the system. The rest of the failure states lead to a complete system failure.

Table 4-1 Failure State Probability of a Three Terminal Topology with Switching Possibility

Failure State	Subsystem Status (1=working, 0=out)			Probability
	NL Node	DK Node	Off Node	
1	1	1	1	$P_1 = A_{NL} \times A_{DK} \times A_{OFF}$
2	0	1	1	$P_2 = U_{NL} \times A_{DK} \times A_{OFF}$
3	1	0	1	$P_3 = A_{NL} \times U_{DK} \times A_{OFF}$
4	1	1	0	$P_4 = A_{NL} \times A_{DK} \times U_{OFF}$
5	0	0	1	$P_5 = U_{NL} \times U_{DK} \times A_{OFF}$
6	0	1	0	$P_6 = U_{NL} \times A_{DK} \times U_{OFF}$
7	1	0	0	$P_7 = A_{NL} \times U_{DK} \times U_{OFF}$
8	0	0	0	$P_8 = U_{NL} \times U_{DK} \times U_{OFF}$

The probability of a failure state is the product of the availability of the working subsystems and the unavailability of failed subsystems. The sum of the probabilities of all failure states should be 1. To gain more clear insight, several failure states are briefly explained. Taking failure state 1 as an example, all subsystems are available, thus the probability of this state is the product of the three subsystems' availabilities. In failure state 2, since the NL onshore node is out of work, the probability is the product of the unavailability of the NL onshore node and the availabilities of the DK onshore node and the offshore node.

This probability can be used to calculate the duration of the failure states per year.

$$\text{Outage_Duration_TT_sn} = P_n \cdot 8760 \text{ hours/year} \quad (4.23)$$

Where,

Outage_Duration_TT_sn = The duration when the three-terminal HVDC system with switching possibilities is in failure state n

P_n = The probability of failure state n

Next, the failure states 2, 3, and 4 can be used to calculate other reliability indices. The estimated energy not transmitted due to these failure states will be beneficial to understand how much energy loss or energy excess per year results from failures. During failure state n , the unavailable subsystems will receive and supply zero energy. Only the available subsystems export and import the energy. This causes (theoretical) excess or lack of energy in the HVDC system, which is used as a reliability indicator in this study. The energy transmitted stated in Eq. 4.24 is the sum of the export and import energy in each subsystem.

$$E_{\text{nottransmitted-year-TT}} = E_{\text{transmitted-hour-TT}} \times 8760 \text{ hour/year} \times P_n \quad (4.24)$$

Where,

$E_{\text{nottransmitted-year-TT}}$ (GWh/year) = The total energy not transmitted per year in the three-terminal topology

$E_{\text{transmitted-TT}}$ (GWh/year) = The total energy transmitted per year of the three-terminal topology

All reliability models have created now. The next chapter will demonstrate the results of the reliability analysis described in this chapter.

4.5 MONTE CARLO SIMULATION

In the Monte Carlo simulation, random numbers of Times To Failure (TTF) and Times To Repair (TTR) of each subsystem inside the converter station are generated using the negative exponential distribution. The inputs parameters of the simulation are the MTTF and MTTR of each subsystem, the annual load flow scenario, and the desired number of TTF/TTR samples, which is chosen to be 1200 in this study. Actually, more samples simulation sample leads to more accurate results. However, due to the limited memory size of MATLAB and the used computer, in which the simulation is undertaken, 1200 is the maximum. The 1200 samples of TTF and TTR are then combined to 1200 Time Between Failures (TBF), which can be found by 4.13. After that, the 'up' state and 'down' state of Time series of 'up' and 'down' states for components 1 to N is formed. The shortest total life (i.e. sum of the up states and down states) of all subsystems inside the converter station is the simulation time of the Monte Carlo simulation, which is approximately 1500 years. This means, the same year (2020) is analysed 1500 times with a resolution of one hour. All the life state data longer than the total simulation time will be neglected for convenience of the analysis, so every subsystem has the same length of life cycle but, obviously, different TTFs and TTRs.

The lifetime cycle of the converter station is the product of all the subsystems life data. It should be noted that there are three converter stations: NL, DK, and offshore. The lifetime of the point to-point and the three-terminal topology are also obtained using the same approach. An example lifetime cycle of the point-to-point connection is shown in Fig. 4-9. The first result will be the availability of all subsystems, including the subsystems within the converter station and the converter

station itself. The availability is the ratio of the number of 'up' state to the total simulation time. The unavailability of the analysed subsystems and systems is simply achieved by Eq. 2.19.

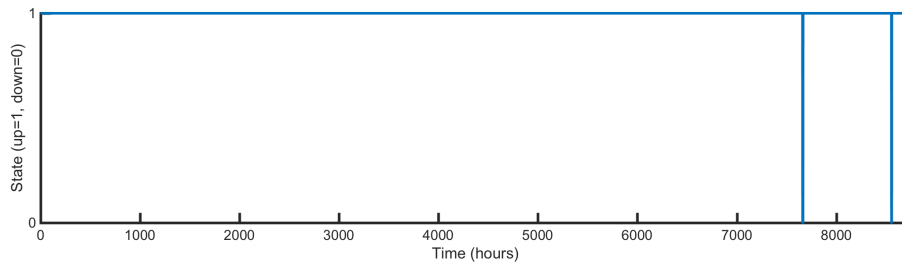


Fig. 4-9 Lifetime Cycle of the Point-to-Point Connection in a Year

Similar to the analysis using the analytical method, the unavailability of all analysed subsystems and systems is used for the calculation of the outage duration. The energy not transmitted can be determined using the lifetime cycle, which was described previously. The energy transmitted in the point-to-point connection is the product of the load flow scenario (which is firstly adapted to the simulation time) and the lifetime cycle of the point-to-point connection. The energy not transmitted is simply the subtraction of the load flow scenario and the energy transmitted. The workflow of the Monte Carlo simulation is shown in Fig. 4-10.

In addition, extra analyses can be done only by executing Monte Carlo simulation. The number of occurrence of the failure states in the whole lifetime cycle counted and divided by the simulation time in years (approximately 1500 year) results in the failure frequency of any system failure (S2-S8). The average duration per interruption can also be calculated by the average of time to repair within the lifetime cycle. The range of time between failures is the clustering of time between failures. The range of 0-3 months, 3-6 months, 6-12 months, and 1-2 years are selected for analysis.

Since the result of the Monte Carlo simulation will slightly vary, the Monte Carlo Simulation is performed a hundred times to determine a the normal distribution. The normal distribution is found to be applicable to fit data for which the precise distribution is still unidentified [60]. In this way, the 95% confidence interval can be determined for the Monte Carlo simulation results.

All the codes for Monte Carlo simulation and the sampling of the result can be found in the Appendix B and Appendix C.

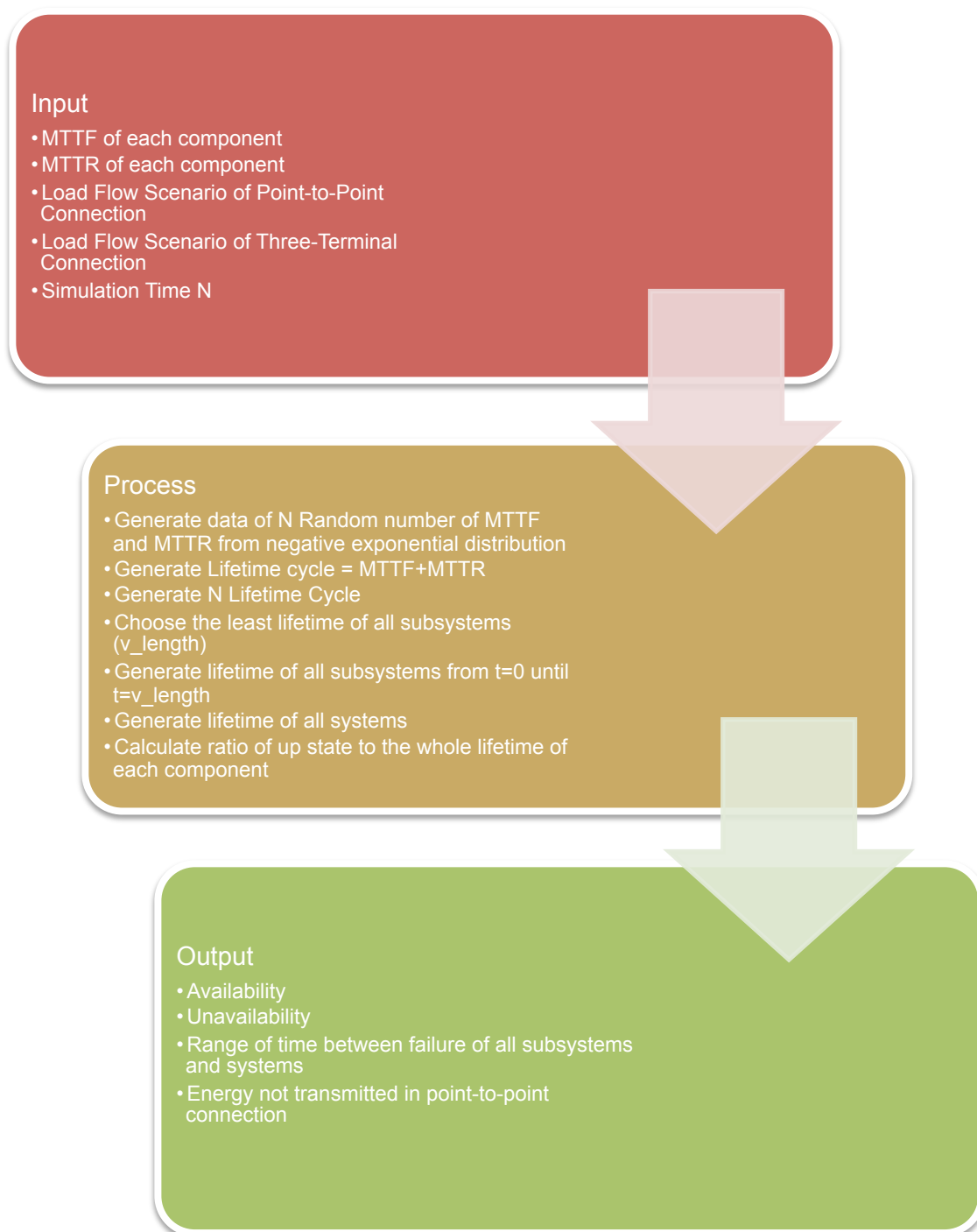


Fig. 4-10 Workflow of the Monte Carlo Simulation

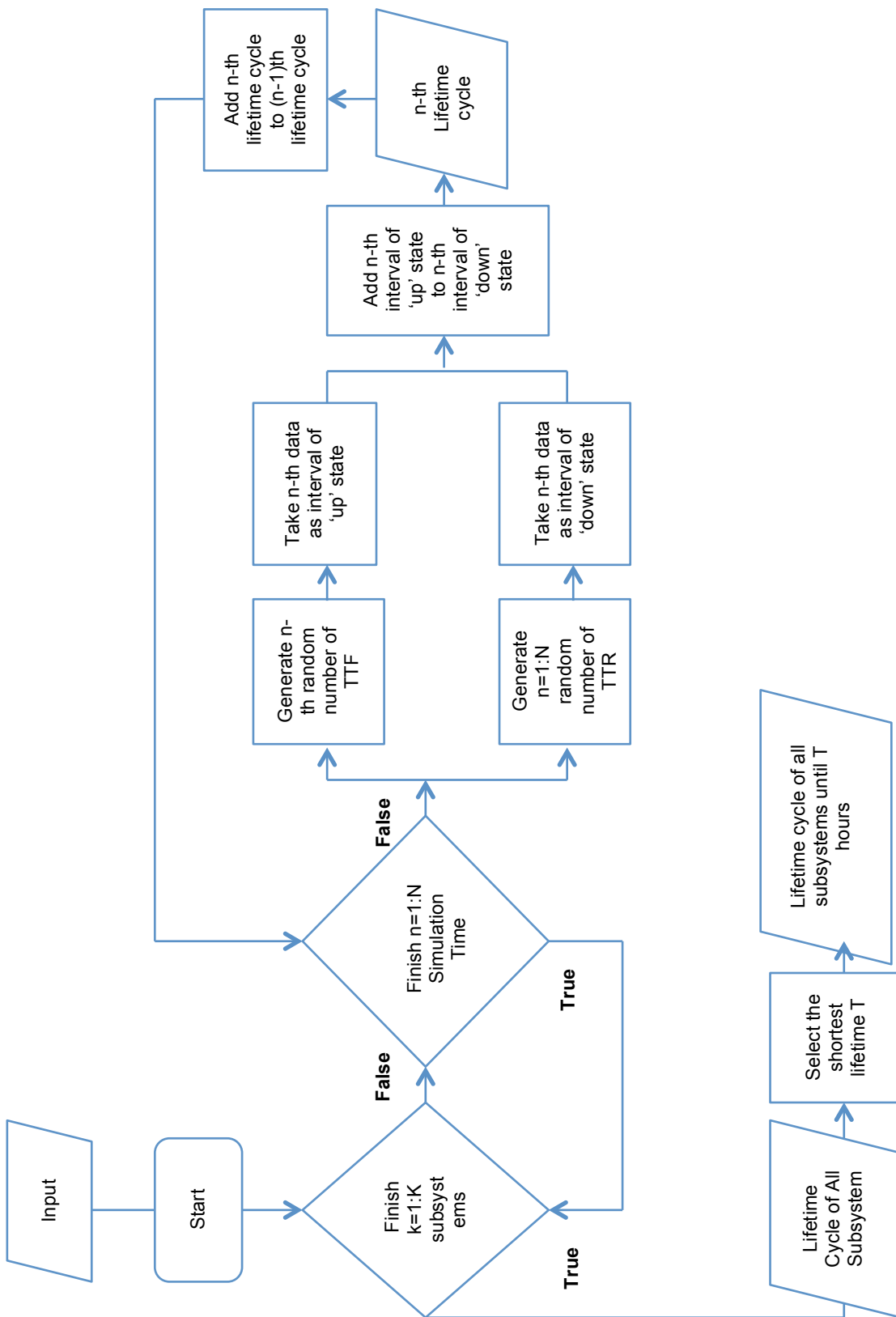


Fig. 4-11 Algorithm of the Monte Carlo Simulation (a)

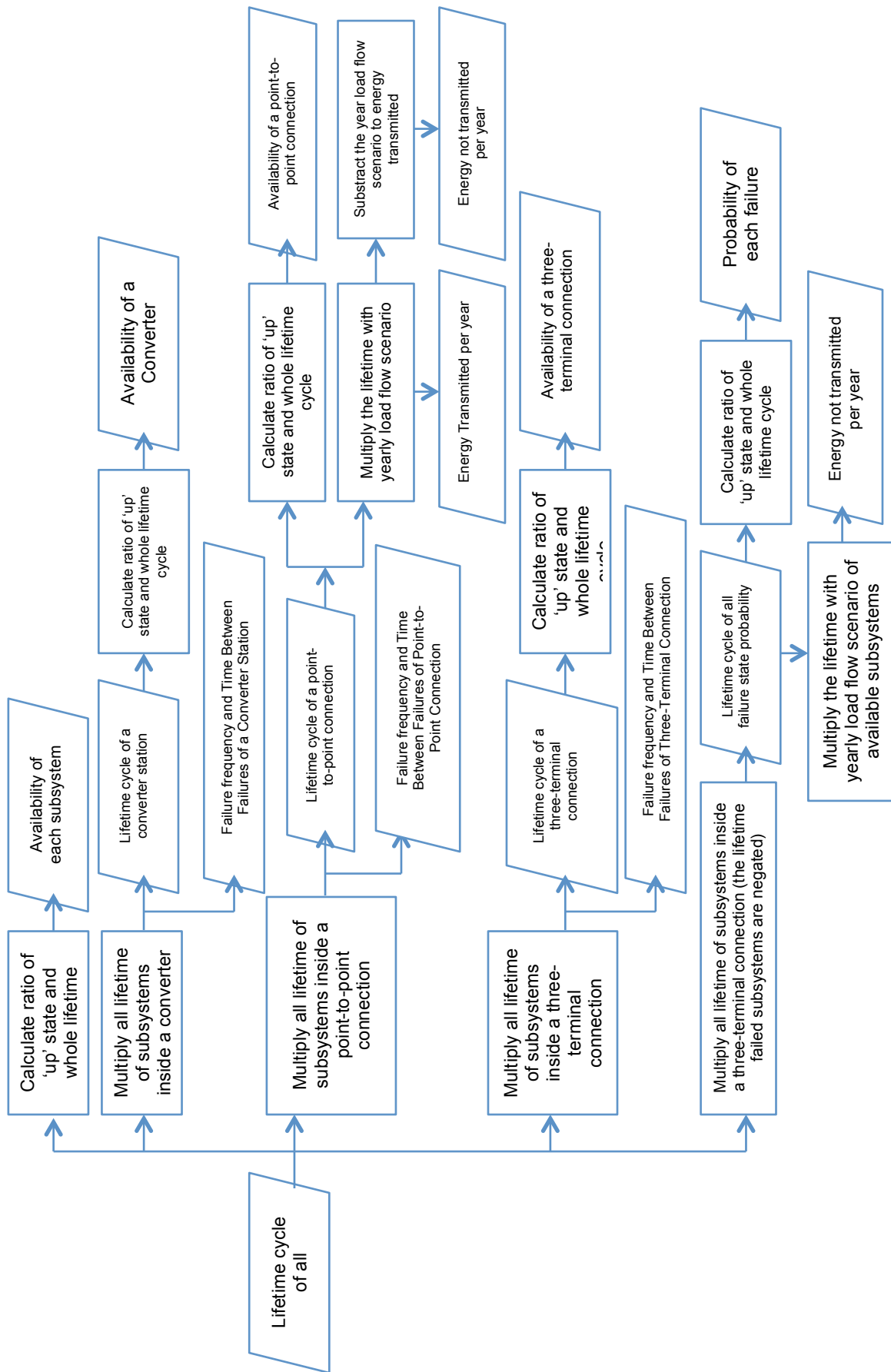


Fig. 4-12 Algorithm of the Monte Carlo Simulation (b)

4.6 CONCLUSION

This chapter discussed the reliability modelling of the components and subsystems inside the HVDC system based on the case study of this master thesis. The first model was the reliability model of the converter unit, which was shown in section 4.1. It includes hundreds of power modules, which consist of two IGBTs and a capacitor. Power module redundancy is also involved in this master thesis, based on a reference. Afterwards, the other subsystems inside the converter station were also modelled in section 4.2 and the availability, unavailability, and the outage duration were calculated. Two approaches are used in this research: an analytical approach and Monte Carlo simulation. The Monte Carlo simulation, which is utilised for modelling the reliability of the converter station and also the system was particularly discussed in section 4.5. The reliability model of all the subsystems, the converter station as a subsystem were modelled in terms of reliability in section 4.2. Similarly to the subsystems assembling the converter station, for the converter station itself the availability, unavailability, and the outage duration were determined. Other additional reliability indicators for the converter stations are the time between failures, the failure frequency, and the average duration per interruption. Next, two HVDC topologies were modelled: a point-to-point topology and a three-terminal configuration. The reliability indicators of these systems are similar to that of the converter station, yet the energy not transmitted through the system is determined using a load flow scenario for one year.

5 Results

In this chapter, the results of the probabilistic reliability analysis of the subsystems, the point-to-point HVDC system and the three-terminal HVDC system are discussed based on the modelling described in chapter 4. In section 5.1, the reliability analysis of the converter is discussed. The reliability analysis of the other components assembling the converter station is described in section 5.2. The analysis of the complete point-to-point connection is described in section 5.3. Finally, section 5.4 discusses the reliability analysis of the offshore converter station and the three-terminal HVDC system. General conclusions are then drawn in section 5.5

5.1 PROBABILISTIC RELIABILITY ANALYSIS OF A CONVERTER UNIT

As mentioned before in section 4.1, the lowest level model, which is the power module, consists of two IGBT cells and a capacitor. The failure rate of the power modules can be calculated using Eq.4.1. The next level model, the converter arm, contains 254 power modules with 4 redundancies and one converter reactor. However, as stated in section 3.2.2, the converter reactor is modelled as one single component outside the converter unit. The reliability of the power module can be represented by its reliability function, applying Eq.4.4. From the reliability function, the hazard rate can be calculated, which is illustrated in Fig. 5-1.

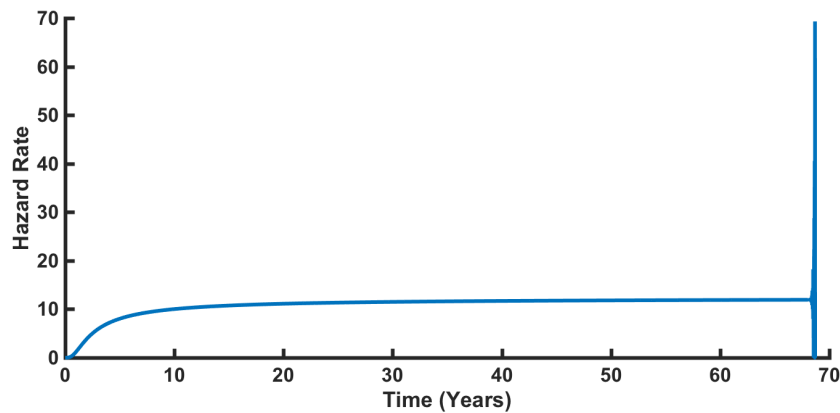


Fig. 5-1 Hazard Rate of the Converter unit

It can be seen from the figure that the hazard rate increases in the first years, stays constant afterwards and then becomes unstable after about 68 years. This occurs because after that time, the reliability function approaches zero and consequently, based on Eq.5.1, the natural logarithm will approach (minus) infinity. This causes instability when calculating the hazard rate at about 68 years for the figure.

$$h_{3c}(t) = -\frac{1}{R_{3c}(t)} \frac{d \ln[R_{3c}(t)]}{dt} \quad (5.1)$$

Where,

$R_{3c}(t)$ = Reliability of the three phase converter unit

$h_{3c}(t)$ = Hazard rate of the three phase converter unit

Another observation is the reliability function, which is shown in Fig. 5-2. Compared to the reliability function of the converter unit without any redundancy, which can be seen in Fig. 5-3 (modelled by the negative exponential distribution), it shows a different curve characteristic. Therefore, the negative exponential distribution cannot be applied in this model. However, the expected Time to Failure (TTF) can be calculated by taking the integral of the reliability function (Eq. 4.7). This result will be used for further analysis in the analytical approach.

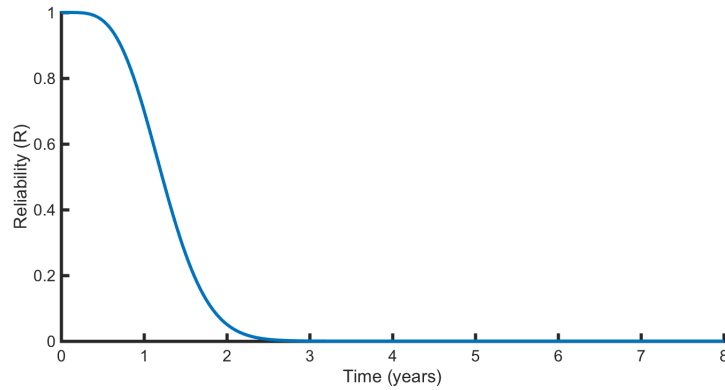


Fig. 5-2 Reliability Curve of The Converter unit with Four Redundant Power Modules

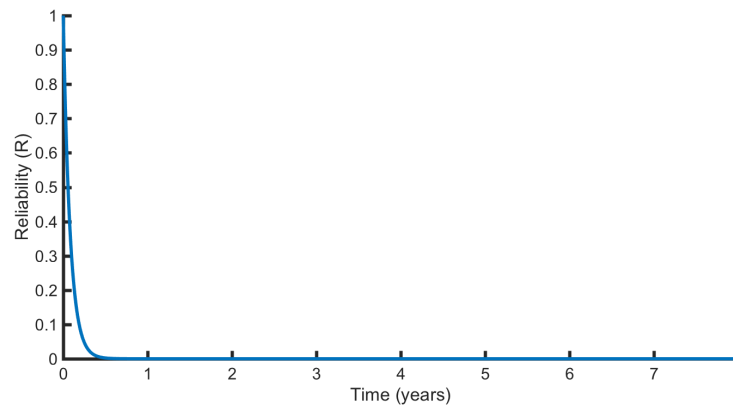


Fig. 5-3 Reliability Curve of The Converter unit without Redundancy.

One converter unit consists of two polarities and three phases. In other words, there are six converter arms installed in the converter unit. Table 5-1 shows a list of failure rates and MTTFs of the subsystem.

Table 5-1 List of Reliability Indices of Components inside Converter unit

Reliability Indices	Value
Failure Rate - DC capacitor (/year)	8.7600e-6
Failure Rate - Sub-module (/year)	8.0088e-3
TTF - Converter Arm (year)	2.4388
TTF – Converter unit (year)	1.2508

The Mean Time to Repair (MTTR) of the converter unit, defined here as the installation time to replace the failed component, was listed in section 3.2.2 as 3 hours. The data of converter unit MTTR is taken from [48].

In the analytical approach, all components will be modelled by negative exponential distributions. Hence, a negative exponential distribution is fit to the

converter unit reliability by using curve fitting tool in MATLAB. The result is shown in Fig. 5-4.

$$R(t) = e^{-\lambda t} \quad (5.2)$$

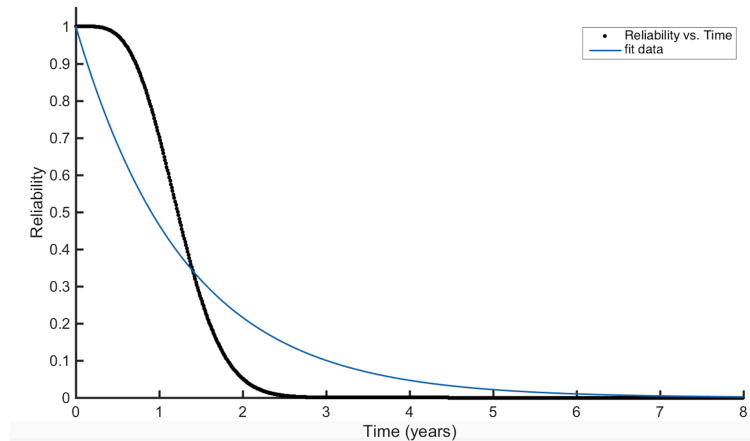


Fig. 5-4 Fitted Converter unit Reliability using General Negative Exponential Distribution

From the result, it can be seen that the negative exponential distribution is not appropriate to model the reliability of the converter unit very well. Thus, another curve fitting is performed. The Weibull distribution described by Eq. 5.3 is now fit to the model, of which the result is shown in Fig. 5-5. (The blue line) The Weibull distribution is a well-known model to fit curves that have non-constant hazard rates.

$$R(t) = e^{-\left(\frac{t}{b}\right)^c} \quad (5.3)$$

Where,

b = Scale parameter

c = Shape parameter

The curve fitting in MATLAB shows that the value of b is **1.384** (lower limit = 1.382, upper limit = 1.385, 95% confidence level) and the value of c is **3.212** (lower limit = 3.197, upper limit = 3.226, 95% confidence level). The values of b and c are then used for further analysis using Monte Carlo simulation. This means that in the Monte Carlo simulation, TTFs are sampled from the Weibull distribution with parameters b and c .

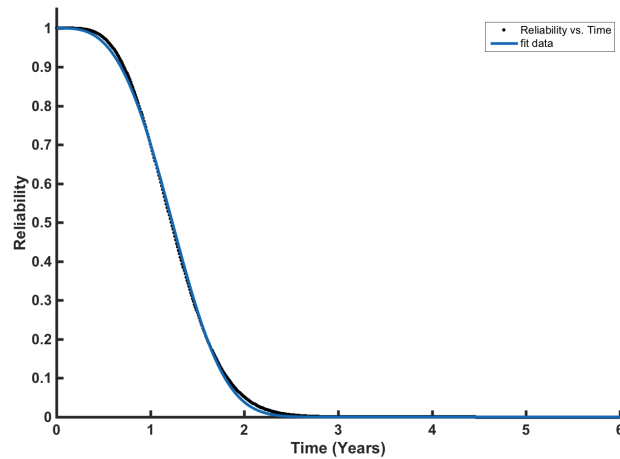


Fig. 5-5 Fitted Converter unit Reliability using Eq. 5.3

The MTTR of the converter unit for Monte Carlo simulation analysis is similar to that used in the analytical approach. The next analysis of the converter unit will be discussed in the next section.

5.2 PROBABILISTIC RELIABILITY ANALYSIS OF A CONVERTER STATION

The results of the reliability analysis of the two converter stations are described in this section. Section 5.2.1 discusses the results of the analysis of the onshore converter stations in the Netherlands and Denmark. The offshore converter station reliability analysis results are discussed in section 5.2.2.

5.2.1. Onshore Converter Stations

In this section, the reliability analysis of all the components in the onshore converter station is performed. The availability of all the components and the HVDC systems, which will be discussed in the next section, are calculated using two methods: an analytical approach and Monte Carlo simulation. The calculation of the unavailability by the analytical approach uses the equations described in Eq. 2.18 and 2.19. In the Monte Carlo simulation, random numbers of all components are generated using the reliability parameters of the components. A more accurate result can be achieved by a longer simulation time. The simulation time is about 1500 (simulated) years, considering the memory size in MATLAB and the used computer. Next, the availability of each component is calculated. In the Monte Carlo simulation, this process is performed 100 times to find a (normal) distribution of the Monte Carlo simulation results. After that the 95% confidence intervals can be determined for the Monte Carlo simulation results.

Table 5-2 Reliability Parameters of all Subsystems in the Onshore Subsystem

Subsystems	MTTF (Years)	MTTR (Hours)
Control System	1.6	3
Onshore Transformer	95	1008
Converter unit	1.2508	3
Converter Reactor	7	24
DC Switchyard	4.02	26.06

All reliability parameters of the components in the NL and DK converter stations are reshown in Table 5-2. It is assumed that all subsystems in the NL converter station and DK converter station are identical. In addition, it should be noted that the converter unit reliability parameters in Table 5-2 are used only in the analytical approach. All reliability analysis results of components in NL onshore and in the DK onshore nodes are shown in Table 5-3. From the table, it can be seen that there are differences between the results from the analytical approach and the Monte Carlo simulation. For all components that have a relatively small MTTR, the unavailability obtained from the analytical method is outside the confidence limit. On the other hand, the unavailability of the transformer from the analytical approach is within the confidence bounds. This is because for such rare events, in which the probability of failure is extremely large or small, the simulation time required is extremely large to find a single failure in the data [61, 62]. Thus, a longer simulation time is needed, so a more precise and accurate result for the components with a smaller MTTF can be achieved. The different result of the unavailability of the converter unit is due to the different approach to get the value of MTTF. The analytical method uses the first model, in which the MTTF of 1.2508 assumed that it could be directly modelled by a negative exponential distribution. Meanwhile, the computer simulation uses the Weibull distribution, which is considered to be a better fit than the negative exponential. However, as can be seen from the tables, the differences in all the subsystem results are relatively small, thus the Monte Carlo simulation is sufficiently representative to model the reliability of the components.

Table 5-3 Unavailability of Subsystems in the Onshore Converter Station

Subsystems	Analytical	Monte Carlo		
		Average	Lower Limit	Upper Limit
Control System	0.0215%	0.0227%	0.0224%	0.0229%
Onshore Transformer	0.1440%	0.1463%	0.1377%	0.1548%
Converter unit	0.0274%	0.0288%	0.0286%	0.0290%
Converter Reactor	0.0392%	0.0402%	0.0395%	0.0410%
DC Switchyard	0.0742%	0.0727%	0.0717%	0.0736%

Next, it is interesting to compare the unavailability of the subsystems. Fig. 5-6 shows a pie chart of the analytical approach results, while Fig. 5-7 shows a pie chart of the Monte Carlo simulation results. From the figures, it can be seen that the transformer has the highest unavailability of all the components in the onshore converter station. This is because the transformer has the highest MTTR of all components' MTTRs.

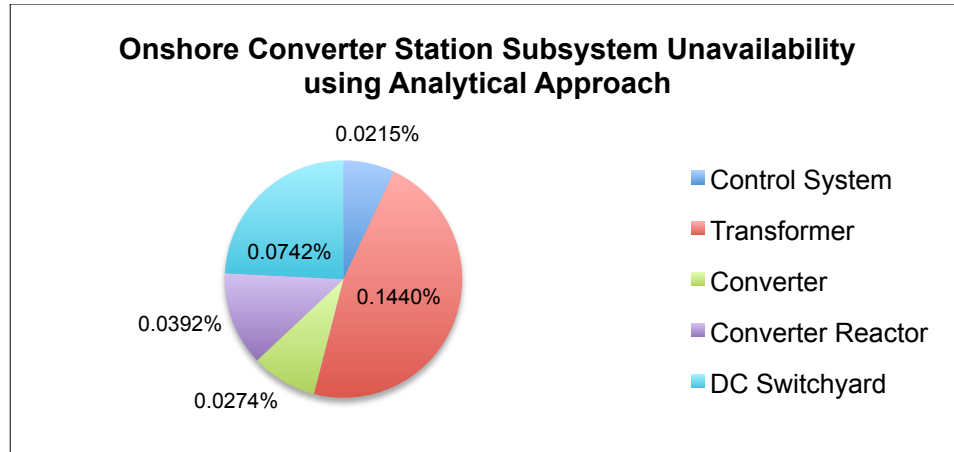


Fig. 5-6 Pie Chart of The Onshore Converter Station Components Unavailability based on Table 5-3 using the Analytical Approach

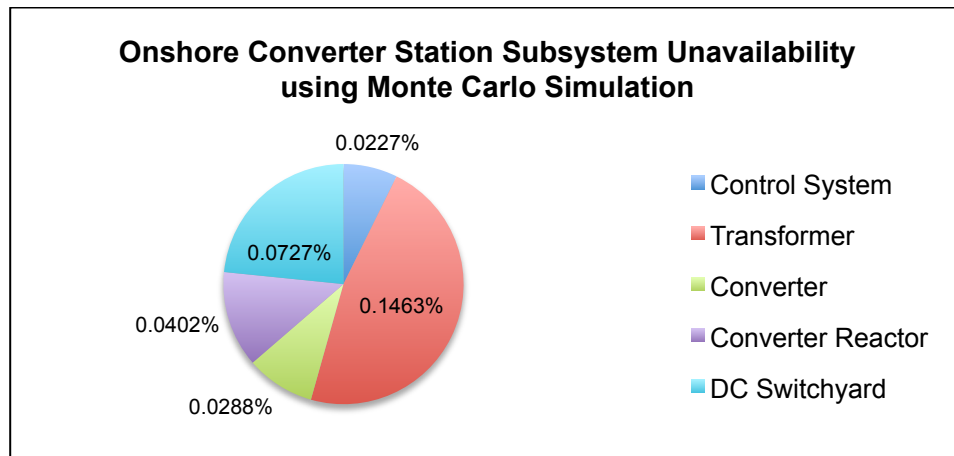


Fig. 5-7 Pie Chart of The Onshore Converter Station Components Unavailability based on Table 5-3 using Monte Carlo Simulation

Table 5-4 Outage Duration of the Subsystems in NL and DK Onshore Converter Station

Components	Duration based on Analytical Approach (Hours/year)	Duration based on Monte Carlo Simulation (Hours/year)	
		NL	DK
Control System	1.9	2.0	2.0
Onshore Transformer	12.6	12.8	13.1
Converter unit	2.4	2.5	2.5
Converter Reactor	3.4	3.5	3.4
DC Switchyard	6.5	6.4	6.5

The annual outage duration can provide more insight than the unavailability. Table 5-4 shows the outage duration for one year (i.e. 8760 hours) for the results found with the analytical method and Monte Carlo simulation. It can also be seen that the difference of the results between the two methods is less than an hour. From the table, it is known that in both approaches, the outage duration of the onshore transformer is the longest compared to the other subsystems. The second longest outage duration is the DC switchyard. This is reasonable because the onshore transformer has the longest time to repair.

Subsystems such as the control system, converter unit, and converter reactor have relatively short times to repair, thus have the shortest outage duration.

5.2.2. Offshore Converter Station

The method to perform reliability analysis on all subsystems inside the offshore converter is similar to that used for the onshore converter stations. The reliability parameters of the components in the offshore converter station are shown in Table 5-5. The results are subsystems availabilities together with the lower and upper limit using 95% confidence interval, as shown in Table 5-6. From the table, similarly to the analysis of the onshore converter stations, the availability of the converter unit achieved by the analytical method is slightly different from that obtained by Monte Carlo simulation due to the different models used in the calculation. However, the result of converter reactor in the offshore converter station is now within the confidence bound. This can be explained by the fact that the highest increase of MTTR of the subsystems is the converter reactor.

Table 5-5 Reliability Parameters of all Subsystems in the Offshore Node

Subsystems	MTTF (Years)	MTTR (Hours)
Control System	1.6	17
Transformer	95	1512
Converter unit	1.2508	3
Converter Reactor	7	192
DC Switchyard	4.02	98.06

Table 5-6 Unavailability of Subsystems in the Offshore Node

Components	Analytical	Monte Carlo		
	Unavailability	Average	Lower Limit	Upper Limit
Control System	0.1215%	0.1214%	0.1202%	0.1226%
Transformer	0.2159%	0.2174%	0.2025%	0.2323%
Converter Unit	0.0274%	0.0289%	0.0287%	0.0290%
Converter Reactor	0.3130%	0.3138%	0.3066%	0.3210%
DC Switchyard	0.2784%	0.2807%	0.2766%	0.2848%

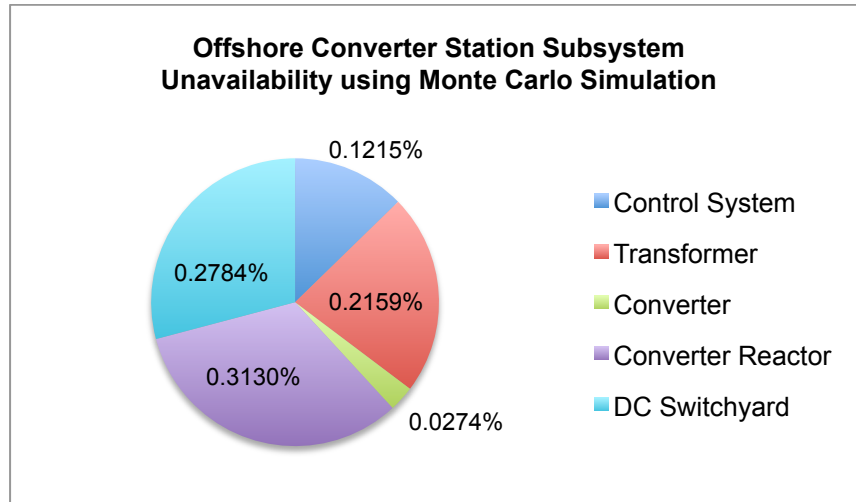


Fig. 5-8 Pie Chart of the Offshore Converter Station Components Unavailability based on Monte Carlo Simulation

To illustrate the results more clearly, a pie chart of the unavailability obtained by the analytical approach and the Monte Carlo simulation are shown in **Error! Reference source not found.** and Fig. 5-8 respectively. From the figures, it can be seen that the converter reactor and the DC switchyard have the highest unavailability of all components.

Table 5-7 Outage Duration of the Components in the Offshore Node

Components	Offshore Node Duration (hours) in 1 year = 8760 hours	
	Analytical	Monte Carlo
Control System	10.6	10.6
Transformer	18.9	19.0
Converter unit	2.4	2.5
Converter Reactor	27.4	27.5
DC Switchyard	24.4	24.6

The annual outage duration of the subsystems in the converter station can be calculated and is shown in Table 5-7. From the table, it can be seen that the converter reactor has the longest outage duration. This is due to the short time to fail and relatively long time to repair. The second longest outage duration is the DC switchyard, which has a short time to fail and a long time to repair as well. From the table, it can also be seen that the results from the analytical method and the Monte Carlo simulation have insignificant difference so the model built in the computer simulation is considered suitable for reliability analysis.

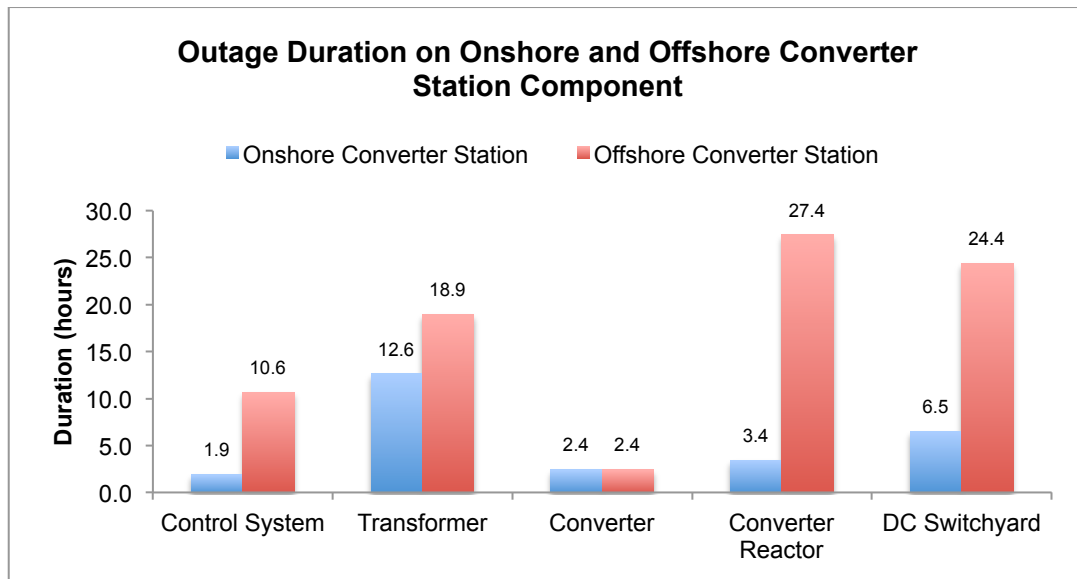


Fig. 5-9 The outage Duration of the Onshore and Offshore Converter Stations

It is interesting to compare the outage duration between the onshore and the offshore converter station. The bar graph, which shows the comparison of those two converter stations, is shown in Fig. 5-9. From the figure, it is known that the converter unit has the same outage duration because it is assumed that the MTTF and the MTTR in both the onshore and offshore converter station are identical. Other subsystems of the offshore converter station have longer outage duration than those in the onshore converter station due to longer repair times. All the components except the converter unit require additional time to transport the spare parts. From these results, it can be concluded that the outage duration of the offshore converter station will be higher than that of the onshore converter station.

5.3 PROBABILISTIC RELIABILITY ANALYSIS OF A POINT-TO-POINT HVDC SYSTEM

As mentioned in section 4.3, the point-to-point connection consists of two onshore nodes, i.e. the NL onshore node and the DK onshore node, and the cables connecting these nodes. In this section, the point-to-point connection reliability analysis is performed using the results of the previous converter station analysis. The point-to-point connection reliability analysis can be performed by the analytical method using Eq. 4.16. Monte Carlo simulation, which has been described in section 5.2 is also executed to verify the results. The reliability analysis of the converter station in the NL onshore node and the DK onshore node, the 325 km DC cables and the point-to-point connection are shown in Table 5-8. It can be seen from the table that all results from the analytical method calculation are within the confidence intervals of the Monte Carlo simulation.

Table 5-8 Unavailability of Subsystems in the Point-to-Point Connection

Components	Analytical	Monte Carlo		
	Unavailability	Average	Lower Limit	Upper Limit
NL Converter Station	0.3060%	0.3103%	0.3016%	0.3190%
DK Converter Station	0.3060%	0.3136%	0.3036%	0.3236%
DC Cables	1.1463%	1.1447%	1.1024%	1.1869%
Point-to-point	1.7503%	1.7596%	1.7263%	1.7928%

The other reliability analysis of the point-to-point connections includes the calculation of the amount of energy not transmitted affected by the failure probability of the network. For this analysis, the load flow scenarios of several examples of existing HVDC systems and an onshore AC connection are used. These existing connections are assumed to be a point-to-point topologies, similar to the case study in this work. The capacity of all connections has been scaled down to the capacity of the case study, which is 700 MW. The result can be obtained by calculation using Eq. 4.18 and is shown in Table 5-9 and Fig. 5-10. The energy not transmitted of the case study is listed as load flow scenario number one. From the table, similar to the analysis above, the energy not transmitted of the four example load flow scenarios calculated by the analytical method is slightly different from the Monte Carlo simulation result, yet still within the range of the confidence limits. Comparing all load flow scenarios, it can be seen that scenario 4 has the lowest energy not transmitted, while scenario 3 has the largest value. This significant difference is due to the different power flow, which is briefly discussed in the next paragraph.

Scenario 1 has 700 MW installed capacity, yet the maximum power transferred is 600 MW, with the longest time transferring the maximum is only 28 hours. Most of the time, the transferred power directly goes down to zero. In addition, there are durations of 40 hours that the system transmits no power. Scenario 2 has a maximum power transferred of 1400 MW before scaling down. Comparing to scenario 1, the power transmitted in scenario 2 fluctuates to 500 MW as well and often transfers over 1400 MW. Thus, the estimated energy not transmitted in scenario 2 is higher than that for scenario 1. In scenario 3, the transmitted power per day fluctuates between 200 MW and 600 MW after scaling down and rarely, zero power is transmitted, only 16 hours is the maximum duration that the power transmitted is constantly zero. Lastly, in scenario 4, the maximum power before scaling down, which is 2800 MW is transferred for only one hour. Even though the power transferred is rarely zero, the amount of energy transmitted per day fluctuates around less than 500 MW, which is significantly lower than its maximum power. Consequently, it has the lowest energy transmitted, thus the lowest estimated energy not transmitted of all HVDC systems. It can therefore be concluded that the amount of not-transmitted energy strongly depends on the load flow scenario of the HVDC connection.

Table 5-9 Expected amount of Energy not Transmitted in the Point-to-Point Connection

Load Flow Scenario	Energy Transmitted (GWh/year)	Analytical (GWh/year)	Monte Carlo (GWh/year)		
			Average	Lower Limit	Upper Limit
1	1853.14	32.44	32.65	32.04	33.27
2	2306.91	40.38	40.65	39.88	41.41
3	4270.75	74.75	75.21	73.79	76.63
4	1371.04	24.00	24.10	23.63	24.58

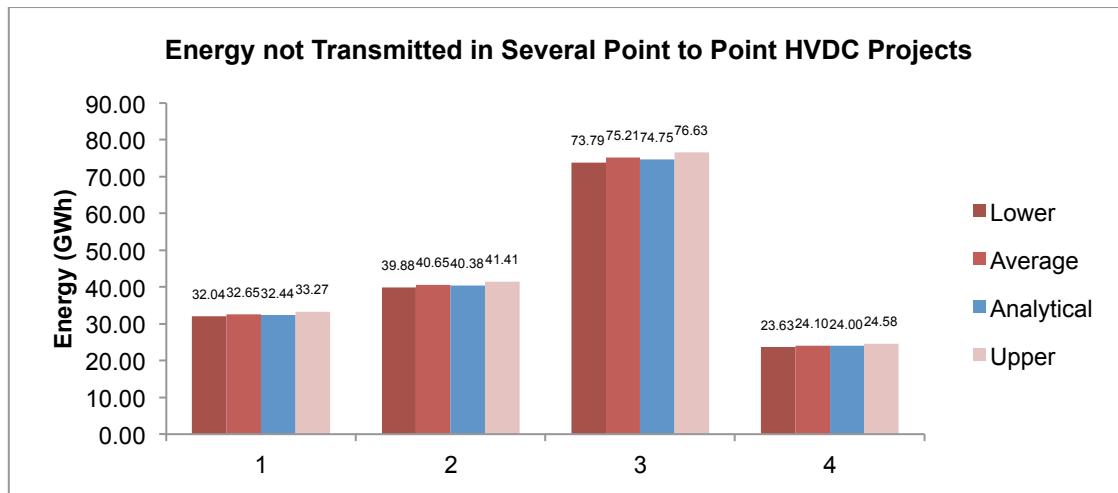


Fig. 5-10 Graph of The Expected not-Transmitted Energy of a Point-to-Point Connection

Other reliability indicators of the point-to-point system that have been calculated in this master thesis are the failure frequency, the average duration per interruption, and the outage duration. The analysis will be shown together with that in the next section, which describes the three-terminal topology.

5.4 PROBABILISTIC RELIABILITY ANALYSIS OF THE THREE-TERMINAL HVDC SYSTEM

In this section the probabilistic reliability analysis of the three-terminal HVDC system is discussed. The three-terminal connection consists of a two-terminal connection, which the reliability analysis was discussed in the previous section, and one offshore converter station with cable to connect it to the two-terminal connection. The system will form a T-connection (re-shown in Fig. 5-11) for which arise two situations are considered: with and without switching possibilities at the T-connection. According to section 4.4, to simplify the analysis, three subsystems are made: the NL node, the DK node, and the offshore node.



Fig. 5-11 Multi-terminal HVDC Layout

5.4.1. Without Switching Possibilities

For the three-terminal configuration, the analysis without switching possibilities means that the failure of at least one subsystem (either the NL, DK or offshore node) will cause a complete failure of the three-terminal HVDC system. The first analysis is the calculation of the unavailability of the three-terminal system, of which the availability can be calculated using Eq. 4.20. The result of the analysis without switching possibility is shown in Table 5-10. In the table, the results of the two approaches (analytical and Monte Carlo Simulation) are shown. The unavailability of the converter stations (NL, DK, and offshore), DC cables of the point-to-point topology and the DC cables of the connection of the offshore converter station towards the point-to-point connection are shown in the table. It can be seen that the unavailability of the offshore converter station is three times larger than that of the onshore converter station. In addition, the results of the analytical approach and the Monte Carlo simulation are sufficiently similar. The small difference is acceptable as the results of the analytical approach of all subsystems are within the lower and upper limits of the 95% confident intervals.

Table 5-10 Unavailability of The Subsystems in Offshore Converter Station

Subsystems/Systems	Analytical	Monte Carlo		
	Unavailability	Average	Lower Limit	Upper Limit
NL Converter Station	0.3060%	0.3103%	0.3016%	0.3190%
DK Converter Station	0.3060%	0.3136%	0.3036%	0.3236%
DC Cables – Point to Point	1.1463%	1.1447%	1.1024%	1.1869%
Offshore Converter Station	0.9528%	0.9587%	0.9412%	0.9762%
DC Cables - Offshore	0.2485%	0.2543%	0.2370%	0.2715%
Three Terminal	2.9283%	2.9497%	2.9088%	2.9907%

In the three-terminal configuration without switching probabilities, there are two system states: the 'up' state P_1 , in which the system is working; and the 'down' state P_2 , in which the system is out of service. The probability of each state is shown in Table 5-11.

Table 5-11 Probability and Duration of Subsystem Failure by the Analytical Method

Subsystems/Systems	Probability
P_1	97.0717%
P_2	2.9283%

Next, from the Monte Carlo simulation, the average duration per interruption of the NL, DK, onshore nodes, the offshore node, the point-to-point and three-terminal configuration is determined and shown in Table 5-12. Another analysis from the Monte Carlo Simulation is the calculation of the failure frequency of the subsystems and the complete system, as can be seen in the same table. From the results, it is known that the cables connecting the NL and DK onshore nodes and offshore nodes to the point-to-point topology have a small impact on the average duration per interruption because the point-to-point system failure frequency is equal to the sum of the NL converter station and the DK converter station. Meanwhile, the outage duration can also be obtained by multiplying the unavailability of the subsystem and the system by 8760 hours/year. All the results are shown in Table 5-12. In the table, the unavailability used for the calculation is the unavailability from the analytical approach. This is taken to check whether the Monte Carlo simulation can verify and represent the analytical model. It can be seen from the table that it gives slightly different results, but less than one hour difference. It can be seen that most of the Monte Carlo simulation results are slightly higher values than in the analytical approach. More accurate results cannot be obtained due to the memory size of MATLAB and the used computer.

Table 5-12 Other Analysis Results from Monte Carlo Simulation

Subsystem / System	Failure Frequency (/year)	Average Duration per Interruption (Hours/year)
NL	1.83	14.8
DK	1.83	14.9
Offshore	1.82	45.9
Point to Point	3.67	41.8
Three Terminal	5.42	47.4

Table 5-13 The Outage Duration of the Case Study Subsystems and System

Subsystem	Outage Duration (hours/year)	
	Analytical Approach	Monte Carlo Simulation
NL	26.80	27.18
DK	26.80	27.47
Offshore	83.47	83.98
Point to Point	153.32	154.14
Three Terminal	256.52	258.40

From the Monte Carlo simulation, the time between failures can also be observed in this case. The variation of the time between failures of the three subsystems, two-terminal connection and three-terminal connection are calculated and 50 years lifetime is taken as an example to give more clear insight. The result is shown in Fig. 5-12. From the figures, it is shown that all the total number of failures in each subsystem/system is near to the failure frequency per year multiplied by 50 years despite of small differences. This means that the Monte Carlo simulation with the simulation time given for the reliability model is sufficient enough for further analysis. Next, the onshore converter station, both NL and DK have the same failure frequency as that in the offshore converter station, as shown in Table 5-12. This is acceptable since

$$f = \frac{1}{MTTF + MTTR} \quad (5.4)$$

The MTTR of the subsystems in the converter station are all small thus can be neglected in $f = \frac{1}{MTTF}$. Based on the reliability parameters of the subsystems inside the converter station shown in Table 3-9 and Table 3-10, the MTTF of all subsystems in both the onshore and offshore converter station are all the same, thus the failure frequency of the NL, DK, and offshore converter station should be nearly similar. The slight difference between the onshore converter station and the offshore converter station might be due to the higher MTTR of the subsystem in the offshore converter station, thus a decrease of the failure frequency. The highest number of time between interruptions is in the interval of 0-3 months, which also occurs in the system analysis (point-to-point and three-terminal configuration). The converter reactor, which has the least time between failures in all converter stations, should be taken into account for the improvement of system. The data can be applied so that one should be aware that there is higher possibility of failure occurrence in the next 0-3 months after interruptions due to small MTTF such as converter units and control systems. The result is also useful to describe how frequent the failure is occurred so that if higher time between failures is required, several improvements such as improving the quantity of the maintenance can be done.

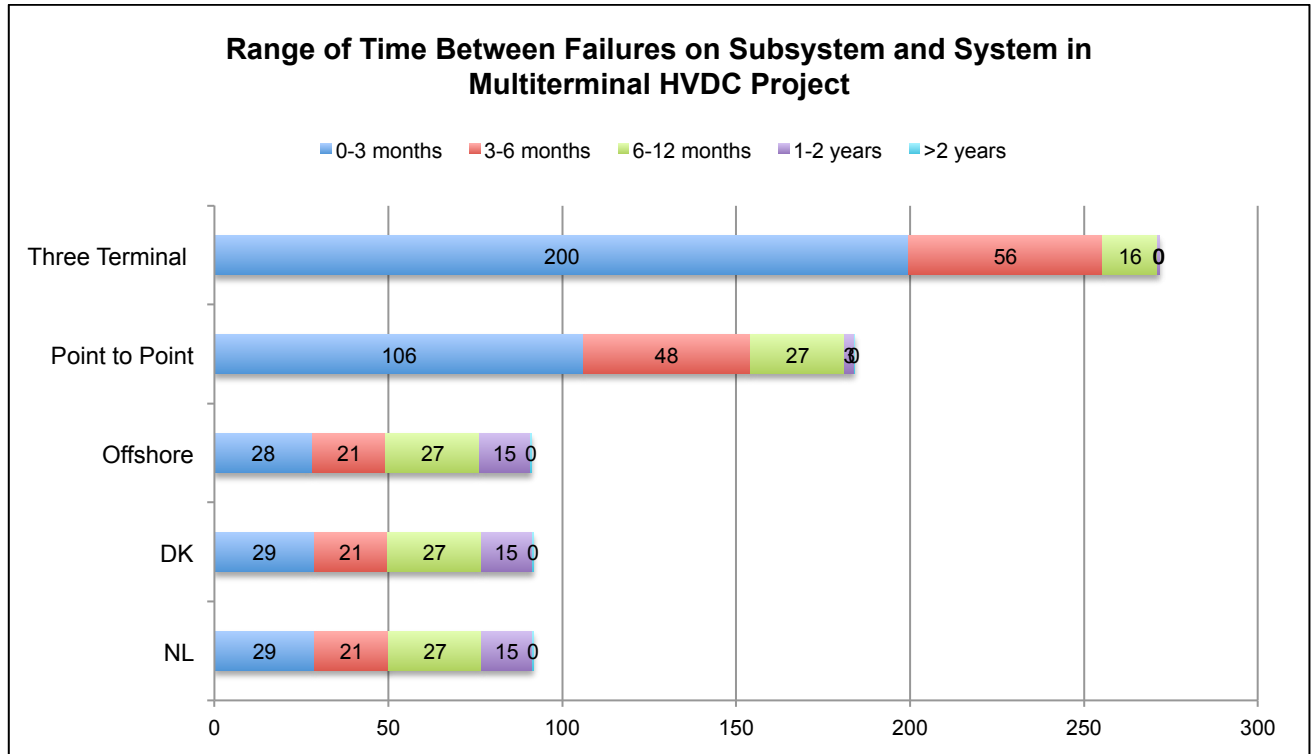


Fig. 5-12 Range of Time Between Failures in the Subsystems and HVDC System in the Multiterminal HVDC Project

From all reliability analysis results, it is shown that the unavailability obtained from Monte Carlo simulation is mostly higher than that from the analytical approach. This can be explained as follow: the time to repair in hours generated in Monte Carlo simulation is occasionally less than one hour. To simplify the simulation, those numbers are rounded to one. Consequently, it will increase the total time of repair, and thus rises the down time and unavailability. Therefore, it can be deduced that the Monte Carlo simulation in this master thesis gives slightly pessimistic results. This is reasonable rather than rounding the time to repair to zero, which is obviously impossible as repairs are neglected then.

5.4.2. With Switching Possibilities

The next analysis is the three-terminal topology considering the switching possibilities. As mentioned in chapter 4.4, there are three subsystems evolved in the analysis. Thus, there will be $2^3 = 8$ possible failure states.

Table 5-14 Probability and Duration of Subsystem Failure States by the Analytical Method

States	Availability of the Subsystems			Probability	Duration (1 year = 8760 hours)
	NL Node	DK node	Off Node		
P ₁	1	1	1	97.0717%	8503.5 hours/y
P ₂	0	1	1	0.6445%	56 hours/y
P ₃	1	0	1	1.0777%	94 hours/y
P ₄	1	1	0	1.1780%	103 hours/y
P ₅	0	0	1	0.0072%	38 minutes/y
P ₆	0	1	0	0.0078%	41 minutes/y
P ₇	1	0	0	0.0131%	69 minutes/y
P ₈	0	0	0	0.0000868%	27 seconds/y

Table 5-15 Probability and Duration of Subsystem Failure States by Monte Carlo Simulation

States	Availability of the Subsystems			Probability			Duration (1 year= 8760 hours)
	NL Node	DK Node	Off Node	Average	Lower Limit	Upper Limit	
P ₁	1	1	1	97.0503%	97.0912%	97.0093%	8501.6 hours/y
P ₂	0	1	1	0.6568%	0.6371%	0.6765%	58 hours/y
P ₃	1	0	1	1.0742%	1.0479%	1.1005%	94 hours/y
P ₄	1	1	0	1.1901%	1.1653%	1.2149%	104 hours/y
P ₅	0	0	1	0.0079%	0.0063%	0.0096%	42 minutes/y
P ₆	0	1	0	0.0072%	0.0064%	0.0080%	38 minutes/y
P ₇	1	0	0	0.0134%	0.0115%	0.0153%	70 minutes/y
P ₈	0	0	0	0.0001%	0.0000%	0.0002%	32 seconds/y

Table 5-14 and Table 5-15 show the probability of the failure states and the status of the three subsystems, using the availability obtained from the analytical method and Monte Carlo simulation. The mean availability from the Monte Carlo simulation shown in Table 5-15 is used for the calculation of the yearly outage duration. To get more insight into the unavailability, the outage duration per year of all failure probabilities is shown in the same tables. From the results, it is known that the longest subsystem outage duration is when the offshore node failed, which is 103 hours/year and 104 hours/year based on calculation by the analytical approach and the Monte Carlo simulation, respectively. Several results also give slightly different numbers but all the probabilities produced by the analytical approach are still within the limits of the confidence intervals. The longest outage duration when one subsystem failed is the failure of the offshore node because all the components need longer time to repair than that in the onshore nodes, both DK and NL. For further research, longer simulation time of the Monte Carlo simulation is required to obtain both accurate and precise availability results. In addition, from the table it is shown that the longest outage duration of two failed subsystems occurs for the failure of the offshore node and the DK onshore node, which is 70 minutes/year. This is reasonable since the DK node includes the longest DC cables, which is 225 km. However, the failure probability of states 5, 6, 7 and 8 results in a complete system failure thus it can be concluded based on the analytical approach and Monte Carlo simulation, the system suffers from complete outage for 148 minutes and 150 minutes, respectively. Meanwhile, based on the

analytical and Monte Carlo simulation results, the system suffers from a partly outage (state 2, 3, and 4) for 253 hours and 256 hours.

Table 5-16 The Snapshot of Energy not Transmitted per Year in Three Terminal Topology using Analytical Result

Failure	The Amount of Energy (MWh) Per Hour			The Amount of Energy Not Transmitted (MWh) per Hour	The Amount of Energy Not Transmitted (GWh) per Year	Energy Excess (GWh) per Year	Energy Losses (GWh) per Year	Total energy not Transmitted (GWh/year)
	NL	DK	Off					
SCENARIO 1	-700	0	700					
No Failure	-700.00	0.00	700.00	0.00	0.00			
NL	0.00	0.00	700.00	700.00	39.52			
DK	-700.00	0.00	700.00	0.00	0.00			
OFF	-700.00	0.00	0.00	-700.00	-72.23			
NL-DK	0.00	0.00	700.00	700.00	0.44			
NL-Offshore	0.00	0.00	0.00	0.00	0.00			
DK-Offshore	-700.00	0.00	0.00	-700.00	-0.80			
						39.96	-73.04	113.00
SCENARIO 2	0	-700	700					
No Failure	0.00	-700.00	700.00	0.00	0.00			
NL	0.00	-700.00	700.00	0.00	0.00			
DK	0.00	0.00	700.00	700.00	66.08			
OFF	0.00	-700.00	0.00	-700.00	-72.23			
NL-DK	0.00	0.00	700	700.00	0.44			
NL-Offshore	0.00	-700	0.00	-700.00	-0.48			
DK-Offshore	0.00	0.00	0.00	0.00	0.00			
						66.53	-72.71	139.24
SCENARIO 3	-700	350	350					
No Failure	-700.00	350.00	350.00	0.00	0.00			
NL	0.00	350.00	350.00	700.00	39.52			
DK	-700.00	0.00	350.00	-350.00	-33.04			
OFF	-700.00	350.00	0.00	-350.00	-36.12			
NL-DK	0.00	0.00	350	350.00	0.22			
NL-Offshore	0.00	350	0.00	350.00	0.24			
DK-Offshore	-700	0.00	0.00	-700.00	-0.80			
						39.98	-69.96	109.94
SCENARIO 4	350	-700	350					
No Failure	350.00	-700.00	350.00	0.00	0.00			
NL	0.00	-700.00	350.00	-350.00	-19.76			
DK	350.00	0.00	350.00	700.00	66.08			
OFF	350.00	-700.00	0.00	-350.00	-36.12			
NL-DK	0.00	0.00	350	350.00	0.22			
NL-Offshore	0.00	-700	0.00	-700.00	-0.48			
DK-Offshore	350	0.00	0.00	350.00	0.40			
						66.71	-56.36	123.06

The next analysis is the energy not transmitted due to several failure states. Two approaches are performed: the snapshots and the year scenario. The snapshots show the load flow in a specific point of time. The analysis of the expected energy not transmitted per year using the snapshots is executed with the

assumption that the energy transmitted through the DC cables is constant and the scenario enables the onshore node to either only export or import. The offshore node always supplies energy to one of the onshore nodes. The year scenario, on the other hand, allows the onshore nodes two options: import or export depending on the market. However, similar to the snapshot, the offshore node only takes part to give energy to the onshore nodes. The output of this analysis is the energy excess, the energy loss, and the total energy not transmitted, assuming that the power flow cannot be redirected.

Four scenarios are made within the snapshot scenarios. Table 5-16 shows the amount of energy not transmitted per hour and per year in MWh and GWh respectively based on these four scenarios. Each scenario has four failure states: no failure, DK, NL, offshore, NL-DK, NL-offshore, and DK-offshore. All scenarios are briefly described in the following paragraph. The complete failure is excluded from the analysis because the failure of all nodes does not permit the energy to be transported through the three-terminal system, hence zero energy is transmitted via the system and this is out of interest.

Snapshot scenario 1 permits the offshore nodes to provide 700 MW only to the NL onshore node. Thus, in the table, the Netherlands receives a power of 700 MW and it can be said that the Netherlands onshore node supplies -700 MW. The Denmark onshore node in this scenario plays no role both to export and import the energy. The failure of the Denmark onshore node, hence, does not have an impact on the three-terminal HVDC system, as can be seen in row 5. If there are no failures, all energy of 700 MWh/hour from the offshore node is transmitted to the Netherlands, and the Netherlands receives the energy of 700 MWh/hour, thus all energy is transmitted and the estimated energy not transmitted is zero, as shown in row 3 column 5 and 6. When the Netherlands onshore node is down, the amount of energy not transmitted is an excess energy from offshore node, which is 700 MWh/hour. The fault of nodes that should receive energy leads to the generation dispatch cost included the Netherlands' fault. When the offshore node is out of work, there is energy loss of 700 MW, which leads to generation dispatch cost to prevent transmission congestion. Snapshot scenario 2 has the same characteristic as snapshot scenario 1, yet in this snapshot, Denmark is the country that receives the energy from the offshore node. In snapshot scenario 3, the Netherlands is the node that demands the supply, yet the energy is provided by the offshore node and the Denmark onshore node equally. When the Denmark part of the network suffers from an outage, the Netherlands can still receive half of the energy demand but it results in half of energy demand as an energy losses. Since there is no possibilities that the faulted NL onshore node get any supply form the three-terminal system, included energy excess, this causes redispatch costs, but only half of the snapshot scenario 1's. The same situation happens if the offshore node failed. However, when the Netherlands suffers from failure, it generates energy excess in the system of 700 MW. Snapshot scenario 4 has the same condition as snapshot scenario 3, yet Denmark is the onshore node that receives the power.

The energy not transmitted per year is the reliability indicator that would be achieved. This gives insight about how many energy not transmitted per year regarding to the probability of the four scenarios occur in a year. The equation for this analysis can be found in Eq. 4.24. The results are shown in Table 5-16. The energy not transmitted of each scenario is distinguished whether it is an energy excess or energy loss. It cannot be directly concluded that the lowest energy losses and the highest energy excess will give the highest profit. It depends on the energy price in the Netherlands and the Denmark. Nevertheless, It is interesting to know several consequences arisen from the results. Taking snapshot scenario 2 as an example, the energy excess caused by the Denmark down state is then transmitted to the Netherlands onshore node with lower price since Denmark poses no demand of energy from this three-terminal HVDC system. The energy losses due to failure in the offshore node causes the Denmark pay higher price to fulfil its

demand. Thus, the price will vary depending on the country. If the energy price in the Netherlands and Denmark is the same, the price excess energy paid by the offshore node to be transmitted to either Denmark or the Netherlands will be equal. Likewise, the price of energy loss suffered by Denmark and the Netherlands will be similar. Thus, the least excess energy and the least energy loss among all the scenarios will be the most profitable option. With this assumption, snapshot scenario 3 is preferable.

The second scenario of analysis on energy not transmitted in three-terminal configuration is the year scenario. In this scenario, the data of the amount of energy supply or demanded per hour in one year is available in each node (DK, NL, offshore). Similarly to the snapshot scenarios, each scenario has four failure states: No Failure, DK failure, NL failure, and offshore failure. Moreover, there are four other scenarios with this scenario based on the offshore node preference to which the energy is transmitted: NL preference, DK preference, equal preference, and "Follow Exchange" preference. The scenarios are described below.

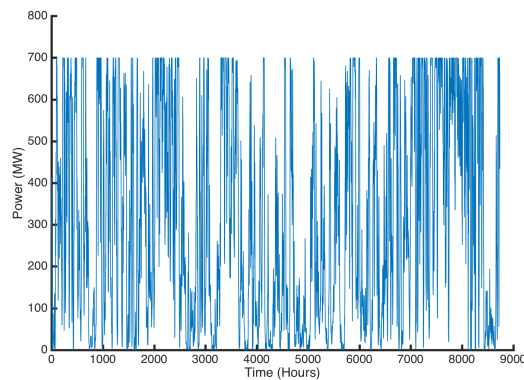


Fig. 5-13 The Year Scenario of The NL Preference in The Offshore Node

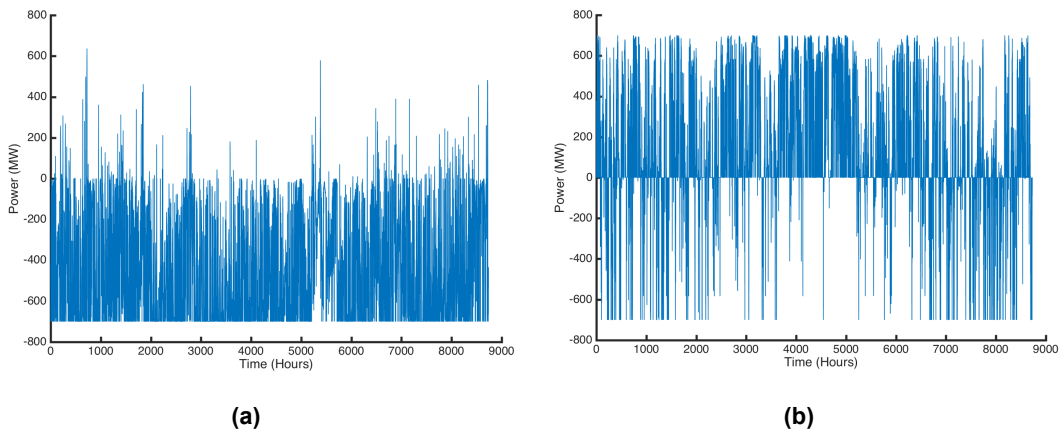


Fig. 5-14 The Year Scenario of The NL Preference in (a) NL Onshore Node and (b) DK Onshore Node

In the NL-preference scenario, the generated offshore wind power is transferred to NL, unless due to the network capacity, the power is transmitted to DK. Fig. 5-13 shows the energy year scenario of the offshore node. It is shown in the picture that the power is all beyond zero. It means that the offshore node exports the electrical supply. Fig. 5-15 shows the NL onshore node and DK onshore node energy year scenario. Most of the power in Fig. 5-15(a) is lower than zero (negative), meaning that the NL onshore node imports the energy from other nodes. To be more precise, Table 5-17 shows the data of all energy transmitted, both export and import of three subsystems in each preference. From the table, it

can be seen that NL imports 3888 GWh/ year energy. NL receives the supply from both offshore node (2774 GWh/year) and DK node (1454 GWh/year), while occasionally, due to the condition of power capacity, DK also receive the relatively low energy of 374 GWh/year. The offshore generates electrical energy of 2774 GWh/year in each preference.

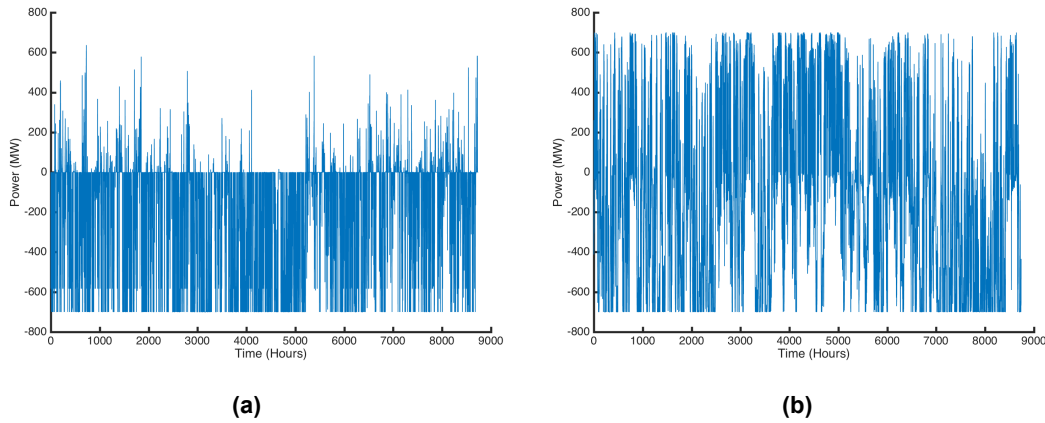


Fig. 5-15 The Year Scenario of The DK Preference in (a) NL Onshore Node and (b) DK Onshore Node

In the DK-preference scenario, DK onshore node imports the highest energy, which is 2327 GWh/year, compared to the imported energy of NL onshore node, which is 1788 GWh/year. However, DK onshore node also still exports relatively high energy of 1254 GWh, while the NL onshore node only gives a supply of 8667 GWh/year. To see it more clearly, the graph can be seen in Fig. 5-15. In two preferences, NL onshore node is the node that actively imports the energy.

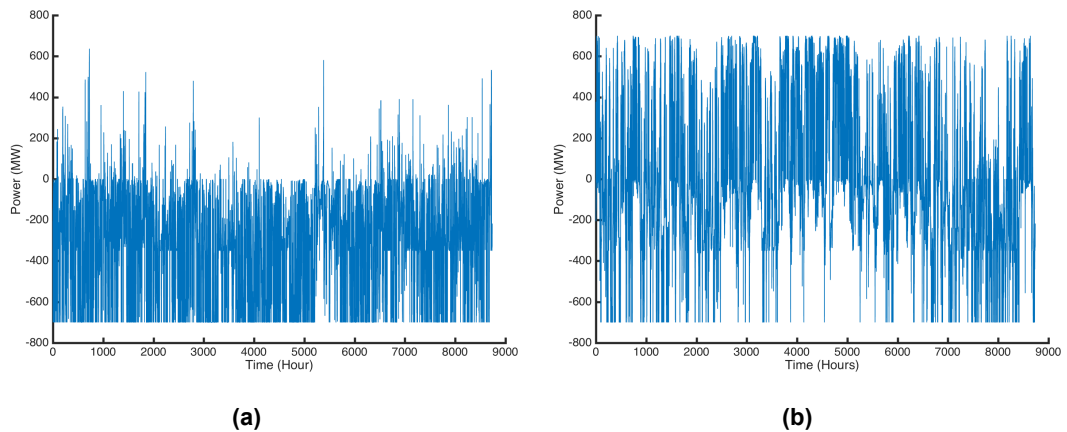


Fig. 5-16 The Year Scenario of The Equal Preference in (a) NL Onshore Node and (b) DK Onshore Node

In equal preference, the offshore node will equally transfer the energy to both the NL onshore node and the DK onshore node. In this preference, the NL onshore node receives the highest energy supply, which is 2840 GWh/year, compared to the NL onshore node, which are lower than half of NL onshore node imported energy, 1340 GWh/year. The NL onshore node receives energy from the DK onshore node, which is 1352 GWh/year. From the graphs shown in Fig. 5-16, DK receives less energy in this preference than in the previous preference, while NL receives more.

The last preference is “follow exchange” preference. The generated wind power of offshore node follows the scenario of energy exchange between NL and

DK. Both DK and NL export and import more energy in this preference than in the equal preference, as can be seen in Fig. 5-17.

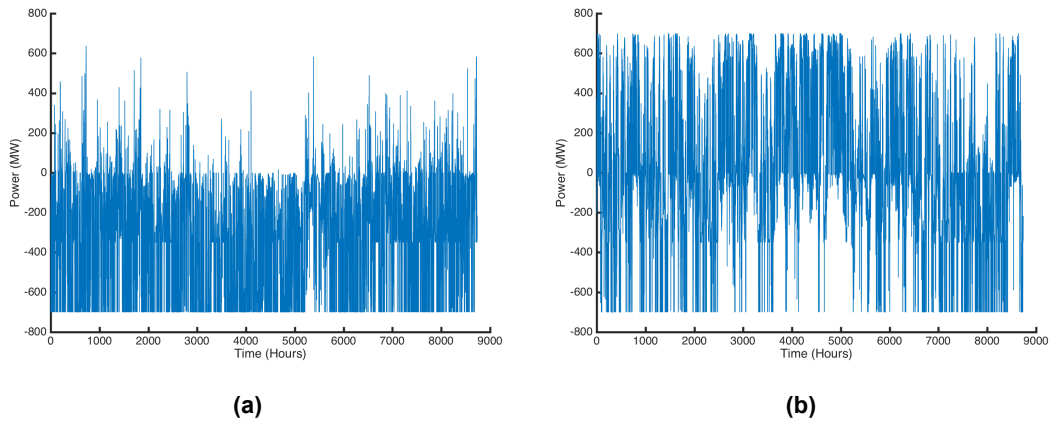


Fig. 5-17 The Year Scenario of The Equal Preference in (a) NL Onshore Node and (b) DK Onshore Node

Table 5-17 Year Scenario of Energy Transmitted in Three Terminal Topology

Preference	Subsystem	Energy Transmitted in a Year (MWh/year)	
		EXPORT	IMPORT
NL	NL	3.344.E+04	-3.888.E+06
	DK	1.454.E+06	-3.741.E+05
	Offshore	2.774.E+06	0.000.E+00
DK	NL	8.667.E+04	-1.788.E+06
	DK	1.254.E+06	-2.327.E+06
	Offshore	2.774.E+06	0.000.E+00
Equal	NL	5.355.E+04	-2.840.E+06
	DK	1.352.E+06	-1.340.E+06
	Offshore	2.774.E+06	0.000.E+00
Follow Exchange	NL	8.667.E+04	-2.949.E+06
	DK	1.454.E+06	-1.366.E+06
	Offshore	2.774.E+06	0.000.E+00

The energy not transmitted due to failure probability can be achieved by calculation using Eq. 4.24. The failure states are mentioned in Table 4-1. However, the failure states considered in the analysis are only state 2, 3, and 4, which are the failure of NL onshore node, DK onshore node, and offshore node respectively. This is because the other failure states will cause the complete losses and this is not of interest to be discussed. The result of this analysis followed by all preference is shown in Table 5-18.

In NL preference, the NL onshore node plays a role as the highest energy importer in the three-terminal HVDC system. The failure of NL onshore node does not enable the DK onshore node and the offshore node to transmit the energy to the NL onshore node. Consequently, the excess energy is resulted, which is 24.84 GWh/year. The failure of DK onshore node and offshore node cause the energy

should be transferred to the NL onshore node cannot be transmitted. Thus it causes the energy loss due to the failure of DK onshore node and offshore node, which are 11.64 GWh/year and 32.68 GWh/year respectively. The total of energy excess and the energy loss in this preference with 3 failure possibilities are 24.84 GWh/year and 32.69 GWh/year, respectively.

Table 5-18 Year Scenario of Energy not Transmitted per Year in Three Terminal Topology using Analytical Result

Preference	Energy Transmitted in a Year After Failure (GWh/year)			Energy Excess (GWh/year)	Energy Loss (GWh/year)	Total Energy not Transmitted in a Year (GWh/year)
	NL	DK	Offshore			
NL	24.84	-11.64	-32.68	24.84	-32.69	57.53
DK	10.96	11.57	-32.68	22.53	-32.68	55.21
Equal	17.96	-0.14	-32.68	17.96	-32.82	50.78
Follow Exchange	18.45	-0.95	-32.68	18.45	-33.63	52.07

In the DK preference, the NL failure will cause the imported and exported energy not transmitted. Because the NL supply energy much less than the offshore node and DK onshore node, the NL onshore node failure gives no significant impact on energy loss. Moreover, due to high supply to the NL onshore node, the failure leads to the generation of excess energy of 10.96 GWh/year. When the DK onshore node is out of, it will lead to energy excess in the three-terminal HVDC system because DK onshore node receive the highest energy, which are 11.57 GWh/year. The offshore node outage, similarly with the previous scenario will affect to the energy loss of the system, which are 32.68 GWh/year. The amount of energy loss due to the failure of the offshore node is typical in every scenario. With three failure possibilities mentioned above, the total energy excess is the sum of the excess energy due to NL onshore node and DK onshore node, which are 22.53 GWh/year.

In the equal and the "Follow Exchange" preference, the NL still acts as the highest energy importer, thus the failure leads to the excess energy and will be the total of the excess energy of the preferences considering three failure state, which are 17.96 GWh/year and 18.45 GWh/year respectively. The energy loss is contributed by the failure of DK and offshore node, which are 32.86 and 33.63 GWh/year.

All the results exclude the energy losses of the NL and DK networks due to the failure of the NL and DK onshore node. The analysis only discusses the surplus and deficit energy within the system. Hence, the effect of failure in NL and DK onshore node is there are zero energy transmitted from NL and DK onshore node to the three-terminal system and from three-terminal system to NL and DK onshore node. After that, it is actually interesting to estimate which preference is the most advantageous for three-terminal HVDC system. However, there are several other factors such as the price and the market. The price that should be paid for the onshore nodes receive the excess energy and suffer from energy loss varies to time, season, and the energy market with the countries. Nevertheless, taking equal preference as an example, the 17.96 GWh/year energy excess should be marketed to DK network due to NL onshore node failure. The price could be lower than in the scenario when there is no failure in the system. If for example, the price of excess energy in both networks (The Netherlands and Denmark) is typical regardless of time and the season when the energy excess exists, the least energy excess will be more profitable for wind offshore company provider, hence the equal

preference is chosen as the best option. On the other hand, if the prices that should be paid by the country who suffer from energy loss and need extra energy from other networks in two countries are similar, also regardless of the time and the season when the energy loss exists, the least energy losses will be the most commercial. Thus, DK preference is preferable. From the analysis, the best scenario depends also on the parties (onshore node and offshore node).

Several factors affecting the option of the preferences such as price, time and season, and the parties are beyond this master thesis and can be done for the further works.

5.5 CONCLUSION

This chapter described the reliability analysis of all subsystems and the complete HVDC system of the case study based on the reliability models explained in chapter 4. In the last chapter, it is mentioned that two approaches are used to model the reliability and the results were shown in this chapter.

Section 5.1 explained the reliability analysis of the converter unit based on the model in section 4.1. From the reliability calculation and failure rate of the IGBT and capacitor listed in section 3.2.2, it was shown that it cannot be modelled by a negative exponential distribution, as was assumed before. The Weibull distribution is found to be the best fit to determine the reliability parameters of the converter unit. The mean time to failure of the converter unit can be achieved by calculating the integral of the reliability and results in a MTTF of 1.2508.

Section 5.2 showed the reliability analysis of the converter station, assembled by several subsystems such as: transformer, converter unit, converter reactor, control system, and DC switchyard. There are two types of converter stations in the system based on the case study: onshore and offshore converter station. The unavailability and the outage duration were shown in this section. It was found that the longest outage duration in the onshore and offshore converter station calculated by the two approaches is possessed by the transformer and the converter reactor, respectively.

Section 5.3 demonstrated the point-to-point system reliability analysis. The energy not transmitted of using the load flow scenarios of four example connections was shown. Since each connection has different characteristics, it cannot be directly compared. In section 5.4, the three-terminal configuration reliability analysis both with and without switching possibilities was discussed. In the situation without switching possibilities, the probability of two states ('up' and 'down' state) produced in section 5.4.1, all the unavailability and the outage duration of the NL, DK, offshore converter station, the point-to-point connection and the three-terminal topology were shown. The result of failure frequency, the average duration per interruption and the range of time between failures, which were obtained from Monte Carlo simulation, are shown in the same section. The results will be useful as a description of the system and data for improving the reliability of the system using several actions of asset management. In section 5.4.2, the three-terminal configuration with switching possibilities produces eight failure states. The probability of each failure state is shown in the same section. The data were used to analyse the energy not transmitted through the system. There are two methods to calculate the energy not transmitted: using the snapshots and the annual load flow scenario. Each method utilises four scenarios as described in the section. It was obtained from the explanation that it cannot be directly deduced which scenario is the most profitable to be applied due to several factors affected such as energy price in each country, the season, redispatch cost in each country and energy market occurred in both countries.

In all results obtained from both analytical and Monte Carlo simulation, it is found that the Monte Carlo simulation is a good method to verify the results from analytical approach, considering that it gives more pessimistic results.

The next chapter will show the combined conclusion of all chapters in this master thesis.

6 Conclusion & Recommendations

This final chapter gives a brief summary of the most important conclusions drawn from the discussion in this master thesis. After that, the recommendations, which will be useful for future work are described.

6.1 CONCLUSION

The renewable energy resources are now the prioritised sources for new generation capacity in 2016. New transmission systems are expected to transfer the energy with high availability. HVDC is now becoming a popular option due to higher efficiency and compatibility for transferring electrical energy over long distances and from/to power systems with different frequency. Moreover, multi-terminal HVDC is preferred because of the growing electricity market and the need for high flexibility of the electricity supply. The newest technology is the Modular Multilevel Converter (MMC), a converter technology, which creates a flexible and scalable DC voltage level. Two types of MMC are available: half-bridge MMC and full-bridge MMC. Half-bridge MMC is widely used since it has less power losses and costs than the full-bridge MMC. The design of this kind of transmission system should meet high reliability to achieve good quality of the power flow. To investigate the reliability of the system, one should analyse the reliability of each component/subsystem assembling the HVDC system. This research answered the question of how the reliability of multi-terminal HVDC systems based on half-bridge MMC can be modelled.

To answer this question, the components and the subsystems inside the converter station and connection were studied. The reliability parameters were determined as observed in several sources. It was found that the reliability parameters of the subsystems are chosen with the assumption that the reliability can be modelled by a specific probability distribution, which is the negative exponential distribution. There are a lot of subsystems inside the converter station, yet five subsystems were chosen based on the available reliability parameters: the transformer, converter reactor, converter station, control system and DC switchyard. After determining the reliability parameters of each subsystem, the reliability models of the components were constructed based on reliability theory. It was noted that the converter unit was modelled with redundancy. All subsystems and finally the complete HVDC system (point-to-point and three-terminal connection) were modelled by two approaches: an analytical approach and Monte Carlo simulation. The reliability of the components and the complete HVDC system in this master thesis were described by the unavailability, the outage duration, the energy not transmitted through the systems, the failure frequency, the average duration per interruption, and time between failures.

From the results, it was found that the transformer and the converter reactor have the largest unavailability and thus have the highest outage duration in the onshore and offshore converter stations, respectively. In addition, the offshore converter station has the highest outage duration of all converter stations in the system (NL, DK and offshore converter station) because it has the longest 'down' state, hence affects the system reliability the most. The failure frequency, the average outage duration and the range of time between failures were provided and several actions regarding asset management could be executed. The energy not transmitted through the point-to-point system for four different load flow scenarios

was calculated and compared and it was concluded that the expected energy not transmitted strongly depends on the load flow scenario of the HVDC connection. Similarly, the energy not transmitted for the three-terminal configuration with several scenarios could not be directly determined because it is also influenced by other factors such as energy market, season, energy price and generation redispatch costs in each country, which is not the scope of this research. However, the results show that implementation of switching possibilities in the three-terminal configuration allows an amount of energy generated and transferred from the onshore node can still be transmitted to any onshore node. This would be more profitable for the offshore wind provider and the countries involved, comparing to the condition if there are no switching possibilities, which results in a complete system failure in case of faults in one of the nodes.

6.2 RECOMMENDATION

There are a lot of methods to set up the reliability model of an HVDC system. However, the availability of reliability parameters of several components, especially for new technologies such as MMC is limited. In the future, if other reliability parameters become available, such as transition rates, it will result in more realistic reliability models and other methods can be applied such as Markov models and state enumeration. Moreover, if the information about of the failure mechanisms and failure modes is available, a method such as Failure Mode and Effect Analysis can also be executed.

From the results of the energy not transmitted of a point-to-point and three-terminal configuration, cost benefit analysis will be interesting to implement using several data, such as the energy market and energy prices.

Bibliography

- [1] A. Vaughan. (2017, July 17). *Almost 90% of new power in Europe from renewable sources in 2016*. Available: <https://www.theguardian.com/environment/2017/feb/09/new-energy-europe-renewable-sources-2016>
- [2] A. Nghiem and A. Mbistrova, "Wind in power," WindEurope, Brussels, 2017.
- [3] S. Lazarou, C. F. Covrig, I. Colak, P. Minnebo, H. Wilkening, and G. Fulli, "Behaviour of multi-terminal grid topologies in renewable energy systems under multiple loads," in *2012 International Conference on Renewable Energy Research and Applications (ICRERA)*, 2012, pp. 1-4.
- [4] J. Schachner, "Power Connections for Offshore Wind Farms," Diploma, Department of Electrical Engineering, University of Leoben, Leoben, 2004.
- [5] SIEMENS. (January 9). *DC Technology for far offshore platforms*. Available: <http://www.energy.siemens.com/nl/en/power-transmission/grid-access-solutions/dc-technology.htm>
- [6] ABB. (January 9). *Technical advantages*. Available: <http://new.abb.com/systems/hvdc/why-hvdc/technical-advantages>
- [7] M. K. Bucher, R. Wiget, G. Andersson, and C. M. Franck, "Multiterminal HVDC Networks: What is the Preferred Topology?," *IEEE Transactions on Power Delivery*, vol. 29, no. 1, pp. 406-413, 2014.
- [8] D. Van Hertem and M. Ghandhari, "Multi-terminal VSC HVDC for the European supergrid: Obstacles," *Renewable and Sustainable Energy Reviews*, vol. 14, no. 9, pp. 3156-3163, 2010/12/01/ 2010.
- [9] E. N. Abildgaard and M. Molinas, "Modelling and Control of the Modular Multilevel Converter (MMC)," *Energy Procedia*, vol. 20, pp. 227-236, 2012/01/01/ 2012.
- [10] S. Debnath, J. Qin, B. Bahrani, M. Saeedifard, and P. Barbosa, "Operation, Control, and Applications of the Modular Multilevel Converter: A Review," *IEEE Transactions on Power Electronics*, vol. 30, no. 1, pp. 37-53, 2015.
- [11] J. Setreus and L. Bertling, "Introduction to HVDC Technology for Reliable Electrical Power Systems," in *Probabilistic Methods Applied to Power Systems, 2008. PMAPS '08. Proceedings of the 10th International Conference on*, 2008, pp. 1-8.
- [12] B. W. Tuinema, J. L. R. Torres, and M. A. M. M. v. d. Meijden, *Reliability of Sustainable Power System*. Delft: Delft University of Technology, 2016.
- [13] ABB, "Introducing HVDC," ed. Ludvika, Sweden: ABB AB, 2014.
- [14] ReliaSoft. (2014, 9 January). *RBDs and Analytical System Reliability*. Available: http://reliawiki.org/index.php/RBDs_and_Analytical_System_Reliability
- [15] M. Davies, M. Dommaschk, J. Dorn, J. Lang, D. Retzmann, and D. Soerangr, "HVDC PLUS – Basics and Principle of Operation," 2011, Available: www.siemens.com/energy/hvdcplus.
- [16] K. Friedrich, "Modern HVDC PLUS application of VSC in Modular Multilevel Converter topology," in *2010 IEEE International Symposium on Industrial Electronics*, 2010, pp. 3807-3810.
- [17] R. Leelaruij, J. Setreus, G. Olguin, and L. Bertling, "Availability Assessment of the HVDC Converter Transformer System," in *Probabilistic Methods Applied to Power Systems, 2008. PMAPS '08. Proceedings of the 10th International Conference on*, 2008, pp. 1-8.
- [18] S. Li, Y. Ma, Y. Hua, and P. Chen, "Reliability Equivalence and Sensitivity Analysis to UHVDC Systems Based on the Matrix Description of the F&D Method," *IEEE Transactions on Power Delivery*, vol. 31, no. 2, pp. 456-464, 2016.

- [19] H. D. Kochs, P. Kongniratsaikul, and F. Lutz, "Comparing system reliability considering insufficient knowledge: Application to HVDC converter stations," in *2012 IEEE Power and Energy Society General Meeting*, 2012, pp. 1-8.
- [20] E. N. Dialynas and N. C. Koskolos, "Reliability modeling and evaluation of HVDC power transmission systems," *IEEE Transactions on Power Delivery*, vol. 9, no. 2, pp. 872-878, 1994.
- [21] S. Zadkhast, M. Fotuhi-Firuzabad, F. Aminifar, R. Billinton, S. O. Faried, and A.-A. Edris, "Reliability Evaluation of an HVDC Transmission System Tapped by a VSC Station," in *IEEE Transactions on Power Delivery*, 2010, vol. 25, no. 3, pp. 1962-1970.
- [22] R. Billinton, M. Fotuhi-Firuzabad, and S. O. Faried, "Reliability evaluation of hybrid multiterminal HVDC subtransmission systems," *IEE Proceedings - Generation, Transmission and Distribution*, vol. 149, no. 5, pp. 571-577, 2002.
- [23] L. Devi, C. Saibabu, and S. Sivanagaraju, "Reliability Evaluation of Multi Terminal HVDC transmission Systems," *International Journal of Recent Engineering Research and Development (IJRERD)*, vol. 01, no. 08, pp. 26-34.
- [24] W. An *et al.*, "Reliability evaluation and comparison for different topologies of VSC-HVDC distribution networks using analytical and simulation methods," in *12th IET International Conference on AC and DC Power Transmission (ACDC 2016)*, 2016, pp. 1-6.
- [25] A. Beddard and M. Barnes, "VSC-HVDC Availability Analysis," The University of Manchester, 2011.
- [26] J. Guo, X. Wang, Z. Bie, and Y. Hou, "Reliability modeling and evaluation of VSC-HVDC transmission systems," in *2014 IEEE PES General Meeting | Conference & Exposition*, 2014, pp. 1-5.
- [27] K. Rudion, Z. A. Styczynski, A. G. Orths, M. Powalko, and H. Abildgaard, "Reliability investigations for a DC offshore power system," in *2013 IEEE Power & Energy Society General Meeting*, 2013, pp. 1-5.
- [28] J. Wang, M. Ding, and S. Li, "Reliability Analysis of Converter Valves for VSC-HVDC Power Transmission System," in *2010 Asia-Pacific Power and Energy Engineering Conference*, 2010, pp. 1-4.
- [29] J. Guo, J. Liang, X. Zhang, P. Judge, X. Wang, and T. Green, "Reliability Analysis of MMCs Considering Sub-module Designs with Individual or Series Operated IGBTs," *IEEE Transactions on Power Delivery*, vol. PP, no. 99, pp. 1-1, 2016.
- [30] B. Wang, X. Wang, Z. Bie, P. D. Judge, X. Wang, and T. C. Green, "Reliability Model of MMC Considering Periodic Preventive Maintenance," *IEEE Transactions on Power Delivery*, vol. 32, no. 3, pp. 1535-1544, 2017.
- [31] V. Najmi, "Modeling, Control and Design Considerations for Modular Multilevel Converters," Master of Science, Virginia Polytechnic Institute, Virginia Tech, Blacksburg, 2015.
- [32] ABB. (November 30). *Economic and environmental advantages*. Available: <http://new.abb.com/systems/hvdc/why-hvdc/economic-and-environmental-advantages>
- [33] SIEMENS, "High Voltage Direct Current Transmission - Proven Technology for Power Exchange", S. AG, Ed., ed. Erlangen, Germany: Siemens AG, 2011.
- [34] F. Nozari and H. S. Patel, "Power electronics in electric utilities: HVDC power transmission systems," *Proceedings of the IEEE*, vol. 76, no. 4, pp. 495-506, 1988.
- [35] W. Wang, G. Wang, and M. Andersson, "Development in UHVDC Multi-Terminal and VSC DC Grid," in *International High Voltage Direct Current Conference (HVDC 2016)* Shanghai, 2016.
- [36] Wikipedia. (2017, June 14). *HVDC converter station*. Available: https://en.wikipedia.org/wiki/HVDC_converter_station
- [37] O. Lennerhag and V. Traff, "Modelling of VSC-HVDC for Slow Dynamic Studies," Master, Department of Energy and Environment, Chalmers University of Technology, Gothenburg, 2013.

- [38] A. I. Stan and D. I. Stroe, "Control of VSC-Based HVDC Transmission System for Offshore Wind Power Plants," Master, Department of Energy Technology, Aalborg University, Denmark, 2010.
- [39] J. S. Harsha, G. N. Shilpa, E. Ramesh, L. N. Dayananda, and C. Nataraja, "Voltage Source Converter Based HVDC Transmission," in *International Journal of Engineering Science and Innovative Technology (IJESIT)*, 2012.
- [40] C. Du, "The control of VSC-HVDC and its use for large industrial power systems," Department of Electric Power Engineering, CHALMERS UNIVERSITY OF TECHNOLOGY, Göteborg, Sweden, 2003.
- [41] SKM, "Calculating Target Availability Figures for HVDC Interconnectors," Sinclair Knight Merz, Newcastle, 2012.
- [42] O. E. Oni, I. E. Davidson, and K. N. I. Mbangula, "A review of LCC-HVDC and VSC-HVDC technologies and applications," in *2016 IEEE 16th International Conference on Environment and Electrical Engineering (EEEIC)*, 2016, pp. 1-7.
- [43] M. Davies, M. Dommaschk, J. Dorn, J. Lang, D. Retzmann, and D. Soerangr, "HVDC Plus - Basics and Principle of Operation," 2008.
- [44] ALSTOM, "HVDC for beginners and beyond," ALSTOM Grid Worldwide Contact Centre.
- [45] R. L. Sellick and M. Åkerberg, "Comparison of HVDC Light (VSC) and HVDC Classic (LCC) site aspects, for a 500MW 400kV HVDC transmission scheme," in *10th IET International Conference on AC and DC Power Transmission (ACDC 2012)*, 2012, pp. 1-6.
- [46] K. Koreman, "New principles of design and operation for HVDC grids," ed. Netherland: Tennet, 2016, p. 36.
- [47] G. STAMATIOU, "Converter interactions in VSC-based HVDC systems," LICENTIATE OF ENGINEERING, Department of Energy and Environment, CHALMERS UNIVERSITY OF TECHNOLOGY, Gothenburg, 2015.
- [48] C. MacIver, "A Reliability Evaluation of Offshore HVDC Transmission Network Options," Doctor of Philosophy, Department of Electronic and Electrical Engineering, University of Strathclyde, 2015.
- [49] C. MacIver, K. R. W. Bell, and D. P. Nedić, "A Reliability Evaluation of Offshore HVDC Grid Configuration Options," *IEEE Transactions on Power Delivery*, vol. 31, no. 2, pp. 810-819, 2016.
- [50] M. Bahrman, "HVDC Development Topics," ed: ABB, 2008.
- [51] C. MacIver, K. R. W. Bell, D. P. Nedi, and x, "A Reliability Evaluation of Offshore HVDC Grid Configuration Options," *IEEE Transactions on Power Delivery*, vol. 31, no. 2, pp. 810-819, 2016.
- [52] R. Faizal, "MODELLING OF SUMATRA-JAVA HVDC TRANSMISSION SYSTEM AND SYSTEM IMPACT ANALYSIS," Master, Institut Teknologi Bandung, 2014.
- [53] Å. H. Kjørholt, "HVDC Transmission Using a Bipolar Configuration Composed of an LCC and MMC," Master, Department of Electric Power Engineering, Norwegian University of Science and Technology, Trondheim, Norway, 2014.
- [54] D. F. Menzies, J. Graham, and F. U. Ribeiro, "'Garabi' the Argentina – Brazil 1000 MW Interconnection Commissioning and Early Operating Experience," presented at the ERLAC Conference, Foz do Iguaçu, Brazil, 2001.
- [55] PALISADE. (2017, July 17). *Monte Carlo Simulation*. Available: http://www.palisade.com/risk/monte_carlo_simulation.asp
- [56] C. Singh and J. Mitra, "Monte Carlo simulation for reliability analysis of emergency and standby power systems," in *Industry Applications Conference, 1995. Thirtieth IAS Annual Meeting, IAS '95., Conference Record of the 1995 IEEE*, 1995, vol. 3, pp. 2290-2295 vol.3.
- [57] S. Martin, "Siemens wins order for HVDC link between Denmark and Holland," ed. Erlangen: Siemens AG, 2016.
- [58] S. Martin, "Siemens wins order for HVDC link between Denmark and Holland," ed. Erlangen: Siemens, 2016.

- [59] R. Ø, C. Öhlén, J. Solvik, J. Thon, K. Karijord, and T. Gjengedal, "Design, operation and availability analysis of a multi-terminal HVDC grid - A case study of a possible Offshore Grid in the Norwegian Sea," in *2011 IEEE Trondheim PowerTech*, 2011, pp. 1-7.
- [60] Wikipedia. (2017, July 11). *Normal Distribution*. Available: https://en.wikipedia.org/wiki/Normal_distribution
- [61] W. Oberle, "Monte Carlo Simulations: Number of Iterations and Accuracy," US Army Research Laboratory, Maryland 2015.
- [62] W. Wu, F. Gong, G. Chen, and L. He, "A fast and provably bounded failure analysis of memory circuits in high dimensions," in *2014 19th Asia and South Pacific Design Automation Conference (ASP-DAC)*, 2014, pp. 424-429.
- [63] E. Tran and P. Koopman, "Mission Failure Probability Calculations for Critical Function Mechanizations in the Automated Highway System," in "Robotics Institute Technical Report," Carnegie Mellon University, Pittsburgh, Pennsylvania 1997.
- [64] J. Thomas. (2006). *One Single Component Reliability Monte Carlo Chronological Method*. Available: <https://www.mathworks.com/matlabcentral/fileexchange/10679-one-single-component-reliability-monte-carlo-chronological-method?focused=5069123&tab=function>

Appendix A

THE SIMULATION OF RELIABILITY ANALYSIS OF CONVERTER UNIT

This section illustrates the reliability analysis of the converter unit. The input data such as the simulation time, failure rate of the lowest level, which is the IGBT, is shown in section Input. The process include the calculation of the reliability, the series connection, the parallel connection [63], which assembles the converter unit, described in section Process. Section Output demonstrate the reliability analysis such as the reliability, MTTF and hazard rate of the converter unit

- **Input**

- Simulation Time

```
function t= getglobalx;  
global t  
t=0:0.01:5000;
```

- Converter Unit Simulation

```
global t  
fr_igbt=0.004;  
submodule = calc_rel(fr_igbt);  
fr_i=1/trapz(t,submodule);  
  
% reliability of the capacitor bank  
% assume that if one capacitor fails, the capacitor bank  
fails  
fr_capacitor=2e-10*8760; % failure rate of one capacitor  
fr_capbank=fr_capacitor % failure rate of 5 reliability-  
series-connected component
```

- **Process**

- Reliability Calculation

```
function [reliability]=calc_rel(lambda)  
% t=0:0.01:100;  
global t  
t1=length(t);  
for t2=1:t1;  
    for n=1:length(lambda)  
        reliability(t2,n)=exp(-lambda(n)*t(t2));  
    end;  
end;
```

- Series Connection

```
function [reliability] = series(series_rel);  
col = size(series_rel,2);  
global t  
t1=length(t);  
for t2=1:t1;  
    temp = 1;  
    for count = 1:col,
```

```

        temp1 = temp*series_rel(t2,count);
        temp = temp1;
    end;
    reliability(t2,1) = temp;
end;

```

➤ Parallel Connection

```

function [reliability] = parallel(parallel_rel);
reliability = [];
col = size(parallel_rel,2);
global t
t1=length(t);
for t2=1:t1;
    temp = 1;
    for count = 1:col
        temp2 = temp*(1 - parallel_rel(t2,count));
        temp = temp2;
    end;
    reliability(t2,1) = 1- temp;
end;

```

```
capbank_rel=calc_rel(fr_capbank);
```

➤ Reliability Calculation of The Converter Unit

```

% 2 submodules and one capacitor bank in one power
module/two-level module
pm          = series([repmat(submodule,1,2) capbank_rel]);
fr_pm=1/trapz(t,pm);

% 258 min power modules/two-level modules in one arm with 4
redundants
pm_min      = 254;
pm_num      = 4+pm_min;
t1          = length(t);
for t2      = 1:t1
    R0       = 0;
    for i    = pm_min:pm_num
        R     = R0+nchoosek(pm_num,i)*pm(t2).^i*(1-
pm(t2)).^(pm_num-i);
        R0    = R;
        arms_rel_sv(t2,1) = R;
    end;
end;
fr_arms_rel_sv=1/trapz(t,arms_rel_sv)
% 3 arms per phase
phase_rel_sv      = series(repmat(arms_rel_sv,1,3));

% 2 side per converter
converter_rel_sv   = series (repmat(phase_rel_sv,1,2));

```

• Output

```

% calculate the MTTF
MTTF=trapz(t,converter_rel_sv);

% calculate the failure rate of the converter
for t2          = 1:t1
    ln_converter_rel_sv (t2,1) =
log(converter_rel_sv(t2,1));

```

```
diff_ln_con_rel_sv      = diff(ln_converter_rel_sv);
end;

diff_t=transpose(diff(t));
num_ln=length(diff_ln_con_rel_sv);

for aa=1:num_ln
    failure_rate_sv(aa)= -
1*diff_ln_con_rel_sv(aa)/diff_t(aa);
end;
```


Appendix B

THE MONTE CARLO SIMULATION OF THE SUBSYSTEMS AND SYSTEMS RELIABILITY ANALYSIS

This section describes the algorithm of the reliability analysis on the subsystems and systems, based on the case study. All basic data, included parameters of the converter unit, MTTF and MTTR of all subsystems inside the converter station are listed in section Input. The random sampling using negative exponential distribution is executed in section Generation of Lifetime Series. The data are processed in section Output for further analysis such as.

- the unavailability of all subsystems inside the converter station and
- the unavailability of the DC cables,
- the unavailability of three converter stations (NL, DK, offshore),
- the energy not transmitted through point-to-point configuration,
- the energy not transmitted through three-terminal configuration,
- the average duration per interruptions of all subsystems and systems.
- the failure frequency of all subsystems and systems.
- The range of time between failures of all subsystems and systems.

• Input

```
format long;
format compact;
data=load('scenario2020_offshoreHVDC.mat');
cobra=abs(data.NL_EEM380_COBRA);
norned=abs(data.NL_EEM380_NorNed12);
britned=abs(data.NL_MVL380_BritNed);
MEE_DE=abs(data.NL_MEE380_DE);
N=1200;

% MTTF Data of Subsystems inside the NL Converter
Station
MTTF_CS=1.6; % MTTF of Control System 1
MTTF_TON=80; % MTTF of Onshore Transformer 2
MTTF_PR=7; % MTTF of Converter Reactor 3
MTTF_DCS=4.02; % MTTF of DC Switchyard 4
MTTF_CBL_NL=438300/8736; % MTTF of NL Subsea Cable 5

% MTTF Data of Subsystems inside the DK Converter
Station
MTTF_CS2=1.6; % MTTF of Control System 6
MTTF_TON2=80; % MTTF of Onshore Transformer 7
MTTF_PR2=7; % MTTF of Converter Reactor 8
MTTF_DCS2=4.02; % MTTF of DC Switchyard 9
MTTF_CBL_DK=438300/(8736*2.25); % MTTF of DK Subsea
Cable 10

% MTTF Data of Subsystems inside the Offshore Converter
Station
MTTF_CS3=1.6; % MTTF of Control System 11
MTTF_TOFF=80; % MTTF of Offshore Transformer 12
MTTF_PR3=7; % MTTF of Converter Reactor 13
MTTF_DCS3=4.02; % MTTF of DC Switchyard 14
MTTF_CBL_offshore=438300/(8736*0.7); % MTTF of offshore
Subsea Cable 15
```

```

%      MTTR Data of Subsystems inside the NL Converter
Station
MTTR_CS=3/8736; % MTTR of Control System 1
MTTR_TON=1008/8736; % MTTR of Onshore Transformer 2
MTTR_PR=24/8736;% MTTF of Converter Reactor 3
MTTR_DCS=26.06/8736; % MTTF of DC Switchyard 4
MTTR_CBL_NL= 1560/8736; % MTTR of NL Subsea Cable 6

%      MTTR Data of Subsystems inside the DK Converter
Station
MTTR_CS2=3/8760; % MTTR of Control System 5
MTTR_TON2=1008/8760; % MTTR of Onshore Transformer 6
MTTR_PR2=24/8736;% MTTF of Converter Reactor 7
MTTR_DCS2=26.06/8736; % MTTF of DC Switchyard 8
MTTR_CBL_DK= 1560/8736; % MTTR of DK Subsea Cable 13

%      MTTR Data of Subsystems inside the Offshore Converter
Station
MTTR_CS3=17/8736; % MTTR of Control System 10
MTTR_TOFF=1512/8736; % MTTR of Offshore Transformer 11
MTTR_PR3=192/8736; % MTTF of Converter Reactor 12
MTTR_DCS3=98.06/8736; % MTTF of DC Switchyard 13
MTTR_CBL_offshore= 1560/8736; % MTTR of offshore Subsea
Cable 14

MTTR_C=3/8736; % MTTR of Converter 16
MTTR_C2=3/8736; % MTTR of Converter 17
MTTR_C3=3/8736; % MTTR of Converter 18

% Coefficient of the converter using Weibull Distribution
b =      2.838;
c =      3.212;

% Arrange MTTF and MTTR of all components into vectors
MTTF_all=[MTTF_CS MTTF_TON MTTF_PR MTTF_DCS MTTF_CBL_NL
MTTF_CS2 MTTF_TON2 MTTF_PR2 MTTF_DCS2 MTTF_CBL_DK MTTF_CS3
MTTF_TOFF MTTF_PR3 MTTF_DCS3 MTTF_CBL_offshore];
MTTR_all=[MTTR_CS MTTR_TON MTTR_PR MTTR_DCS MTTR_CBL_NL
MTTR_CS2 MTTR_TON2 MTTR_PR2 MTTR_DCS2 MTTR_CBL_DK MTTR_CS3
MTTR_TOFF MTTR_PR3 MTTR_DCS3 MTTR_CBL_offshore MTTR_C
MTTR_C2 MTTR_C3];

numMTTF= length(MTTF_all);
numMTTR= length(MTTR_all);

% Define vectors of time to failure (Tup) and time to
repair (Tdn)
Tup=zeros(N,numMTTF);
Tdn=zeros(N,numMTTR);

```

- **Generation of Lifetime Series**

To generate random sampling using negative exponential distribution, “`exprnd`” is used [64]. The converter unit random sampling uses weibull distribution and uses “`rand`” and the parameters for the random sampling. The parameters are stated in the previous section.

```

% Start Monte Carlo Simulation
for i=1:N
for num=1:numMTTF
Tup(i,num)=8736*exprnd(MTTF_all(num));

```

```

        end;
    end;

    for i=1:N
        for num=1:numMTTR
            Tdn(i,num)=8736*exprnd(MTTR_all(num));
        end;
    end;

% Start Monte Carlo Simulation for the Converter
sample_c_nl      = 8736*(-b*log(rand(N,1))).^(1/c);
sample_c_dk      = 8736*(-b*log(rand(N,1))).^(1/c);
sample_c_off     = 8736*(-b*log(rand(N,1))).^(1/c);

% Define roundTup and roundTdn as vectors of Tup and Tdn
rounded number to positive
% integer
roundTup = round(Tup);
roundTdn = round(Tdn);
roundTup_nl = round(sample_c_nl);
roundTup_dk = round(sample_c_dk);
roundTup_off = round(sample_c_off);
roundTup(roundTup==0)=1;
roundTdn(roundTdn==0)=1;
roundTup_nl(roundTup_nl==0)=1;
roundTup_dk(roundTup_dk==0)=1;
roundTup_off(roundTup_off==0)=1;

sumroundTup=sum(roundTup);
sumroundTdn=sum(roundTdn);
sumroundTup_nl=sum(roundTup_nl);
sumroundTup_dk=sum(roundTup_dk);
sumroundTup_off=sum(roundTup_off);

for a=1:numMTTF
    sumTspan(a)=sumroundTup(a)+sumroundTdn(a);
end;

sumTspan_nl=sumroundTup_nl+sumroundTdn(16);
sumTspan_dk=sumroundTup_dk+sumroundTdn(17);
sumTspan_off=sumroundTup_off+sumroundTdn(18);

%Define v1 until v8 as vectors of life state. All interval
time of Tup are defined
%as 1 and All interval time of Tdn as 0
v1=false(sumTspan(1),1);
v2=false(sumTspan(2),1);
v3=false(sumTspan(3),1);
v4=false(sumTspan(4),1);
v5=false(sumTspan(5),1);
v6=false(sumTspan(6),1);
v7=false(sumTspan(7),1);
v8=false(sumTspan(8),1);
v9=false(sumTspan(9),1);
v10=false(sumTspan(10),1);
v11=false(sumTspan(11),1);
v12=false(sumTspan(12),1);
v13=false(sumTspan(13),1);
v14=false(sumTspan(14),1);
v15=false(sumTspan(15),1);
v16=false(sumTspan_nl,1);
v17=false(sumTspan_dk,1);
v18=false(sumTspan_off,1);

```

```

% Define counter that will be useful to make interval Tup
and Tdn as a time
% series
counter1 = 1;
counter2 = 1;
counter3 = 1;
counter4 = 1;
counter5 = 1;
counter6 = 1;
counter7 = 1;
counter8 = 1;
counter9 = 1;
counter10 = 1;
counter11 = 1;
counter12 = 1;
counter13 = 1;
counter14 = 1;
counter15 = 1;
counter16 = 1;
counter17 = 1;
counter18 = 1;

% make the time series and the logic
for i=1:N
    v1(counter1:counter1+roundTup(i,1)-1)=true;

v1(counter1+roundTup(i,1):counter1+roundTup(i,1)+roundTdn(i
,1)-1)=false;
    counter1=counter1+roundTup(i,1)+roundTdn(i,1);

    v2(counter2:counter2+roundTup(i,2)-1)=true;

v2(counter2+roundTup(i,2):counter2+roundTup(i,2)+roundTdn(i
,2)-1)=false;
    counter2=counter2+roundTup(i,2)+roundTdn(i,2);

    v3(counter3:counter3+roundTup(i,3)-1)=true;

v3(counter3+roundTup(i,3):counter3+roundTup(i,3)+roundTdn(i
,3)-1)=false;
    counter3=counter3+roundTup(i,3)+roundTdn(i,3);

    v4(counter4:counter4+roundTup(i,4)-1)=true;

v4(counter4+roundTup(i,4):counter4+roundTup(i,4)+roundTdn(i
,4)-1)=false;
    counter4=counter4+roundTup(i,4)+roundTdn(i,4);

    v5(counter5:counter5+roundTup(i,5)-1)=true;

v5(counter5+roundTup(i,5):counter5+roundTup(i,5)+roundTdn(i
,5)-1)=false;
    counter5=counter5+roundTup(i,5)+roundTdn(i,5);

    v6(counter6:counter6+roundTup(i,6)-1)=true;

v6(counter6+roundTup(i,6):counter6+roundTup(i,6)+roundTdn(i
,6)-1)=false;
    counter6=counter6+roundTup(i,6)+roundTdn(i,6);

    v7(counter7:counter7+roundTup(i,7)-1)=true;

```

```

v7(counter7+roundTup(i,7):counter7+roundTup(i,7)+roundTdn(i,7)-1)=false;
    counter7=counter7+roundTup(i,7)+roundTdn(i,7);

    v8(counter8:counter8+roundTup(i,8)-1)=true;

v8(counter8+roundTup(i,8):counter8+roundTup(i,8)+roundTdn(i,8)-1)=false;
    counter8=counter8+roundTup(i,8)+roundTdn(i,8);

    v9(counter9:counter9+roundTup(i,9)-1)=true;

v9(counter9+roundTup(i,9):counter9+roundTup(i,9)+roundTdn(i,9)-1)=false;
    counter9=counter9+roundTup(i,9)+roundTdn(i,9);

    v10(counter10:counter10+roundTup(i,10)-1)=true;

v10(counter10+roundTup(i,10):counter10+roundTup(i,10)+roundTdn(i,10)-1)=false;
    counter10=counter10+roundTup(i,10)+roundTdn(i,10);

    v11(counter11:counter11+roundTup(i,11)-1)=true;

v11(counter11+roundTup(i,11):counter11+roundTup(i,11)+roundTdn(i,11)-1)=false;
    counter11=counter11+roundTup(i,11)+roundTdn(i,11);

    v12(counter12:counter12+roundTup(i,12)-1)=true;

v12(counter12+roundTup(i,12):counter12+roundTup(i,12)+roundTdn(i,12)-1)=false;
    counter12=counter12+roundTup(i,12)+roundTdn(i,12);

    v13(counter13:counter13+roundTup(i,13)-1)=true;

v13(counter13+roundTup(i,13):counter13+roundTup(i,13)+roundTdn(i,13)-1)=false;
    counter13=counter13+roundTup(i,13)+roundTdn(i,13);

    v14(counter14:counter14+roundTup(i,14)-1)=true;

v14(counter14+roundTup(i,14):counter14+roundTup(i,14)+roundTdn(i,14)-1)=false;
    counter14=counter14+roundTup(i,14)+roundTdn(i,14);

    v15(counter15:counter15+roundTup(i,15)-1)=true;

v15(counter15+roundTup(i,15):counter15+roundTup(i,15)+roundTdn(i,15)-1)=false;
    counter15=counter15+roundTup(i,15)+roundTdn(i,15);

    v16(counter16:counter16+roundTup_nl(i)-1)=true;

v16(counter16+roundTup_nl(i):counter16+roundTup_nl(i)+roundTdn(i,16)-1)=false;
    counter16=counter16+roundTup_nl(i)+roundTdn(i,16);

    v17(counter17:counter17+roundTup_dk(i)-1)=true;

v17(counter17+roundTup_dk(i):counter17+roundTup_dk(i)+roundTdn(i,17)-1)=false;

```

```

        counter17=counter17+roundTup_dk(i)+roundTdn(i,17);

        v18(counter18:counter18+roundTup_off(i)-1)=true;

v18(counter18+roundTup_off(i):counter18+roundTup_off(i)+rou
ndTdn(i,18)-1)=false;
        counter18=counter18+roundTup_off(i)+roundTdn(i,18);

end;

```

```

v_length = 8736*floor(min([length(v1) length(v2) length(v3)
length(v4) length(v5) length(v6) length(v7) length(v8)
length(v9) length(v10) length(v11) length(v12) length(v13)
length(v14) length(v15) length(v16) length(v17)
length(v18)])/8736);

```

```

%take the logic in interval time until v_length

```

```

    v001=v1(1:v_length);
    A_1=mean(v001);
    U_1=1-A_1;
    v002=v2(1:v_length);
    A_2=mean(v002);
    U_2=1-A_2;
    v003=v3(1:v_length);
    A_3=mean(v003);
    U_3=1-A_3;
    v004=v4(1:v_length);
    A_4=mean(v004);
    U_4=1-A_4;
    v005=v5(1:v_length);
    A_5=mean(v005);
    U_5=1-A_5;
    v006=v6(1:v_length);
    A_6=mean(v006);
    U_6=1-A_6;
    v007=v7(1:v_length);
    A_7=mean(v007);
    U_7=1-A_7;
    v008=v8(1:v_length);
    A_8=mean(v008);
    U_8=1-A_8;
    v009=v9(1:v_length);
    A_9=mean(v009);
    U_9=1-A_9;
    v010=v10(1:v_length);
    A_10=mean(v010);
    U_10=1-A_10;
    v011=v11(1:v_length);
    A_11=mean(v011);
    U_11=1-A_11;
    v012=v12(1:v_length);
    A_12=mean(v012);
    U_12=1-A_12;
    v013=v13(1:v_length);
    A_13=mean(v013);
    U_13=1-A_13;
    v014=v14(1:v_length);
    A_14=mean(v014);
    U_14=1-A_14;
    v015=v15(1:v_length);
    A_15=mean(v015);
    U_15=1-A_15;
    v016=v16(1:v_length);
    A_16=mean(v016);

```

```

U_16=1-A_16;
v017=v17(1:v_length);
A_17=mean(v017);
U_17=1-A_17;
v018=v18(1:v_length);
A_18=mean(v018);
U_18=1-A_18;

vv=[v001 v002 v003 v004 v005 v006 v007 v008 v009 v010 v011
v012 v013 v014 v015 v016 v017 v018];

% Calculate the series-connected components logic of N1
onshore node,
% DK onshore node, and offshore node, without DC
switchyard
v_NL_1=(v001&v002&v003&v016);
v_DK_1=(v006&v007&v008&v017);
v_offshore_1=(v011&v012&v013&v018);

% Calculate the series-connected components logic of N1
onshore node,
% DK onshore node, and offshore node
v_NL=(v001&v002&v003&v004&v016);
v_DK=(v006&v007&v008&v009&v017);
v_offshore=(v011&v012&v013&v014&v018);

% Calculate the series-connected components logic of
cobra project
v_cobra=v_NL&v_DK&v005&v010;

% with DC switchyard
v_cobra_offshore=(v_NL&v005)&(v_DK&v010)&(v_offshore&v015);

% Calculate the series-connected components logic of
cobra project
% with offshore node and cable and with DC switchyard
v_no_NL=~(v_NL&v005)&(v_DK&v010)&(v_offshore&v015);
v_no_DK=(v_NL&v005)&~(v_DK&v010)&(v_offshore&v015);

v_no_offshore=(v_NL&v005)&(v_DK&v010)&~(v_offshore&v015);
v_no_NL_DK=~(v_NL&v005)&~(v_DK&v010)&(v_offshore&v015);

v_no_NL_offshore=~(v_NL&v005)&(v_DK&v010)&~(v_offshore&v015
);

v_no_DK_offshore=(v_NL&v005)&~(v_DK&v010)&~(v_offshore&v015
);
v_no_all=~(v_NL&v005)&~(v_DK&v010)&~(v_offshore&v015);

% Calculate of the power transmitted per hour
E_transmitted_cobra = zeros(1,v_length);
E_transmitted_norned = zeros(1,v_length);
E_transmitted_britned = zeros(1,v_length);
E_transmitted_MEE_DE = zeros(1,v_length);
for i=1:v_length
E_transmitted_cobra(i) = v_cobra(i)*cobra(i-
8736*floor((i-1)/8736));
E_transmitted_norned(i) = v_cobra(i)*norned(i-
8736*floor((i-1)/8736));

```

```

        E_transmitted_britned(i) = v_cobra(i)*britned(i-
8736*floor((i-1)/8736));
        E_transmitted_MEE_DE(i) = v_cobra(i)*MEE_DE(i-
8736*floor((i-1)/8736));
    end

```

• Output

➤ Availability and Unavailability

```

% Calculate the availability of the system

```

```

availability_cobra=mean(v_cobra);
unavailability_cobra=1-availability_cobra;
availability_NL=mean(v_NL);
unavailability_NL=1-availability_NL;
availability_DK=mean(v_DK);
unavailability_DK=1-availability_DK;
availability_offshore=mean(v_offshore);
unavailability_offshore=1-availability_offshore;

```

```

availability_all=mean(v_cobra_offshore);
unavailability_all=1-availability_all;

```

```

availability_no_NL=mean(v_no_NL);
availability_no_DK=mean(v_no_DK);
availability_no_offshore=mean(v_no_offshore);
availability_no_NL_DK=mean(v_no_NL_DK);
availability_no_NL_offshore=mean(v_no_NL_offshore);
availability_no_DK_offshore=mean(v_no_DK_offshore);
availability_no_all=mean(v_no_all);

```

➤ Energy not Transmitted in Point-to-Point Connection

```

% Calculate the energy not transmitted through cobra
project in a year

```

```

av_E_transmitted_py_GWh_cobra=
mean(E_transmitted_cobra)*8736/1000;
E_not_transmitted_GWh_cobra= sum(cobra)/1000-
av_E_transmitted_py_GWh_cobra;

```

```

av_E_transmitted_py_GWh_norned =
mean(E_transmitted_norned)*8736/1000;
E_not_transmitted_GWh_norned = sum(norned)/1000-
av_E_transmitted_py_GWh_norned;

```

```

av_E_transmitted_py_GWh_britned =
mean(E_transmitted_britned)*8736/1000;
E_not_transmitted_GWh_britned = sum(britned)/1000-
av_E_transmitted_py_GWh_britned;

```

```

av_E_transmitted_py_GWh_MEE_DE =
mean(E_transmitted_MEE_DE)*8736/1000;
E_not_transmitted_GWh_MEE_DE = sum(MEE_DE)/1000-
av_E_transmitted_py_GWh_MEE_DE;

```

➤ Average Duration per Interruption and Failure Frequency

```

% Calculate the average duration, failure frequency of each
subsystems inside the converter station

```

```

counter_comp=zeros(v_length,numMTTR);

for i=1:numMTTR
    mem_comp = 0;
    j_comp=0;
    for k=1:v_length
        if vv(k,i)==1
            if mem_comp == 1

counter_comp(j_comp,i)=counter_comp(j_comp,i)+1;
                mem_comp = vv(k,i);
            elseif mem_comp == 0;
                j_comp=j_comp+1;

counter_comp(j_comp,i)=counter_comp(j_comp,i)+1;
                mem_comp = vv(k,i);
            end;
            elseif vv(k,i)==0

counter_comp(j_comp,i)=counter_comp(j_comp,i)+1;
                mem_comp = vv(k,i);
            end;
        end;

find1_comp(i) = length(find(0<counter_comp(:,i) &
counter_comp(:,i)<8736/4));
find2_comp(i)=length(find(8736/4<counter_comp(:,i) &
counter_comp(:,i)<8736/2));
find3_comp(i)=length(find(8736/2<counter_comp(:,i) &
counter_comp(:,i)<8736));
find4_comp(i)=length(find(8736<counter_comp(:,i) &
counter_comp(:,i)<8736*2));
find5_comp(i)=length(find(8736*2<counter_comp(:,i)));
end;

freq_comp = zeros(5,numMTTR);
for i=1:numMTTR;
    freq_comp(:,i) =
[find1_comp(i);find2_comp(i);find3_comp(i);find4_comp(i);fi
nd5_comp(i)];
end;

% Calculate the average duration, failure frequency of the
NL converter station

j_NL=0;
mem_NL = 0;
counter_NL = zeros(v_length,1);
outage_NL = zeros(v_length,1);
o_NL=0;

for k=1:v_length
    if v_NL(k)==1
        if mem_NL == 1
            counter_NL(j_NL)=counter_NL(j_NL)+1;
            mem_NL = v_NL(k);
        elseif mem_NL == 0;
            j_NL=j_NL+1;
            o_NL=o_NL+1;
            counter_NL(j_NL)=counter_NL(j_NL)+1;
            mem_NL = v_NL(k);
        end;
    end;
end;

```

```

elseif v_NL(k)==0
    counter_NL(j_NL)=counter_NL(j_NL)+1;
    outage_NL(o_NL) = outage_NL(o_NL)+1;
    mem_NL = v_NL(k);
end;

end;
counter_NL=counter_NL(1:j_NL-1,1);

if outage_NL(o_NL)==0
    outage_NL=outage_NL(1:o_NL-1,1);
else
    outage_NL=outage_NL(1:o_NL,1);
end;

av_outage_NL=mean(outage_NL)/(v_length/8736);
freq_year_NL=length(counter_NL)/(v_length/8736);

find_NL_1=length(find(0<counter_NL & counter_NL<8736/4));
find_NL_2=length(find(8736/4<counter_NL &
counter_NL<8736/2));
find_NL_3=length(find(8736/2<counter_NL &
counter_NL<8736));
find_NL_4=length(find(8736<counter_NL &
counter_NL<8736*2));
find_NL_5=length(find(8736*2<counter_NL));

find_NL=[find_NL_1;find_NL_2;find_NL_3;find_NL_4;find_NL_5]
;

% Calculate the average duration, failure frequency of the
DK converter station

j_DK=0;
mem_DK = 0;
o_DK = 0;
counter_DK = zeros(v_length,1);
outage_DK = zeros(v_length,1);

for k=1:v_length
    if v_DK(k)==1
        if mem_DK == 1
            counter_DK(j_DK)=counter_DK(j_DK)+1;
            mem_DK = v_DK(k);
        elseif mem_DK == 0;
            j_DK=j_DK+1;
            o_DK=o_DK+1;
            counter_DK(j_DK)=counter_DK(j_DK)+1;
            mem_DK = v_DK(k);
        end;
    elseif v_DK(k)==0
        counter_DK(j_DK)=counter_DK(j_DK)+1;
        outage_DK(o_DK) = outage_DK(o_DK)+1;
        mem_DK = v_DK(k);
    end;
end;
counter_DK=counter_DK(1:j_DK,1);

if outage_DK(o_DK)==0
    outage_DK=outage_DK(1:o_DK-1,1);
else
    outage_DK=outage_DK(1:o_DK,1);

```

```

end;

av_outage_DK=mean(outage_DK)/(v_length/8736);
freq_year_DK=length(counter_DK)/(v_length/8736);

find_DK_1=length(find(0<counter_DK & counter_DK<8736/4));
find_DK_2=length(find(8736/4<counter_DK &
counter_DK<8736/2));
find_DK_3=length(find(8736/2<counter_DK &
counter_DK<8736));
find_DK_4=length(find(8736<counter_DK &
counter_DK<8736*2));
find_DK_5=length(find(8736*2<counter_DK));

find_DK=[find_DK_1;find_DK_2;find_DK_3;find_DK_4;find_DK_5]
;

% Calculate the average duration, failure frequency of the
offshore converter station

j_off=0;
mem_off = 0;
o_off=0;
counter_off = zeros(v_length,1);
outage_off = zeros(v_length,1);

for k=1:v_length
    if v_offshore(k)==1
        if mem_off == 1
            counter_off(j_off)=counter_off(j_off)+1;
            mem_off = v_offshore(k);
        elseif mem_off == 0;
            j_off=j_off+1;
            o_off=o_off+1;
            counter_off(j_off)=counter_off(j_off)+1;
            mem_off = v_offshore(k);
        end;
    elseif v_offshore(k)==0
        counter_off(j_off)=counter_off(j_off)+1;
        outage_off(o_off)=outage_off(o_off)+1;
        mem_off = v_offshore(k);
    end;
end;
counter_off=counter_off(1:j_off,1);
if outage_off(o_off)==0
    outage_off=outage_off(1:o_off-1,1);
else
    outage_off=outage_off(1:o_off,1);
end;

av_outage_off=mean(outage_off)/(v_length/8736);
freq_year_off=length(counter_off)/(v_length/8736);

find_off_1=length(find(0<counter_off &
counter_off<8736/4));
find_off_2=length(find(8736/4<counter_off &
counter_off<8736/2));
find_off_3=length(find(8736/2<counter_off &
counter_off<8736));
find_off_4=length(find(8736<counter_off &
counter_off<8736*2));
find_off_5=length(find(8736*2<counter_off));

```

```
find_off=[find_off_1;find_off_2;find_off_3;find_off_4;find_off_5];
```

```
j_cobra=0;
o_cobra=0;
mem_cobra = 0;
counter_cobra = zeros(v_length,1);
outage_cobra = zeros(v_length,1);
```

```
for k=1:v_length
    if v_cobra(k)==1
        if mem_cobra == 1

counter_cobra(j_cobra)=counter_cobra(j_cobra)+1;
            mem_cobra = v_cobra(k);
        elseif mem_cobra == 0;
            j_cobra=j_cobra+1;
            o_cobra=o_cobra+1;

counter_cobra(j_cobra)=counter_cobra(j_cobra)+1;
            mem_cobra = v_cobra(k);
        end;
    elseif v_cobra(k)==0
        counter_cobra(j_cobra)=counter_cobra(j_cobra)+1;
        outage_cobra(o_cobra)= outage_cobra(o_cobra)+1;

            mem_cobra = v_cobra(k);
        end;
end;
counter_cobra=counter_cobra(1:j_cobra,1);
if outage_cobra(o_cobra)==0
    outage_cobra=outage_cobra(1:o_cobra-1,1);
else
    outage_cobra=outage_cobra(1:o_cobra,1);
end;
```

```
av_outage_cobra=mean(outage_cobra)/(v_length/8736);
freq_year_cobra=length(counter_cobra)/(v_length/8736);
```

```
find_cobra_1=length(find(0<counter_cobra &
counter_cobra<8736/4));
find_cobra_2=length(find(8736/4<counter_cobra &
counter_cobra<8736/2));
find_cobra_3=length(find(8736/2<counter_cobra &
counter_cobra<8736));
find_cobra_4=length(find(8736<counter_cobra &
counter_cobra<8736*2));
find_cobra_5=length(find(8736*2<counter_cobra));
```

```
find_cobra=[find_cobra_1;find_cobra_2;find_cobra_3;find_cobra_4;find_cobra_5];
```

```
% Calculate the average duration, failure frequency of the
offshore converter station
```

```
j_all=0;
o_all=0;
mem_all = 0;
counter_all = zeros(v_length,1);
```

```

outage_all = zeros(v_length,1);

for k=1:v_length
    if v_cobra_offshore(k)==1
        if mem_all == 1
            counter_all(j_all)=counter_all(j_all)+1;
            mem_all = v_cobra_offshore(k);
        elseif mem_all == 0;
            j_all=j_all+1;
            o_all=o_all+1;
            counter_all(j_all)=counter_all(j_all)+1;
            mem_all = v_cobra_offshore(k);
        end;
    elseif v_cobra_offshore(k)==0
        counter_all(j_all)=counter_all(j_all)+1;
        outage_all(o_all)= outage_all(o_all)+1;
        mem_all = v_cobra_offshore(k);
    end;
end;
counter_all=counter_all(1:j_all,1);
if outage_all(o_all)==0
    outage_all=outage_all(1:o_all-1,1);
else
    outage_all=outage_all(1:o_all,1);
end;

av_outage_all=mean(outage_all)/(v_length/8736);
freq_year_all=length(counter_all)/(v_length/8736);

find_all_1=length(find(0<counter_all &
counter_all<8736/4));
find_all_2=length(find(8736/4<counter_all &
counter_all<8736/2));
find_all_3=length(find(8736/2<counter_all &
counter_all<8736));
find_all_4=length(find(8736<counter_all &
counter_all<8736*2));
find_all_5=length(find(8736*2<counter_all));

find_all=[find_all_1;find_all_2;find_all_3;find_all_4;find_
all_5];

% end

```

➤ Energy not Transmitted in Point-to-Point Connection

```

E_transmitted_NL_noDK = zeros(1,v_length);
E_transmitted_NL_noNL = zeros(1,v_length);
E_transmitted_NL_nooffshore = zeros(1,v_length);

E_transmitted_DK_noDK = zeros(1,v_length);
E_transmitted_DK_noNL = zeros(1,v_length);
E_transmitted_DK_nooffshore = zeros(1,v_length);

E_transmitted_equal_noDK = zeros(1,v_length);
E_transmitted_equal_noNL = zeros(1,v_length);
E_transmitted_equal_nooffshore = zeros(1,v_length);

E_transmitted_follow_exchange_noDK = zeros(1,v_length);
E_transmitted_follow_exchange_noNL = zeros(1,v_length);
E_transmitted_follow_exchange_nooffshore =
zeros(1,v_length);

```

```

v_NL_c=(v_NL&v005);
v_DK_c=(v_DK&v010);
v_offshore_c=(v_offshore&v015);

for i=1:v_length
E_transmitted_NL_noNL(i) = v_no_NL(i)*(NL_DK_export(i-
8736*floor((i-1)/8736))+NL_offshore_wind(i-8736*floor((i-
1)/8736)));
E_transmitted_NL_noDK(i) = v_no_DK(i)*(NL_NL_export(i-
8736*floor((i-1)/8736))+NL_offshore_wind(i-8736*floor((i-
1)/8736)));
E_transmitted_NL_nooffshore(i) =
v_no_offshore(i)*(NL_DK_export(i-8736*floor((i-
1)/8736))+NL_NL_export(i-8736*floor((i-1)/8736)));

E_transmitted_DK_noNL(i) = v_no_NL(i)*(DK_DK_export(i-
8736*floor((i-1)/8736))+DK_offshore_wind(i-8736*floor((i-
1)/8736)));
E_transmitted_DK_noDK(i) = v_no_DK(i)*(DK_NL_export(i-
8736*floor((i-1)/8736))+DK_offshore_wind(i-8736*floor((i-
1)/8736)));
E_transmitted_DK_nooffshore(i) =
v_no_offshore(i)*(DK_DK_export(i-8736*floor((i-
1)/8736))+DK_NL_export(i-8736*floor((i-1)/8736)));

E_transmitted_equal_noNL(i) =
v_no_NL(i)*(equal_DK_export(i-8736*floor((i-
1)/8736))+equal_offshore_wind(i-8736*floor((i-1)/8736)));
E_transmitted_equal_noDK(i) =
v_no_DK(i)*(equal_DK_export(i-8736*floor((i-
1)/8736))+equal_offshore_wind(i-8736*floor((i-1)/8736)));
E_transmitted_equal_nooffshore(i) =
v_no_offshore(i)*(equal_DK_export(i-8736*floor((i-
1)/8736))+equal_NL_export(i-8736*floor((i-1)/8736)));

E_transmitted_follow_exchange_noNL(i) =
v_no_NL(i)*(follow_exchange_DK_export(i-8736*floor((i-
1)/8736))+follow_exchange_offshore_wind(i-8736*floor((i-
1)/8736)));
E_transmitted_follow_exchange_noDK(i) =
v_no_DK(i)*(follow_exchange_DK_export(i-8736*floor((i-
1)/8736))+follow_exchange_offshore_wind(i-8736*floor((i-
1)/8736)));
E_transmitted_follow_exchange_nooffshore(i) =
v_no_offshore(i)*(follow_exchange_DK_export(i-
8736*floor((i-1)/8736))+follow_exchange_NL_export(i-
8736*floor((i-1)/8736)));

end

NL_av_E_transmitted_py_GWh_noNL= mean(
E_transmitted_DK_noNL)*8736/1000;
NL_av_E_transmitted_py_GWh_noDK=
mean(E_transmitted_NL_noDK)*8736/1000;
NL_av_E_transmitted_py_GWh_nooff=
mean(E_transmitted_NL_nooffshore)*8736/1000;
DK_av_E_transmitted_py_GWh_noNL=
mean(E_transmitted_DK_noNL)*8736/1000;
DK_av_E_transmitted_py_GWh_noDK=
mean(E_transmitted_DK_noDK)*8736/1000;
DK_av_E_transmitted_py_GWh_nooff=

```

```
mean(E_transmitted_DK_nooffshore)*8736/1000;  
equal_av_E_transmitted_py_GWh_noNL=  
mean(E_transmitted_equal_noNL)*8736/1000;  
equal_av_E_transmitted_py_GWh_noDK=  
mean(E_transmitted_equal_noDK)*8736/1000;  
equal_av_E_transmitted_py_GWh_nooff=  
mean(E_transmitted_equal_nooffshore)*8736/1000;  
follow_exchange_av_E_transmitted_py_GWh_noNL=  
mean(E_transmitted_follow_exchange_noNL)*8736/1000;  
follow_exchange_av_E_transmitted_py_GWh_noDK=  
mean(E_transmitted_follow_exchange_noDK)*8736/1000;  
follow_exchange_av_E_transmitted_py_GWh_nooff=  
mean(E_transmitted_follow_exchange_nooffshore)*8736/1000;
```


Appendix C

THE RESULT SAMPLING

Below illustrate the sampling of Monte Carlo simulation results. The results include:

- the unavailability of all subsystems inside the converter station and
- the unavailability of the DC cables,
- the unavailability of three converter stations (NL, DK, offshore),
- the energy not transmitted through point-to-point configuration,
- the energy not transmitted through three-terminal configuration,
- the average duration per interruptions of all subsystems and systems.
- the failure frequency of all subsystems and systems.
- The range of time between failures of all subsystems and systems.

Data of the sampling is defined in section Input. The sampling is executed in section Sampling. The calculation of the average of all the result and the 95% confidence bound is applied in section Process and Output.

- **Input**

```
% Define all the result sampling as vectors
```

```
NN=100;  
U_1=zeros(NN,1);  
U_2=U_1;  
U_3=U_1;  
U_4=U_1;  
U_5=U_1;  
U_6=U_1;  
U_7=U_1;  
U_8=U_1;  
U_9=U_1;  
U_10=U_1;  
U_11=U_1;  
U_12=U_1;  
U_13=U_1;  
U_14=U_1;  
U_15=U_1;  
U_16=U_1;  
U_17=U_1;  
U_18=U_1;  
unavailability_NL=U_1;  
unavailability_DK=U_1;  
unavailability_offshore=U_1;  
unavailability_cobra=U_1;  
v_length=U_1;  
  
E_not_transmitted_GWh_cobra=U_1;  
E_not_transmitted_GWh_norned=U_1;  
E_not_transmitted_GWh_britned=U_1;  
E_not_transmitted_GWh_MEE_DE=U_1;  
unavailability_all=U_1;  
unavailability_all_1=U_1;  
unavailability_no_NL=U_1;  
unavailability_no_DK=U_1;  
unavailability_no_offshore=U_1;  
unavailability_no_NL_DK=U_1;  
unavailability_no_NL_offshore=U_1;
```

```

unavailability_no_DK_offshore=U_1;
unavailability_no_all=U_1;

freq_comp=zeros(5,18,NN);
av_outage_NL=U_1;
av_outage_DK=U_1;
av_outage_off=U_1;
av_outage_cobra=U_1;
av_outage_all=U_1;

find_NL=zeros(1,5,NN);
find_DK=zeros(1,5,NN);
find_off=zeros(1,5,NN);
find_cobra=zeros(1,5,NN);
find_all=zeros(1,5,NN);

```

- **Sampling**

```

for i=1:NN
[E_not_transmitted_GWh_cobra(i),E_not_transmitted_GWh_nornd(i),E_not_transmitted_GWh_britned(i),E_not_transmitted_GWh_MEE_DE(i),U_1(i),U_2(i),U_3(i),U_4(i),U_5(i),U_6(i),U_7(i),U_8(i),U_9(i),U_10(i),U_11(i),U_12(i),U_13(i),U_14(i),U_15(i),U_16(i),U_17(i),U_18(i),unavailability_NL(i),unavailability_DK(i),unavailability_offshore(i),unavailability_cobra(i),availability_all(i),unavailability_all(i),unavailability_all_1(i),availability_no_NL(i),availability_no_DK(i),availability_no_offshore(i),availability_no_NL_DK(i),availability_no_NL_offshore(i),availability_no_DK_offshore(i),availability_no_all(i),v_length(i),av_outage_NL(i),av_outage_DK(i),av_outage_off(i),av_outage_cobra(i),av_outage_all(i),freq_year_NL(i),freq_year_DK(i),freq_year_off(i),freq_year_cobra(i),freq_year_all(i),freq_comp(:,:,i),find_NL(:,:,i),find_DK(:,:,i),find_off(:,:,i),find_cobra(:,:,i),find_all(:,:,i)]=MonteCarlo_program8;
end;

```

- **Process and Output**

The mean of availability and the 95% confidence bound can be achieved using “normfit” in MATLAB

```

[muhat1,sigmahat1,muci1,sgmaci1] = normfit(U_1);
[muhat2,sigmahat2,muci2,sgmaci2] = normfit(U_2);
[muhat3,sigmahat3,muci3,sgmaci3] = normfit(U_3);
[muhat4,sigmahat4,muci4,sgmaci4] = normfit(U_4);
[muhat5,sigmahat5,muci5,sgmaci5] = normfit(U_5);
[muhat6,sigmahat6,muci6,sgmaci6] = normfit(U_6);
[muhat7,sigmahat7,muci7,sgmaci7] = normfit(U_7);
[muhat8,sigmahat8,muci8,sgmaci8] = normfit(U_8);
[muhat9,sigmahat9,muci9,sgmaci9] = normfit(U_9);
[muhat10,sigmahat10,muci10,sgmaci10] = normfit(U_10);
[muhat11,sigmahat11,muci11,sgmaci11] = normfit(U_11);
[muhat12,sigmahat12,muci12,sgmaci12] = normfit(U_12);
[muhat13,sigmahat13,muci13,sgmaci13] = normfit(U_13);
[muhat14,sigmahat14,muci14,sgmaci14] = normfit(U_14);
[muhat15,sigmahat15,muci15,sgmaci15] = normfit(U_15);
[muhat16,sigmahat16,muci16,sgmaci16] = normfit(U_16);
[muhat17,sigmahat17,muci17,sgmaci17] = normfit(U_17);
[muhat18,sigmahat18,muci18,sgmaci18] = normfit(U_18);

```

```

[muhat_NL,sigmahat_NL,muci_NL,sigmaci_NL] =
normfit(unavailability_NL);
[muhat_DK,sigmahat_DK,muci_DK,sigmaci_DK] =
normfit(unavailability_DK);
[muhat_offshore,sigmahat_offshore,muci_offshore,sigmaci_off
shore] = normfit(unavailability_offshore);
[muhat_two,sigmahat_two,muci_two,sigmaci_two] =
normfit(unavailability_cobra);
[muhat_three,sigmahat_three,muci_three,sigmaci_three] =
normfit(unavailability_all);

[muhat_no_NL,sigmahat_no_NL,muci_no_NL,sigmaci_no_NL] =
normfit(availability_no_NL);
[muhat_no_DK,sigmahat_no_DK,muci_no_DK,sigmaci_no_DK] =
normfit(availability_no_DK);
[muhat_no_offshore,sigmahat_no_offshore,muci_no_offshore,si
gmaci_no_offshore] = normfit(availability_no_offshore);
[muhat_no_NL_DK,sigmahat_no_NL_DK,muci_no_NL_DK,sigmaci_no_
NL_DK] = normfit(availability_no_NL_DK);
[muhat_no_NL_offshore,sigmahat_no_NL_offshore,muci_no_NL_of
fshore,sigmaci_no_NL_offshore] =
normfit(availability_no_NL_offshore);
[muhat_no_DK_offshore,sigmahat_no_DK_offshore,muci_no_DK_of
fshore,sigmaci_no_DK_offshore] =
normfit(availability_no_DK_offshore);
[muhat_no_all,sigmahat_no_all,muci_no_all,sigmaci_no_all] =
normfit(availability_no_all);
[muhat_v_length,sigmahat_v_length,muci_v_length,sigmaci_v_l
ength] = normfit(v_length);

```

